The Role of RNA-Binding Protein, Muscleblind-Like 1, in Cardiac Wound Healing and Remodeling

Christina J. Jones

A dissertation
submitted in partial fulfillment of the
requirements for the degree of

Doctor of Philosophy

University of Washington
2018

Reading Committee:
Randall T. Moon, Chair
Jennifer M. Davis
William M. Mahoney

Program Authorized to Offer Degree:

Pharmacology

University of Washington

Abstract

The Role of RNA-Binding Protein, Muscleblind-Like 1, in Cardiac Wound Healing and Remodeling

Christina J Jones

Chair of the Supervisory Committee:
Randall T. Moon, Ph.D.
Pharmacology

Myocardial infarction (MI) triggers cardiomyocyte necrosis and a reparative response that involves deposition of a collagenous, fibrotic scar. Persistent scar formation leads to adverse remodeling of the heart structure and progression to heart failure, which is the leading cause of death worldwide. Although advancements in treatments have allowed patients to live longer, the underlying fibrotic scar is not remedied. The primary effector of cardiac fibrosis is the myofibroblast, which is a specialized, heterogeneous cell type that secretes extracellular matrix (ECM) and functionally contracts to help maintain ventricular wall integrity and prevent heart rupture after acute MI.

Our lab previously identified the RNA-binding protein, Muscleblind-Like 1 (MBNL1), to be robustly upregulated during myofibroblast transformation. MBNL1 (a) stabilizes mRNA transcripts, (b) activates nodal signaling axes that transition fibroblasts into a myofibroblast cell fate and (c) augments fibrosis in the heart after MI. However, there are still several unanswered questions: (1) Which cardiac cell type contributes to MBNL1-mediated fibrotic remodeling after MI? (2) Could genetically dosing

MBNL1 in the heart improve cardiac function post-infarct? (3) What other protein complexes associate with MBNL1 to regulate mRNA maturation and cell differentiation?

In order to answer these questions, we either genetically knocked out or overexpressed *Mbnl1* selectively in two different cells within the heart, fibroblasts and cardiomyocytes, to determine if *Mbnl1* is a global mediator in the fibrotic response. We hypothesized fibroblasts were the main contributor to MBNL1-dependent fibrosis after MI. Indeed, we demonstrated that genetic deletion of *Mbnl1* in resident cardiac fibroblasts diminishes the formation of a fibrotic scar and protects the heart from cardiac dysfunction post-MI. *Mbnl1* depletion in resident cardiac fibroblasts inhibits TGFβ-mediated myofibroblast differentiation, which can be rescued by reintroduction of functional pro-fibrogenic transcripts *serum response factor (Srf)* and *calcineurin (CnA)* that are bound and regulated by MBNL1. A decrease in fibrosis post-MI was also observed in mice with cardiomyocyte-specific *Mbnl1* loss of function, suggesting *Mbnl1* function in cardiomyocytes also contributes to post-infarction wound healing and fibrotic remodeling after MI. Mechanistically, we show for the first time that MBNL1 binds with RNA processing machinery in fibroblasts to promote myofibroblast differentiation. When *Mbnl1* is overexpressed in cardiac fibroblasts and cardiomyocytes, we observed diastolic dysfunction phenotypes in the absence of injury, highlighting MBNL1's regulatory role in maintaining homeostasis in the cell. Collectively, this dissertation addresses the cell-specific role of MBNL1 in cardiac remodeling after MI by genetically manipulating *Mbnl1* levels in both resident cardiac fibroblasts and cardiomyocytes. This work is significant because it will build upon a basic scientific understanding of transcriptome changes during cardiac wound healing and may provide new approaches to functionally repair and heal the myocardium post-MI.

Contents

List of Figures

List of Tables

Acknowledgements

The pursuit of a doctoral degree is a challenging and rewarding process. Many people have contributed directly to this work and my growth as a scientist. First and foremost, I would like to thank my two advisors, Dr. Randy Moon and Dr. Jennifer Davis. Randy afforded me the freedom to explore my own scientific ideas and learn from my failures as a young scientist. His vision for science is unremarkable, and it was a privilege to train in his laboratory. I would also like to thank Dr. Jennifer Davis who graciously took me into her lab with open arms. The countless hours, advice, expertise, and patience has pushed me to grow into a much more thoughtful, well-rounded scientist. It has been exciting to watch the lab grow and expand under her leadership. I would also like to extend my gratitude to my thesis committee. Dr. Bill Catterall has offered a strong biological perspective and was a pleasure to work with while rotating through his lab. Dr. Larry Zweifel has always brought cheer to our committee meetings with intuitive questions. Dr. Bill Mahoney has been an absolute pleasure to work with and was always supportive in both my scientific pursuits as well as career development. I'd also like to thank Dr. Edith Wang who has acted as an unofficial committee member, but has been a great sounding board to scientific ideas. Finally, I would like to thank Judy Austin and Laura Frost who have inspired me to pursue math and science and are still fantastic role models.

I would also like to thank everyone in the Moon lab. I would like to specifically acknowledge Aaron Robitaille for his scientific insight and advice as well as his unwavering passion for all fields of science. He took me under his wing as a new graduate student and trained me on everything from cell culture to mass spectrometry and business development. He has been an instrumental friend and role model, and I'm grateful for his continuing mentorship. I would also like to thank Jeanot Muster for his support and ability to fix almost anything, Charisma Enam for providing emotional support and being my fellow grad student confidant, Jeremy Rabinowitz and Jason Berndt continually asking critical questions

to challenge everyone's views on scientific questions, and Stanley Kim for his company during long hours in the zebrafish facility. I would love to thank all the members of the Moon lab for the constant support, as these were the best people I could have imagined working with: Cat Ray, Lindsey Wimberly, Aurélie Jacquet, Miranda Murray, Nick Strand, Nick Robin, Zhoujin Xu, Peggy Yang, Zsuzsa Agoston, Matthew Pawlus, Tim Petrie, Jessica St. Laurent, and Peter Hofsteen.

Next, I would like to thank everyone in the Davis lab. It has been a fun experiment. You all bring such unique perspectives to the group. I would like to especially thank Darrian Bugg who has tirelessly helped with surgeries and teaching me almost everything there is to know about working with mouse hearts. Ambika Gunaje has been such a great friend, bay-mate, and always willing to give her time to help with any problem I encountered. It was great having her as a lunch buddy and I learned so much about Indian cooking. I would like to thank Emily Olszewski for her upbeat attitude and willing to help with any issues that arose in the lab, Kevin Shi and Guy Everett for their late-night conversations, Peter Kim for his support with engineered patterned cell culture materials, Danny El-Nachef for his expertise in cell cycle and cardiomyocytes, and all the undergraduates would have been a pleasure to mentor a lot of help, including Jasmine Fuerte-Stone, Divya Lakshmanan, Issac Flores, Kacie Yokoro, and Nadia Siddiqui.

I would like to thank the Pharmacology Department and the Institute for Stem Cell and Regenerative Medicine, which have both provided a strong, collaborative environment. This research could not have been possible without the support of my funding sources: HHMI, the Pharmacological Sciences Training Grant, the Wellstone Muscular Dystrophy Grant, and the NIH.

I would like to give a special thanks to my fellow classmates and friends who have provided advice and an awesome support network during graduate school. They are my family away from home and I love them all. Lastly, I would like to thank my family for teaching the value of perseverance and always supporting me in whatever endeavor I pursue.

Dedication

"The heart of animals is the foundation of their life, the sovereign of everything within them, the sun of their microcosm, that upon which all growth depends, from which all power proceeds"

-William Harvey, 1628.

I would like to dedicate this PhD dissertation to my mom and my brother, Matthew, who have been my heart and foundation throughout my entire life and has always believed in me to achieve my goals, no matter how difficult.

1 Introduction

1.1 Project Aims and Objective

Progressive cardiac fibrosis causes an abundance of medical problems including loss of organ function and tissue flexibility that can eventually lead to heart failure. The overall purpose of this thesis is to identify the mechanisms that are involved in cardiac fibrosis and subsequent remodeling after acute myocardial infarction. We hypothesized that MBNL1 regulation specifically in resident cardiac fibroblasts to promote myofibroblast differentiation is a critical contributor to adverse cardiac fibrosis.

My specific objectives were:

1. To determine the contribution of MBNL1 in resident cardiac fibroblasts and cardiomyocytes to cardiac fibrosis and function after acute myocardial infarction.
2. To identify the MBNL1 protein "interactome" during myofibroblast differentiation.

The results attained from these experiments provide deeper insight into MBNL1-regulated terminal cell differentiation during cardiac remodeling post-MI. These insights could reveal potential new avenues for therapeutically targeting cardiac fibrosis while maintaining ventricular wall integrity.

1.2 Cardiovascular Disease

1.2.1 Ischemic Heart Disease: A Global Problem

Heart disease remains the leading cause of deaths worldwide, accounting for 1 in every 4 deaths each year in the United States.[1] Ischemic heart disease is the most common type of heart disease.[2,3] Approximately 720,000 Americans have a new coronary event each year with about 335,000 patients having a recurrent event.[3] Cardiac ischemic occurs when coronary arteries are blocked and is followed almost immediately by loss of function and, within minutes, by cell death (necrosis).[2,4] This type of injury

is termed “myocardial infarction” (MI), or more commonly known as a heart attack. A MI most often occurs in the left ventricle with the blockage of the left anterior descending artery and can ultimately lead to heart failure.[2,5] There are multiple types of MI depending on the degree of coronary artery blockage.[6] For example, when the artery is blocked temporarily and then blood is allowed to re-enter the wound area, we refer to this as ischemia/reperfusion. For the purpose of this document, we will refer to a MI as a permanent occlusion of the coronary artery, unless otherwise noted.

Since the adult human heart has an extremely limited regenerative capacity, patients with chronic heart failure have a survival rate of 50% over 5 years.[3] Current treatment options include palliative small molecule drugs such as ACE inhibitors and beta blockers, ventricular assist devices, and heart transplants.[7] However, there are several limitations to these treatments as heart transplants are only available to about 1 in 1000 patients, and ventricular assist devices are complicated by risk of infection, thrombosis, and power supply.[7] Despite these limitations, advances in these treatments have allowed patients to live longer than ever before, but myocardial infarctions still have high morbidity for patients and still remains a leading cause of mortality worldwide.[3] Reshaping of the heart after MI is termed “cardiac remodeling” and is indicative of morbidity and mortality in patients.[4,8–10] However, heart failure and mortality is not correlated with the severity of the MI, but rather with the amount of fibrotic scar.[4,8–10]

Cardiac fibrosis (scarring) can be categorized into two types – reactive interstitial fibrosis or replacement fibrosis.[11,12] Aortic stenosis which causes ventricular pressure overload is modeled in animals by transverse aortic banding and is characterized by reactive interstitial fibrosis.[13,14] In animal models of acute ischemic injury such as in permanent ligation of the coronary artery or ischemia/reperfusion, the initial injury is characterized by an inflammatory response following by widespread cardiomyocyte death. Replacement fibrosis restores the necrotic area to preserve ventricular integrity and prevent wall rupture.[13] Cardiac fibrosis can also occur in ventricular volume

overload (such as from congenital malformations or pulmonary hypertension), but relatively little is known about fibrosis and the molecular mechanisms underpinning cardiac remodeling in this context.[15] These models demonstrate distinct functions of cardiac fibrosis and need to be taken into consideration when evaluating effective treatment options in heart disease patients.

However, there are currently very limited therapies on the market to treat fibrosis. A small clinical trial was conducted in 2013 to evaluate the effects of an angiotensin II (AngII) receptor inhibitor, losartan, on fibrosis in patients with non-obstructive hypertrophic cardiomyopathy.[16] Although there was a significant change in left ventricular fibrosis by assessment with cardiac magnetic resonance imaging, there was no change in cardiac function or fibrotic metabolites, such as C-terminal propeptide of type I procollagen.[16] Thus, there is still substantial work that needs to be accomplished to understand how the fibrotic scar forms after MI and provide new therapeutic avenues.

1.2.2 The Heart's Response to Myocardial Infarction

Immediately following infarct, up to 1 billion cardiomyocytes die that are replaced by scar rather than new cardiomyocytes.[17] Cardiomyocytes are the major contractile unit of the heart and constitute about 70-85% of the volume of the organ.[18] Unlike most cell types in the human body that have some level of endogenous proliferative capacity to aid in repair after injury, adult cardiomyocytes have an extremely low proliferation rate.[19–22] In fact, less than 1% of cardiomyocytes renew annually in the adult human heart.[19,22,23] Ultimately, the proliferation of existing cardiomyocytes is insufficient to restore the lost myocardial mass with functional muscle.[19,22] Instead, the natural wound healing response after MI involves the coordination of multiple cell types that function to replace the dead cardiomyocytes with a collagenous scar, which is necessary to maintain wall strength and prevent ventricular rupture.[24–28]

This natural wound healing response occurs more rapidly in rodents than in larger animals,[29] and can be explained in three phases: inflammatory, proliferation, and remodeling/scarring. During the inflammatory phase, pro-inflammatory cytokines increase in the necrotic area within hours of the initial

injury.[4,30,31] These cytokines cause an influx of immune cells such as macrophages and neutrophils to the injury site and peak in numbers between two and four days post-injury.[32] The pro-inflammatory cytokines decrease significantly 24-72 hours post-injury and anti-inflammatory mediators increase, marking the transition to the proliferative phase of cardiac repair.[4] At this time, there is a formation of granulation tissue and recruitment of cardiac fibroblasts that phenotypically convert into contractile cells, called myofibroblasts.[4] The increase in myofibroblast numbers peaks within the first week after the initial infarct event and reaches a plateau by two weeks.[33] Fibrogenic factors (such as TGFβ, collagen, fibronectin, elastin, etc.) gradually increase until the remodeling/scarring phase around four weeks post MI.[4,34–36] In the remodeling/scarring phase, cardiac tissue experiences a transition from a reparative process to extensive remodeling of the heart structure to maintain force production.[4] Progressive remodeling of the left ventricle occurs in response to increased wall stress, provoking cardiomyocyte hypertrophy in the infarct border zone and non-infarcted regions, wall thinning due to cardiomyocyte slippage and contraction of the collagenous scar, and dilation of the ventricular chambers, resulting in the reshaping of the ventricular walls from a conical structure to a more globular shape.[11,37] Four weeks after infarct, the thinned mature scar exhibits low myofibroblast and macrophage density with high collagen content.[32,38] Formation of a stable, mature collagen-based scar is associated with extracellular matrix (ECM) crosslinking, fibroblast quiescence, and vascular maturation.[36] Mature collagen fibers are highly stable with a half-life of ~100 days in normal myocardium and tend to be larger in diameter than pre-MI fibers[39]. Additionally, collagen deposition can occur in remote regions from the infarcted zone such as around the coronary arterioles which limit oxygen diffusion and further increases wall stress.[36,39] Differences in the types of fibrosis depend on the disease etiology, and fibrosis can develop in response to injuries that do not cause extensive cardiomyocyte loss. For example, pressure overload (usually caused by hypertension or aortic stenosis) results in interstitial and perivasicular fibrosis, whereas MI can cause widespread collagen deposition.[11–15]

To summarize, the formation of a fibrotic scar initially compensates for the widespread loss of functional cardiomyocytes and can be beneficial to prevent heart rupture; however, maladaptive remodeling of the heart causes extensive fibrosis and wall stiffening, leading to chronically diminished contractility.[39] However, the mechanisms that regulate the transition from the acute wound healing response to chronic cardiac remodeling are not well understood. Recent studies using various model systems have started to explain the dynamics between ECM organization, mechanical stress elicited on the heart, and growth factor signaling pathways that regulate the transition from fibroblast to differentiated myofibroblast.[30,36,40–42] It is still unclear what the contributions of each cell population in the heart are to fibrotic remodeling and how the changing fibrotic environment impacts terminal differentiation of cardiac cells. Since myofibroblasts play a central role in cardiac fibrosis and pathological remodeling post injury, in this chapter, we will discuss the conversion of cardiac fibroblasts into myofibroblasts and the signaling factors and transcriptome regulation that mediate this cellular conversion.

1.3 Cardiac Fibroblasts and Their Conversion into Myofibroblasts

1.3.1 Functional Characteristics

Cardiac fibroblasts and myofibroblasts are key cell types in the regulation of fibrotic remodeling in the heart.[43–45] It is important to note that much of the information that we know about these cell types comes from *in vitro* model systems that do not recapitulate the tissue's microenvironment after cardiac injury. We now know from recent bioengineering approaches that the fibroblast's physical surroundings influence myofibroblast cell fate. For example, increasing the stiffness or changing the topography of the culturing medium can provoke myofibroblast differentiation in the absence of any other exogenous stimuli.[46–48] Until recently, lack of a *bona fide* cell marker to specifically label cardiac fibroblast populations *in vivo* had led to conflicting data, and thus, it is still unclear which key molecular pathways and cell populations contribute to cardiac fibrosis. As a result, there is limited therapeutics to

specifically target cardiac fibroblasts (or myofibroblasts) and mitigate its pathological contribution to disease progression. In this literature review, we will emphasize what is known about the cellular biology and signaling pathways *in vivo* in regards to fibrosis.

Morphologically, fibroblasts can be identified by their flattened spindle shape, extensive rough endoplasmic reticulum, prominent Golgi apparatus, abundant cytoplasmic granular material, and lack of basement membrane.[46,49] They are also able to adhere to culture plates, which enable them to be maintained *in vitro* even when separated from their surrounding cells. Cardiac fibroblasts are typically found *in vivo* in the interstitium with every cardiomyocyte in direct contact with at least one cardiac fibroblast, and thus the location of fibroblasts in close proximity to cardiomyocytes gives optimal spatial positioning for mediating heart functions.[50] Although cardiac fibroblasts are non-excitable cells, they can form gap junctions with cardiomyocytes and are capable of synchronizing contraction of individual cardiomyocytes.[51]

Under physiological conditions in the adult heart, fibroblasts help maintain homeostasis of the ECM, which acts as a scaffold for all cardiac cell types.[52–55] Balanced synthesis and degradation of the ECM is critical for normal cardiac function, and an imbalance can result in pathological myocardial fibrosis with excessive collagen deposition.[38,56] Beyond its role in structural support, the cardiac ECM contains proteins such as TGFβ that are trapped in latent forms and then released in response to mechanical and chemical stimuli.[57–60] Secreted molecules in the ECM are produced by numerous cells including cardiac fibroblasts.[42,61,62] Similar to cellular spatial distribution, the location of growth factors and other matrix proteins in the ECM are spatially optimized to regulate cellular response and can affect cell behavior directly or indirectly through growth factor signaling cascades or mechanical forces.[63,64] Fibroblasts in uninjured, intact tissue are considered quiescent as they are mechanically shielded by crosslinked ECM. Disruption of crosslinked ECM and subsequent changes in the composition, organization, and mechanical property of the ECM causes the release of hormones, growth factors, and

cytokines which causes fibroblasts to phenotypically convert into myofibroblasts.[44,65,66] Myofibroblasts are widely found in injured organs such as the heart, skin, kidney, liver, and lungs where they also function in wound closure and structural integrity of healing scars.[67–70]

Fibroblasts undergo a progressive conversion into matured contractile myofibroblasts by first converting into a protomyofibroblast (Figure 1.1).[71] In dermal wounds, protomyofibroblasts can migrate into the wound area by formation of cytoplasmic actin stress fibers (rather than alpha smooth muscle actin (αSMA)) and small focal adhesion proteins that underlie small traction forces.[44,72] After secreting collagen and fibronectin, protomyofibroblasts align themselves along the primary stress lines in the injured tissue and begin to mature into a myofibroblast.[44,72] High levels of mechanical stress in the wound area progresses protomyofibroblasts into a myofibroblast cell state, characterized by elevated ED-A fibronectin expression, incorporation of αSMA (gene: *Acta2*) into stress fibers, and their ability to contract.[44,70,72,73] However, the protomyofibroblast has not been well defined in cardiac fibroblast differentiation *in vivo* and so it still remains unclear how the distribution of immature and mature myofibroblasts play a role in fibrotic remodeling in the heart after infarct. Fu *et al.* (2018) has started to address this question by using three different mouse lineage-tracing models to identify quiescent resident cardiac fibroblasts, newly activated cardiac fibroblasts, and myofibroblasts.[74] They showed that all three of these populations proliferate within the first week of injury and persist up to 2 months post MI despite proliferation decreasing after 1 week. Notably, myofibroblasts lose αSMA expression over time but remain in the infarct area while the scar matures. The authors of this study termed these cells "matrifibrocytes" as they were genetically distinct from other cells including myofibroblasts after extensive analysis of 5,000 differentially expressed and clustered genes.[74] This study suggests that fibroblasts proliferate and mature to express αSMA after MI, and these cells continue to mature during cardiac remodeling even with a loss of αSMA.

Incorporation of αSMA into stress fibers augments the contractile activity of matured myofibroblasts. These cells contract by developing mature adhesion junctions made of cadherins that are linked to intracellular stress fibers which allows the cell to anchor and confer mechanical tension to the remodeling matrix.[44,45,66,72] In addition to contractile properties, myofibroblasts secrete large amounts of ECM proteins such as glycosaminoglycans, laminin, proteoglycans, periostin, collagen I and III, fibronectin, and fibronectin ED-A isoform, arranged in successive layers of organization.[36,39,44,65]

Cardiac myofibroblasts can persist for an extended duration after initial activation.[56] After the second week post-injury the number of myofibroblasts decrease, but there are still a small number of cells present long-term after injury.[75] In the rat, myofibroblasts have been found six month after MI.[76] In post-mortem human myocardium, myofibroblasts have been found months and even years after MI.[56,77] However, it is still currently unknown how the population of myofibroblasts diminishes over time.

For a long time, it was believed that myofibroblasts undergo apoptosis upon completion of tissue repair.[45,71,78] It was also thought that myofibroblasts could not revert back to a fibroblast phenotype after TGFβ treatment in culture.[79] Although culturing cardiac fibroblasts on tissue culture plastic can mechanically activate them to convert into a myofibroblast cell fate, some studies show culturing differentiated myofibroblasts *in vitro* on soft substrates that more closely mimic healthy tissue causes a partial reversion to a quiescent mesenchymal state.[47,80,81] For example, when valvular fibroblasts are cultured on stiff substrates, they express αSMA stress fibers, but light-mediated reduction in substrate modulus results in a loss of αSMA stress fibers and a reduction of *Acta2* and *Ctgf* gene expression.[47]

Additionally, with new tools available and further insight into fibroblast functions, researchers now conclude that myofibroblasts have the capacity to revert to a quiescent fibroblast in multiple organ systems *in vivo*.[82–87] Sulforaphane treatment reduces αSMA, Col1a1, and Col1a2 protein expression, blocks collagen contraction in culture, and reverts myofibroblasts to thin, spindle-shaped morphology in

fibroblasts isolated from idiopathic pulmonary fibrosis patients or cells treated with TGFβ.[84] Myofibroblast dedifferentiation in lung fibroblasts was confirmed in another study showing TGFβ-treated fetal and adult lung fibroblasts had reduced αSMA and Col1a1 protein and gene expression after prostaglandin E_2 treatment.[83] The dedifferentiation of lung myofibroblasts could be through a non-canonical ERK/MAPK/MyoD dependent mechanism, but this not been tested *in vivo.*[82] Using a *Col1a2-cre* and *Vimentin-cre* lineage tracing mouse models, Kisseleva *et al.*(2012) and Troeger *et al.* (2012) showed after cessation of carbon tetrachloride insult, liver myofibroblasts can revert back to a fibroblast-like cell state that is phenotypically similar but genetically distinct from quiescent hepatic stellate cells and downregulate αSMA protein expression as well as fibrogenic genes such as *Col1a1, Acta2, Tgfbr1, Smad7,* and *Timp1*.[86,88] In the heart, Kanisicak *et al.* (2016) promoted myofibroblast transformation in *Postn-GFP*+ cells with AngII and phenylephrine (PE) for two weeks and showed cessation of AngII/PE infusion resulted in reversion of these cells back towards quiescence. After two weeks following cessation, *Postn-GFP*+ cells were still present but they lacked αSMA protein expression *in vivo*. Furthermore, the reverted cells showed an increased in *Tcf21* and *Pdgfrα* gene expression as well as downregulation of *Acta2, Col1a1, Fn, Fibrillin, Mfap2, and Cthrc1* gene expression, consistent with a quiescent phenotype.[87] Although these studies have confirmed myofibroblasts can revert to quiescence, they have also uncovered more unanswered questions. Why do *Postn*+ cells remain in the infarct zone even with the regression of fibrotic gene expression and αSMA protein production? Can myofibroblasts revert back to a quiescent cell state after acute ischemic injury such as permanent coronary artery ligation? Fu *et al.* (2018) suggests αSMA+ cells subside after MI, but a more mature matrifibrocyte cell type remains.[74] Since reverted myofibroblasts have a higher responsiveness to recurring fibrogenic stimulation and are more prone to activation,[47,83,86,88] can reverted myofibroblasts be maintained in a quiescent cell state? Would eliminating myofibroblast populations affect the integrity of the scar? Fu *et al.* (2018) attempted to address this in a cryoinjury model and showed diphtheria toxin

ablation of *Acta2* lineage-traced matrifibrocytes resulted in reduced collagen content and organization; however, this still needs to be evaluated in the context of MI and other cell populations. It is obvious more work needs to be completed to understand phenotypic conversion of cardiac myofibroblasts back into a quiescent state *in vivo* after cardiac injury.

1.3.2 Cardiac Fibroblast and Myofibroblast Cellular Heterogeneity

A clear understanding of the fibroblast lineage and how fibroblast populations react to injury would provide a basis to investigate anti-fibrotic strategies to target these populations. As discussed in the next section, several research groups have suggested that fibroblast and myofibroblast populations are heterogeneous and might react differently in variable cardiac fibrotic models to contribute to pathological remodeling (Figure 1.1).

1.3.2.1 Fibroblast Origins

Fibroblasts are developmentally derived from two main areas in the heart: the endocardium and the epicardium.[19,89–93] Recent lineage tracing approaches have revealed that the majority of fibroblasts originate from the epicardium during development soon after the heart has looped.[89,91,93] Specifically, over 80% of residing adult fibroblasts were labeled with the epicardial lineage marker Wilms tumor 1 (*Wt1-cre*) or T-box 18 (*Tbx18-cre*), whereas ~20% were labeled with the endocardial lineage marker *Tie2-cre* or Nuclear Factor of Activated T-Cells (*Nfatc1-cre*). [91,94] Another subset of fibroblasts originates from Paired Box 2 (*Pax3-cre*) labelled cells and was found in the outflow tract region of the heart during development. These *Pax3*+ cells are derived from neural crest cells and reside in the right atrium.[90,94]

Furthermore, in addition to *Wt1* and *Tbx18*, we now know the majority of epicardial-derived embryonic cardiac fibroblasts express platelet-derived growth factor receptor alpha (*Pdgfrα*), transcription factor 21 (*Tcf21*), and thymus cell antigen 1 (*Thy1*).[89,93–95] In the absence of *Tcf21* or *Pdgfrα*, there is a lack of Thy1+ fibroblasts and expression of ECM components (such as *Col1a1, Col3a1, Ctgf,*

Col6a1, Ddr2, Postn) as well as Postn protein expression in the left ventricle, but it is unclear if these same genes impact the development of endocardial-derived or neural crest-derived fibroblast populations.[89,93] However, other fibroblasts sources do not seem to compensate for the loss of fibroblasts since adult *Tcf21* and *Pdgfrα* knockout mice continue to lack perivascular collagen content and ECM proteins into adulthood, although these mice still are able to form vascular smooth muscle cells.[89,93] *Thy1*+ cardiac fibroblasts were negative for other cell markers (CD45, CD31, CD11b, and Ter119), had fibrotic gene markers (*Col1a1* and *Ddr2*), retained mesenchymal morphology, and expressed αSMA+ stress fibers after TGFβ treatment in culture.[94] This suggests that the majority of resident cardiac fibroblasts in the heart arise from *Thy1, Wt1, Tbx18, Tcf21,* and *Pdgfrα* mesenchymal lineages.

1.3.2.2 Fibroblast Response to Injury

Recent studies show that cardiac fibroblasts from distinct lineages (i.e. from *Wt1*-cre and *Tie2*-cre mouse lines) in the heart do not change in anatomical distribution or ratio of cell contribution and have similar gene expression profiles and phenotypes after pressure overload injury.[91,94] These studies suggest that although the populations may be derived from diverse origins, they stimulate similar gene programs during the injury response.

However, some *in vivo* studies suggest that other cell types differentiate into myofibroblasts from various sources such as pericytes, circulating fibrocytes from bone marrow, or through endothelial-to-mesenchymal transition (EndoMT) or epithelial-to-mesenchymal transition (EMT). However, these studies relied on insufficient fibroblast markers such as fibroblast specific protein 1 (FSP1) which has been shown to also label hematopoietic cells, endothelial cells, and vascular smooth muscle cells.[89,96–101] Other independent labs have since confirmed that these sources give rise to a negligible amount of myofibroblasts after pressure overload injury.[91,93,102] Using a *Vav-cre* mouse line, Moore-Morris *et al.* (2014) did not find any of these cells to co-label with *Col1a1-GFP* after aortic banding, suggesting that

reactive fibroblasts do not arise from a blood lineage. They also used *VE-cadherin-cre* (endothelial) and tamoxifen-inducible *Wt1-cre* and *Tbx18-cre* mouse lines to show EndoMT and EMT did not contribute to *Col1a1*+ cells after transverse aortic constriction (TAC). [91] These results were also confirmed by transplantation of hematopoietic stem cells labeled with RFP and bone marrow stromal cells labeled with GFP in which GFP+ and RFP+ cells were not present in fibroblast populations after TAC.[94] Furthermore, a parabiosis study showed fibrocytes can migrate into the wound area after pressure overload but do not differentiate into myofibroblasts.[94] However, it is unclear if these cell sources contribute to myofibroblast populations after myocardial infarction.

Importantly, *Tcf21*+ resident cardiac fibroblasts migrate to and populate areas of fibrosis in the injured adult mouse heart.[95] *Wt1*+ and *Tbx18*+ epicardial derived fibroblasts can also give rise to a large percentage of the total fibroblasts in the left ventricle of a failing mouse heart after pressure overload and co-label with *Col1a1*, but they rarely become αSMA+.[91,94] However, epicardial and interstitial fibrosis after ischemia/reperfusion injury in mouse hearts and human hypertensive hearts show expression of *Tcf21, Wt1,* and *Tbx18.*[95] Additionally, Kanisicak *et al.* (2016) developed a tamoxifen-inducible *Postn* knock-in mouse line and used lineage tracing to show that the *Postn* genetic locus specifically labels essentially all cardiac myofibroblasts that arise from *Tcf21*+ cardiac fibroblasts [87,93]. Since all of these markers define resident cardiac fibroblasts, these data suggest that resident cardiac fibroblasts, rather than fibroblasts from circulating bone marrow cells or fibroblasts from resident endothelial cells, are the major cell type that infiltrate the wound site and give rise to myofibroblasts in injury models.[87,91,94]

On the other hand, in models of chemically-induced fibrosis, *Gli1*+ resident perivascular cells express αSMA protein in the heart, lung, liver, and kidney microvasculature and form αSMA+ stress fibers *in vitro,* suggesting they adopt a myofibroblast fate.[103] Cell-specific genetic ablation of *Gli1* substantially reduced fibrosis in the heart and kidney and improved left ventricular systolic function. However, some αSMA+ myofibroblasts still appeared, suggesting a heterogenous lineage for the

myofibroblast population.[103] Although this has not been recapitulated in a MI model, this study suggests that other cell populations could mediate the fibrotic response. The physiologic role of pericytes versus resident cardiac fibroblasts in regulating acute and chronic cardiac fibrosis still needs to be identified.

Nonetheless, how genetic heterogeneity affects myofibroblast function is still an area of open investigation and needs to be studied in multiple cardiac injury contexts *in vivo*. It is also currently unknown whether all fibroblast populations contribute to the fibrotic response as the type of cardiac injury might induce different populations of cells to become myofibroblasts (Figure 1.1).[95] As such, myofibroblasts derived from different cell sources could have different contributions to fibrosis.

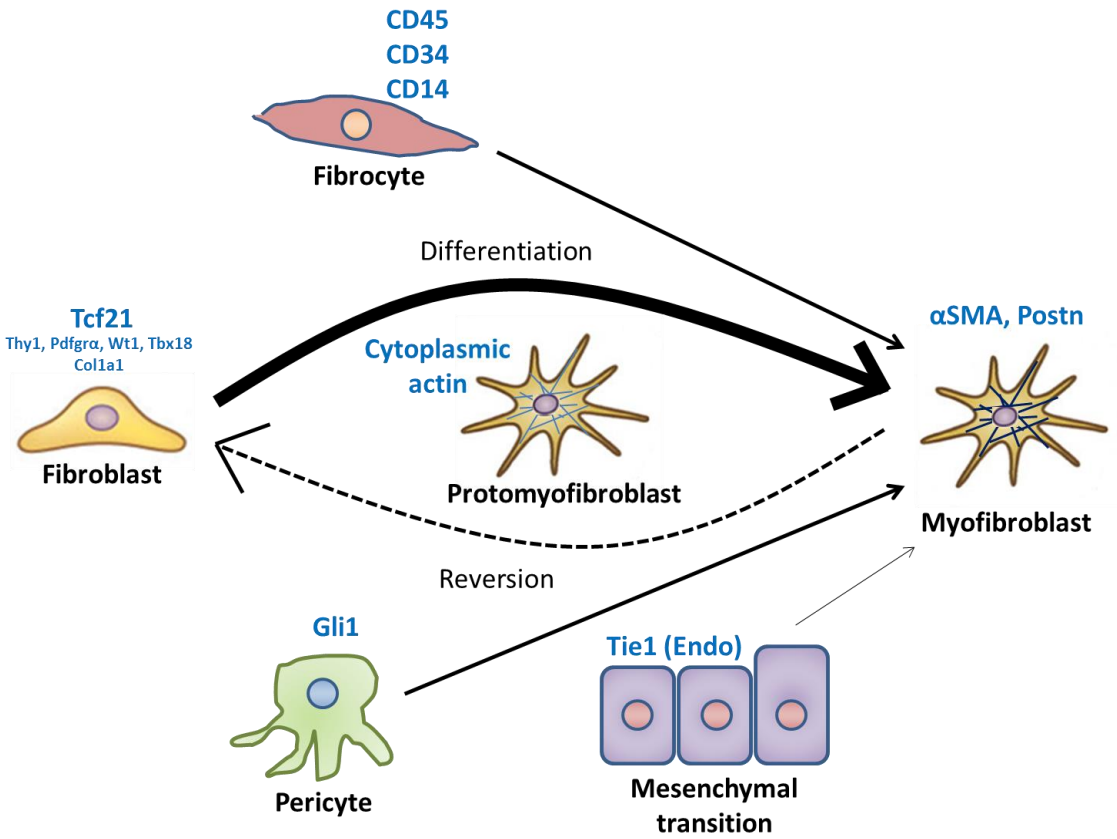

Figure 1.1. Myofibroblast cell sources.
Fibroblasts undergo a progressive conversion into myofibroblasts by first converting into protomyofibroblasts that express cytoplasmic actins (light blue lines). Mature myofibroblasts are characterized by prominent αSMA+ stress fibers (dark blue lines). *Tcf21*+ resident cardiac fibroblasts give rise to the majority of myofibroblasts that secrete collagen (Co1a1) and periostin (Postn). Resident cardiac fibroblasts also express *Thy1, Pdgfrα*, *Wt1,* and/or *Tbx18* although these markers vary depending on type of cardiac injury. CD45+/CD34+/CD14+ hematopoietic circulating fibrocytes and *Gli1*+ pericytes can contribute to myofibroblast population after ischemic/reperfusion injury. Pressure overload can cause a small percentage of

cells to undergo endothelial or epithelial to mesenchymal transition and form myofibroblasts. Image adapted from Stempien-Otero et al. (2016) *JMCC.*[104]

1.3.2.3 Markers for Fibroblasts and Myofibroblasts

In the fibroblast biology field, there has historically been a lack of consensus in defining a specific fibroblast marker. Some of the more classic markers used in numerous *in vitro* and *in vivo* studies include *Vimentin, Thy1, Fsp1, Ddr2, Tcf21, Pdgfrα,* and *Col1a1*. Although these factors are expressed in fibroblasts, most of them are also expressed in numerous other cell types [87,91,99,105–107]. For example, although *Pdgfrα* is strongly expressed in fibroblasts, it is also detected in endothelial cells and cardiomyocytes in the adult heart, suggesting it is not a suitable marker for specifically marking adult fibroblast populations [89–91,94,107]. Of the markers noted above, only *Tcf21* contributes to the resident adult cardiac fibroblasts.[93] Using the information gathered from these studies, our lab uses *Tcf21* as a specific marker for resident cardiac fibroblasts.

Furthermore, understanding which precursor cell type gives rise to myofibroblasts after injury is confounded by the fact that there is limited knowledge of the molecular markers that define myofibroblast populations.[42] *In vitro,* myofibroblasts are routinely defined by their morphologic, contractile, and ECM secreting properties. Morphologically, myofibroblasts are broad, flattened cells that can have protruding dendritic processes. The term myofibroblast was originally used to describe a cell with morphological characteristics of both smooth muscle cells ("myo-") and fibroblasts during skin wound healing.[108] However, defining cardiac myofibroblast populations by morphology alone, without a specific fibroblast marker, makes it difficult to discern these cells *in vivo.*

To date, αSMA and Postn are used as the most reliable markers for myofibroblasts.[73,87,109,110] Postn is a secreted matricellular protein involved in cellular adhesion and collagen organization that is not found in the majority of quiescent fibroblasts or other cells such as endothelial cells or vascular smooth muscle cells.[64,87,101,111–113] In fact, only ~10% of quiescent cardiac fibroblasts express *Postn*, but this percentage increases significantly after MI and *Postn*-positive cells are mainly detected in the injury

site, suggesting it may be a good marker for myofibroblasts, but not quiescent fibroblasts, *in vivo.*[101,102,109] TGFβ treatment in cultured fibroblasts and cardiomyocytes results in an upregulation of Postn expression specific to cardiac fibroblasts.[113,114] *Postn* is upregulated before and during cardiac remodeling following infarction and pressure overload and correlates with the amount of collagen produced, suggesting it plays a key role in fibrotic remodeling.[115] Notably, global deletion of the *Postn* gene in mice disrupts cardiac fibroblast function and causes a reduction of fibrosis after infarction (and in pressure overload) and subsequent ventricular wall rupture due to a defect in the formation of a protective scar.[112,115] When *Postn* is depleted after the initial infarct, mice have reduced cardiac fibrosis without compromising scar stability and systolic cardiac function is improved compared to littermate controls.[111] Thus, genetic manipulation of *Postn* provides a useful tool for probing myofibroblast differentiation and cardiac remodeling.

1.4 Signaling Pathways that Regulate Myofibroblast Differentiation

Researchers are still trying to understand how extracellular signals in the wound area transduce into intracellular cues for fibroblast differentiation into myofibroblasts and persistence of myofibroblasts in pathological remodeling. Growing evidence suggests agents that regulate the functional responses of cardiac fibroblasts after injury operate through intracellular signaling cascades that converge at the transcriptional level to coordinate gene programs. Some of these signaling pathways include beta-adrenergic receptor (β-AR), AngII, endothelin-1 (ET-1), transient receptor potential channels (TRP), integrins, tumor necrosis factor alpha (TNFα), TGFβ, norepinephrine (NA), among many others including mechanical stretch.[39,42,62,104,116,117] There is great scientific interest in the modification of these signaling pathways as they provide a plethora of potentially novel therapeutics strategies.[39,62,116–118] The subsections below will review our current knowledge of the more well-characterized signaling pathways that promote myofibroblast differentiation and are more pertinent to our research as MBNL1 directly regulates these pathways.[69]

1.4.1 TGFβ Signaling

Transforming growth factor β1 (TGFβ) is a secreted protein expressed by mesenchymal cells, macrophages, monocytes, and resident cardiac fibroblasts and acts as a potent mediator of cardiac fibrotic remodeling and universal myofibroblast differentiation from fibroblasts derived from multiple tissues.[43,117,119–125] Under physiological conditions, latent TGFβ is chemically bound and trapped in the ECM, but mechanical liberation and enzymatic cleavage events release biologically active TGFβ which acts on fibroblasts to promote differentiation into myofibroblasts.[44,59,126,127] Perpetual canonical TGFβ signaling results in the persistence of myofibroblasts in the injury site, and TGFβ prevents cardiac fibroblast apoptosis after ischemia reperfusion injury.[128]

In canonical TGFβ signaling, TGFβ binds to its cell surface receptor, a heterodimer of TGFβ receptor type I (TGFβR1) and II (TGFβR2), and in turn, phosphorylates SMAD2/3 which promotes interaction with SMAD4 and subsequent translocation into the nucleus for transcriptional induction of matrix genes, such as *Col1a1, Col1a2, Col3a1, Col5a2, Col6a1, Col6a3, Fn, TnC, and Timp-1*.[129–131] SMAD6/7 promote TGFβR1 degradation and inhibit canonical TGFβ signaling by competing with SMAD2/3.[132] Canonical TGFβ signaling is upregulated in skin,[133] lung,[134–136] liver,[137] and kidney[138,139] fibrosis animal models, suggesting TGFβ signaling plays a global role in promoting fibrosis in multiple organ systems. In fact, studies using *Smad3* loss of function mouse models show *Smad3* depletion protects against fibrosis in the eye[140] and chemically-induced fibrosis in the kidney[141] and vasculature.[142]

In the mouse heart, there is an increase in phosphorylated SMAD2 protein expression after ischemic reperfusion, suggesting a promotion of TGFβ signaling activation.[143] However, *Smad2* knockout mice are embryonic lethal so studies of this gene has been limited.[144] Data from *Smad3* knockout mice show a decrease in αSMA+ myofibroblasts *in vivo* and reduced αSMA protein expression and myofibroblast contractile function *in vitro* compared to wildtype mice.[125,133] After coronary artery ischemic reperfusion, *Smad3* deletion protects against diastolic dysfunction and remodeling, and *Smad3*

null mice had reduced collagen deposition compared to wildtype mice despite an increase in the number of myofibroblasts and TGFβ-responsive genes *Acta2, Col1a1, Col3a1,* and *Fn* during the first week following injury.[125,131,143,145] Additionally, myofibroblasts from *Smad3* deficit mice fail to form αSMA stress fibers, migrate, and contract collagen *in vitro,* and the αSMA promoter contains SMAD3 binding sites,[125] suggesting canonical TGFβ signaling regulates the contractile function of myofibroblasts. Furthermore, overexpression of inhibitory SMAD6/7 failed to block TGFβ-mediated αSMA stress fiber formation *in vitro*.[119] These studies suggest that SMAD3 is necessary for ECM formation and subsequent fibrotic remodeling but not myofibroblast differentiation. When *Tgfbr1/2, Smad3,* or *Smad2/3* (but not *Smad2*) was genetically removed specifically in *Tcf21+* and *Postn+* cardiac fibroblasts, a reduction of myofibroblast differentiation and cardiac fibrosis was also observed following pressure overload, addition of TGFβ ligand, or transgenic overexpression of *Tgfβ*. However, this was not observed when *Smad2/3* was deleted in cardiomyocytes, providing evidence that *Smad2/3* effects on fibrosis are specific to the cardiac fibroblast.[133]

Targeting TGFβ signaling factors upstream of SMAD proteins had more significant effects on fibrosis and cardiac remodeling. For example, genetic deletion of *Tgfbr1/2* in *Postn+* cardiac fibroblasts or *αMhc+* cardiomyocytes had reduced cardiac fibrosis and fibrotic gene expression, preserved systolic and diastolic function, and less cardiac hypertrophy following pressure overload compared to littermate controls.[133] Knockdown of TGFβR1 *in vitro* also blocked TGFβ-mediated myofibroblast transformation.[119] This added effect could be due to the fact that TGFβR1/2 lie upstream of both canonical and non-canonical TGFβ signaling. Additionally, the fact that inhibition of SMAD signaling does not completely attenuate the fibrotic response and evidence of interplay between SMAD signaling and other signaling pathways suggest multiple signaling pathways converge to promote fibrotic remodeling after cardiac injury.[125,129,143,146] A prime example is crosstalk between GSK3β signaling and SMAD3 in which genetic

deletion of *Gsk3β* in cardiac fibroblasts activated TGFβ/SMAD3 signaling and promoted fibrosis after MI.[146]

Non-canonical TGFβ signaling also plays a crucial role in myofibroblast differentiation and cardiac remodeling.[117,119] TGFβ can act via non-canonical signaling primarily through TGFβR2[147–150] by recruiting TGFβ activated kinase (TAK1) and TAK1 binding protein (TAB) to activate a mitogen-activated protein kinase (MAPK) signaling cascade with downstream targets such as c-Jun N-terminal kinase (JNK) and p38 kinase.[42,151] Koitabashi *et al.,* showed induced genetic knockdown of *Tgfbr2* functionally inhibited non-canonical TGFβ signaling and reduced cardiac fibrosis and remodeling after pressure overload compared to littermates.[147] In contrast, TAK1 protein expression is normally low in the adult mouse heart, but upon transgenic activation of *Tak1* in cardiomyocytes, mice experience cardiac hypertrophy, interstitial fibrosis, and impairment of systolic and diastolic function.[152] However, the role of TAK1 in cardiac fibroblasts has not been directly tested. Transgenic overexpression of MAPK Kinases 3 and 6 (*Mkk3* and *Mkk6*), which act downstream of TAK1, results in interstitial fibrosis and premature death but with no signs of cardiac hypertrophy, although mice did have enlarged atria and indicators of dilated cardiomyopathy.[153] However, this study was performed in a cardiomyocyte-specific mouse model, and thus the increase in fibrosis is an indirect reaction to changes in cardiomyocyte function. MKK3/6 activation induces fibrosis by increasing αSMA transcriptional activity and αSMA+ stress fibers in fibroblasts.[119] Downstream of MKK3/6, the mitogen-activated protein kinase p38α, which is encoded by the *Mapk14* gene, is upregulated during the cardiac injury response.[154] Loss of *Mapk14* blocks cardiac fibroblast differentiation into myofibroblasts and attenuates fibrosis after ischemia reperfusion injury or with addition of neuroendocrine agonists.[154] Transgenic mouse models expressing dominant negative mutants of MKK3, MKK6, and p38α have greater cardiac hypertrophy, resistance to fibrosis, and increased *Nfat* transcriptional activity after pressure overload than littermate controls.[155,156] However, these studies were performed in cardiomyocyte-specific transgenic mouse models, so the fibrotic

phenotype observed is likely secondary to cardiomyocyte dysfunction. Collectively, these data provide evidence that both canonical and non-canonical TGFβ signaling regulates myofibroblast contractility, ECM secretion, and cardiac remodeling, but components of these molecular pathways might control distinctive myofibroblast functions. Targeting one branch of TGFβ signaling for antifibrotic therapies might improve the ineffectiveness of current treatments that globally inhibit TGFβ signaling.[157] However, the differential effects in *Tak1* vs. *Mkk3/6* and *p38α* transgenic models suggest TAK1 may regulate other signaling branches such as IκB kinase,[158] thus it is important to understand how other pathways and their interactions regulate myofibroblast differentiation and the fibrotic response.

1.4.2 TRP Channel Ca^{2+} Signaling

Myofibroblast differentiation is also associated with Ca^{2+} influx via TRP, calcineurin, and NFAT signaling pathways.[42] There are several TRP channels that comprise a superfamily consisting of canonical (TRPC), melastatin (TRPM), vanilloid (TRPV), polycystin (TRPP), ankyrin (TRPA), and mucolipin (TRPML) channels.[159] TRP channels are activated by mechanical stretch and allow non-specific entry of cations such as Ca^{2+}, Mg^{2+}, and Na^{+} into the cell.[159] TRPM7, TRPC3, TRPC6, and TRPV4 are all involved myofibroblasts differentiation, but TRPM7 and TRPC3 seem to be specific to atrial fibroblasts whereas TRPC6 and TRPV4 function in ventricular fibroblast differentiation.[119,160–163] For example, Du *et al.* showed TRPM7 protein expression, endogenous currents, and calcium influx are upregulated in atrial fibroblasts isolated from atrial fibrillation patients, and this is specific to TRPM7 and not TRPC1, TRPC6, TRPV2, or TRPV4 channels. They also demonstrated fibroblasts from atrial fibrillation patients have an increased propensity for myofibroblasts differentiation without TGFβ treatment, and this effect is eliminated with shRNA knockdown of *Trpm7*. TGFβ increases TRPM7 protein expression and activity and is correlated with increased myofibroblast differentiation from human atrial fibroblasts *in vitro*, suggesting TGFβ regulates TRPM7 expression and activity.[161] Harada *et al.* showed TRPC3 is also

necessary for atrial fibroblast differentiation by causing calcium influx and NFAT-mediated downregulation of microRNA-26.[164]

TRPV4 is a mechanosensitive ion channel that mediates myofibroblast differentiation via integration of mechanical signals.[160] Specifically, knockdown of *Trpv4* using siRNA or a small molecule antagonist blocks Ca^{2+} influx as well as TGFβ and tension-dependent myofibroblast differentiation.[160] The authors of this study speculate that increased ECM stiffness and cell contraction could activate integrins that release latent TGFβ to form a positive mechanical feedback loop that promotes myofibroblast differentiation. This idea is supported by a study showing TRPV4 is required for tension-induced integrin signaling.[165] In a lung model, TRPV4 channel activity is upregulated in lung fibroblasts plated on stiff matrices as well as in lung fibroblasts derived from idiopathic pulmonary fibrosis patients.[166] This study showed TRPV4 activity potentiates TGFβ-dependent myofibroblast differentiation via actomyosin remodeling and nuclear localization of MRTF-A.[166] However, TRPV4 mechanisms have not been directly tested in the heart *in vivo*.

TRPC6 was discovered as a myofibroblast differentiation regulator in a genome-wide screen.[119] Adenoviral overexpression of *Trpc6* promotes myofibroblast differentiation *in vitro* in both cardiac and dermal fibroblasts.[119] TGFβ preferentially increased *Trpc6* gene expression over other canonical TRP channels such as *Trpc1, Trpc3, and Trpc4,* and αSMA stress fiber formation and contractile activity was also specific for adenoviral overexpression of *Trpc6*. Furthermore, *Trpc6* genetic deletion in mice blocked TGFβ- and AngII-mediated myofibroblast differentiation, indicating that *Trpc6* is both necessary and sufficient for fibroblast transformation into myofibroblasts [119]. Mechanically, TGFβ and AngII increase *Trpc6* gene expression through a p38 MAPK/SRF-dependent activation of the *Trpc6* promoter.[119] TRPC6 also propagates Ca^{2+} signaling through calcineurin signaling via NFAT and functions to induce αSMA incorporation into stress fibers *in vitro*.[119] Although SRF can directly regulate *Trpc6* expression, active calcineurin and *Trpc6* overexpression can rescue the loss of SRF to promote

myofibroblast differentiation, suggesting that NFAT and SRF can function in parallel to induce myofibroblast transformation.[119] This was the first study to show a comprehensive mechanism for the role of the TRPC6 channel in myofibroblast differentiation.

TRPC6 plays a crucial role in wound healing and cardiac fibrosis and remodeling. Genetic ablation of *Trpc6* in mice results in the failure to close dermal wounds and ventricular wall rupture after permanent coronary artery occlusion due to a decrease in myofibroblast numbers and a reduction in scar formation.[119] Further confirmation of the TRPC6/calcineurin/NFAT signaling pathway in wound healing was observed *in vivo* as adenovirus delivery of constitutively active calcineurin was able to rescue the defective dermal wound closure in *Trpc6* knockout mice.[119]

The studies illustrated above also suggest calcium signaling is a key effector in myofibroblast differentiation. For example, overexpression of calcineurin promotes cardiac fibroblasts to differentiate into myofibroblasts, and genetic deletion of calcineurin or pharmacological inhibition of calcineurin signaling blocks TRPC6-mediated myofibroblast differentiation, ECM production, and αSMA transcriptional activity.[119,167–169] This suggests that TRPC6 mediates myofibroblast differentiation through calcineurin signaling. Calcineurin is also required for TGFβ-mediated accumulation of ECM proteins fibronectin and collagen type IV in mesangial cells.[168] Calcineurin involvement in myofibroblast differentiation is corroborated in a study showing expression of a constitutively active variant of calcineurin promotes αSMA stress fiber formation and functional contraction of collagen.[119] Additionally, mechanical stretch can increase the expression of myofibroblast genes, such as *Col1α1, Col1α3, Fn,* and *Actα2,* through calcineurin-NFAT pathways, and αSMA stress fibers can form in the absence of TGFβ release from the ECM.[169,170]

These studies are further supported in myofibroblasts from other tissue compartments. For example, Ca^{2+} influx and ensuing cell contraction is observed in hepatic myofibroblast-like cells *in vitro* and *in vivo* from cells isolated from rats with chemically-induced liver injury.[171,172] Ca^{2+} influx is also

strongly correlated with gut myofibroblast proliferation and migration.[173,174] Extracellular calcium is also necessary for TGFβ-mediated myofibroblast differentiation from lung fibroblasts.[166] Finally, NFAT is required for pulmonary myofibroblast contraction.[175] These studies suggest Ca^{2+}/calcineurin/NFAT signaling could provide potential avenues for therapeutics not only in treating cardiac fibrosis but also fibrosis in other organ systems.

1.4.3 SRF Signaling

Fibroblasts physically interact with the extracellular environment to allow for integration of mechanical and chemical inputs into transcriptional events. Serum response factor (SRF) is a transcription factor involved in smooth muscle cell differentiation and contractile properties of myofibroblasts by binding to CArG box elements located near transcriptional start sites in genes such as *Myh11, Acta2, Col1a1,*and *Col1a2* among others.[176–178] SRF functions downstream of TGFβ and AngII signaling.[42] These extracellular ligands bind to TGFβRs and G-protein coupled receptors (GPCRs), respectively, to activate Rho GTPases such as RhoA and RhoB.[179,180] Upon activation, Rho GTPases induce Rho assisted kinase (ROCK) or mDia to polymerize F-actin and deplete the pool of free G-actin monomers. G-actin is normally bound to members of the related transcription factor family (MRTF) consisting of MRTF-A and MRTF-B and maintain MRTFs in the cytosol, but upon actin polymerization, MRTFs can translocate to the nucleus where they bind with SRF to stimulate target gene expression.[181–187] Since SRF target genes encode structural components of the cytoskeleton (such as actin) and regulators of actin dynamics (such as vinculin), MRTF/SRF signaling through cytoskeleton reorganization initiates such events as cellular migration, adhesion, and contraction.[188]

Reorganization of actin cytoskeleton into stress fibers and induction of myofibroblast gene expression is directly linked to SRF signaling.[104,189] ROCK inhibition via small molecules or siRNA in lung, skin, and cardiac fibroblasts blocks TGFβ-dependent stress fiber formation and expression of ECM genes and proteins such as Col1a1, Col1a2, and Fn. Studies *in vitro* show myofibroblast differentiation is

stimulated by overexpression of MRTF-A.[170,187,190] In contrast, loss of *Mrtfa* by expression of a dominant negative isoform, shRNA targeting, or genetic deletion in lung fibroblasts disrupts myofibroblast differentiation and collagen synthesis.[170,187,191] Global loss of *Mrtfb* is embryonic lethal and has not been tested for its role in myofibroblast differentiation.[192,193] Bleomycin insult in lung tissue results in an accumulation of SRF in myofibroblast nuclei.[194] Adenoviral overexpression of SRF in lung and cardiac fibroblasts promotes αSMA protein expression and stress fiber formation.[119,189,194] Furthermore, myofibroblast differentiation *in vitro* with TGFβ or AngII can be inhibited using adenoviral overexpression of a short hairpin RNA (shRNA) directed at SRF, suggesting SRF plays a key regulatory role in the myofibroblast gene program and potentially in the fibrotic injury response.[119,189,194,195]

In fact, several studies show a direct role of Rho GTPase/MRTF/SRF signaling in fibrotic remodeling. In the chick, C3 transferase enzymatic inhibition of endogenous Rho prevents the assembly of actin and results in a failure to close dermal wounds.[196] *Rock1* knockout mice fail to form myofibroblasts *in vivo* and (compared to wildtype mice) show a decrease in fibrosis after ischemia/reperfusion with preserved cardiac function comparable to sham mice.[197] Global *Mrtfa* deletion results in reduced fibrosis and ECM and contractile gene expression (*Col1a1, Col3a1, Elastin,* and *Acta2*) following MI.[187] Notably, targeted deletion of *Srf* in *Tcf21*+ cardiac fibroblasts resulted in heart rupture after permanent coronary artery ligation due to a reduction in protective fibrosis and delayed wound closure in Postn+ dermal fibroblasts.[69] These studies provide evidence that SRF is a critical transcription factor during myofibroblast differentiation and fibrotic remodeling.

Mechanical tension can also signal SRF in the absence of chemical ligands. As stated previously, culturing fibroblasts on stiff surfaces can promote myofibroblast differentiation and is likely mediated through Rho GTPase/MRTF/SRF signaling as a stiffer modulus promotes translocation of MRTF-A into the nucleus.[170,198–200] Direct mechanical manipulation using collagen-coated magnetic beads attached to β1 integrins on human gingival fibroblasts resulted in myofibroblast transformation, and siRNA

knockdown of *Mrtfa* or mDia or small molecule inhibition of ROCK blocked mechanically-induced αSMA promoter activity, protein expression, and stress fibers as well as contractile function.[170,201] In contrast, stabilization of filamentous actin by jasplakinolide stimulates αSMA protein and gene expression in the absence of any ligand, suggesting mechanical forces can directly activate transcriptional programs. This is recapitulated *in vivo* as liver, lung, and heart tissues increase in stiffness over time after injury, suggesting mechanical forces could promote a positive feedback loop that extends myofibroblast activity and fibrosis.[4,41,126,202,203] An elevated level of stiffness after injury also maintains TGFβ in its active state, which reinforces the differentiation signal.[59,81,104,126,127,204]

However, the timing of signaling activation can vastly change how organs respond to injury. For example, Sandbo *et al.* (2011) demonstrated in human pulmonary fibroblasts that ROCK inhibition with a small molecule or actin depolymerization with latrunculin B blocked TGFβ-induced SRF activation and αSMA gene and protein expression but had no effect on phosphorylated SMAD2 protein expression.[205] To further this notion, TGFβ-dependent gene expression of Rho/MRTF/SRF signaling factors precedes activation of ROCK and formation of αSMA stress as cycloheximide (a translational inhibitor) prevents stress fiber formation without affecting SMAD-dependent *Pai1* gene transcription.[69,119,205–208] This could possibly explain why *Mrtfα* knockout mouse hearts do not rupture following permanent coronary artery ligation, but does not explain why *Srf* knockout in TCF21+ cells results in heart rupture by the same means.[69,187] Global deletion of *Mrtfb* or *Srf* is embryonic lethal, suggesting *Mrtfa* knockout mice could experience some aspect of functional compensation.[192,193,209] Georges *et al.* (2007) noted tissue stiffness and an increase in αSMA myofibroblast numbers in the liver precedes matrix deposition, suggesting a temporal regulation in fibrotic remodeling.[202] This is also true in the heart as the initial stages of the injury response involves formation of a provisional matrix before collagen cross-linking.[44,66,126,127]

Taken together, these studies highlight that multiple signaling pathways promote and are critical for the differentiation of fibroblasts in myofibroblasts (Figure 1.2). In fact, SRF signaling also overlaps

with TRPC6 signaling. SRF-mediated transcription of TRPC6 is required for induction of Ca^{2+}/Calcineurin/NFAT signaling. However, activation of TRPC6 and calcineurin in *Srf*-deficient fibroblasts can still promote myofibroblast differentiation, suggesting TRPC6 and calcineurin act downstream of *Srf* transcription.[119] Although our group as well as others suggests that these signaling pathways interact, they likely function in parallel to regulate cell differentiation.[42,104,119,205] This is supported by a study in renal tubular epithelial cells showing both SMAD- and Rho-dependent signals are required to fully revert mesenchymal cells to an epithelial phenotype, suggesting these pathways likely don't elicit redundant functions.[210] Researchers still do not fully understand how independent signaling pathways converge to alter wound healing and fibrosis. This could explain why targeting individual signaling pathways has not been successful in fully reducing fibrosis in the heart after injury.[39,117,118,211–213] Thus, elucidating the mechanism of how these signaling pathways regulate myofibroblast differentiation and fibrotic remodeling in the heart could provide insight into designing better anti-fibrotic therapies.

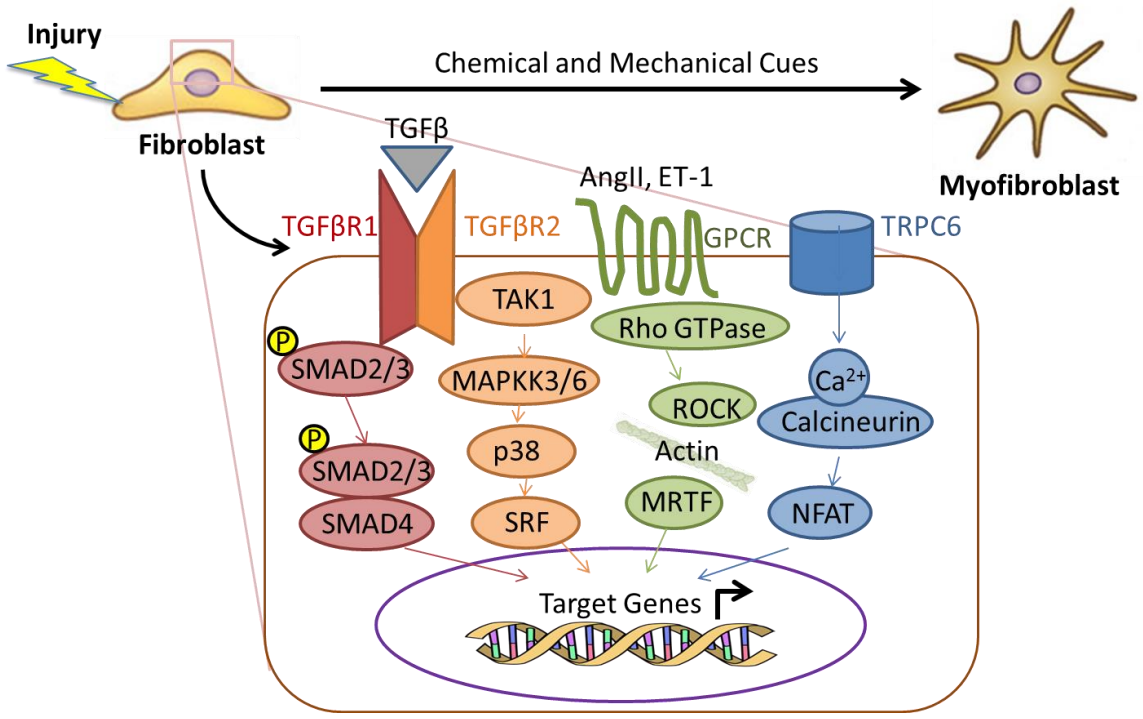

Figure 1.2. Signaling pathways in myofibroblast differentiation.
TGFβ binds to a heterodimer receptor consisting of TGFβR1 and TGFβR2 and signals through a SMAD-dependent canonical pathway (red) or SRF-mediated noncanonical pathway (orange). Actin cytoskeletal dynamics and MRTF translocation to the

nucleus are regulated through Rho GTPase/ROCK signaling after a GPCR is stimulated by AngII or ET-1 (green). Myofibroblast gene transcription can also be activated through TRPC6/Ca^{2+}/Calcineurin/NFAT signaling (blue). Mechanical cues can also stimulate TRP ion channels, Rho/MRTF and p38 signaling, and release latent TGFβ. Together these signaling pathways converge on target genes to promote myofibroblast differentiation. Target genes include *Acta2, Trpc6, Col1a1, Col3a1, Postn,* and *Fn ED-A.* Image adapted from Davis et al. (2014) *JMCC.*[42]

1.5 Transcript Regulation by RNA-Binding Proteins

Although there has been extensive work done to understand transcriptional profiles during myofibroblast differentiation, there is still a large disconnect as to how signaling pathways that induce gene expression lead to myofibroblast differentiation. RNA-binding proteins (RBPs) are central to transcriptional regulation and have emerged as downstream factors in signaling networks that regulate differentiation and disease.[214] RBPs were first discovered as proteins that present mRNA to the degradation machinery, but we now know they regulate all aspects of RNA processing and gene expression including splicing, stability, cellular localization, and rate of translation.[215,216] RBPs interact with target mRNA at the 5'- and 3'-untranslated regions (UTRs) as well as at non-coding intronic and coding exonic regions called *cis*-regulatory elements. RBPs assemble into the spliceosome with small RNA complexes forming heterogenous ribonucleoprotein particles (hnRNPs). These complexes coordinate splicing of pre-mRNA which leads to functionally distinct mature mRNAs. In humans, alternative splicing (AS) and alternative polyadenylation (APA) occur in approximately 80-90% of protein-coding genes resulting in over 200,000 unique protein-coding transcripts. The prevalence of these events underlies the importance of tight albeit dynamic regulation of splicing events for normal physiological function.[217] The region where the RBP binds on its target influences the event that is catalyzed, and access to the target RNAs is determined by expression levels of individual RBPs.[215] However, dysfunction in disease settings is associated with reversion to fetal mRNA and protein isoforms underlying the pathological phenotypes. For example, RNA-seq analysis of postnatal mouse cardiomyocytes and cardiac fibroblasts shows there are extensive changes in gene expression and AS within a month after birth, which correlate with a downregulation of *Celf1* and an upregulation of

Mbnl1.[218] Additionally, when *Celf1* is re-expressed in adults or *Mbnl1* is depleted, genes affected by AS during normal development, such as *Tnnt2* and *Cacna1s*, have a reversion towards a neonatal splicing pattern.[218] The fetal splicing patterns correlate with disease phenotypes such as T-tubule disorganization and aberrant gating of Ca(v)1.1 calcium channel seen in muscle cells from myotonic dystrophy patients.[218–220] The studies above suggest there is differential gene expression in cardiac fibroblasts compared to cardiomyocytes. For example, isolated cardiac fibroblasts from neonatal to adult showed a downregulation in mitochondria metabolism and an upregulation in transcription regulation and adhesion. On the other hand, isolated cardiomyocytes from neonatal to adult showed the opposite result.[218] However, it is still unclear how AS is regulated in the fibroblast during myocardial infarction.

Although AS and APA has been known phenomenon for decades, recent advancements in deep-sequencing technologies has allowed for a more comprehensive understanding of AS and APA across the transcriptome.[221] Comparison of pathways regulated in cardiac hypertrophy induced by TAC to those regulated at different stage of development revealed genes involved in ECM and cell morphology were upregulated in hypertrophy and were more likely to be regulated by AS. Additionally, there was an activation of a fetal post-transcriptional program in the heart in response to pressure overload.[222] In another study using 3' end RNA sequencing, Creemers *et al.* (2016) directly measured global patterns of APA in healthy and failing human heart specimens. Using PANTHER comparisons (Protein Analysis Through Evolutionary Relationships), the researchers found that genes with shortened 3' UTRs in heart failure patients were enriched for RNA binding whereas genes with longer 3' UTRs were enriched for cytoskeletal organization and actin binding [221]. Global shortening of 3' UTRs were also found using microarrays and RNA-sequencing technologies in hypertrophied mouse hearts with a decrease in overall amount of miRNA repression[222,223], suggesting APA plays a key role in regulating gene expression in heart pathophysiology. Generally, there is an inverse correlation between 3' UTR length and the level of gene expression. In fact, shorter mRNA 3' UTR isoforms can produce 10-fold more protein by escaping

miRNA-mediated repression [224]. Thus, an APA shift toward a proximal cleavage site results in shorter 3' UTRs and increased gene expression, whereas a shift toward a distal cleavage site leads to downregulation of the mRNA. Furthermore, splicing regulation is coupled closely with transcription [225]. For example, in hypertrophic mice, genes with upregulated expression are positively correlated with inclusion and exclusion of internal exons one week after TAC[222]. Additionally, miRNA target genes are upregulated during hypertrophy in a TAC model, indicating a global de-repression of miRNA targeting and consequent increase in protein production, which could explain the rapid enlargement of the heart in response to mechanical stress.[222]

Several RBPs increase in expression and activity during remodeling after MI. For example, *HuR/Elavl1* (Hu Antigen R/Embryonic Lethal, Abnormal Vision, Drosophila-Like 1) expression is highly upregulated in the myocardium after permanent coronary artery ligation.[226] Compared to controls, shRNA-mediated knockdown of HuR in the myocardium improved left ventricular dysfunction after MI by abating the inflammatory response, attenuating cardiomyocyte cell death, and reducing myocardial infarct size [226]. However, these experiments were performed in IL-10 knockout mice, suggesting that HuR could be a target of IL-10. However, a similar improvement in fibrosis and cardiac function and remodeling with shRNA HuR treatment was also observed in WT mice, suggesting HuR is partially required for the fibrotic response.[226] Interestingly, these results also showed a correlation with a reduction in TGFβ expression, suggesting there could be an intersection of TGFβ signaling and HuR function.[226] In fact, HuR controls TGFβ-induced fibrosis in the liver by regulating expression of *TGFβ, Acta2*, and *p21* in the cytoplasm.[227] TGFβ signaling is known to activate p38 MAPK and phosphorylate HuR and translocate it to the cytoplasm. Thus, TGFβ signaling and HuR likely act in a feed-forward activation loop during the fibrotic response. All in all, these studies highlight the importance of post-transcriptional regulation via RBPs in heart development and disease. However, how RBPs in *fibroblasts* regulate fibrotic remodeling after MI is still a large area of research currently unexplored.

1.5.1 Muscleblind-like proteins

Our group recently conducted an unbiased genome-wide screen to gain a more global map of gene networks that promote myofibroblast differentiation and discovered a RBP, Muscleblind-like 1 (MBNL1), as a novel post-transcriptional regulator of myofibroblast differentiation.[69] Muscleblind-like proteins are a deeply conserved family of RNA-binding factors that were first discovered in *Drosophila* encoded by the *mbl* gene, and loss of *mbl is* associated muscle and eye developmental defects.[228,229] The mammalian genome contains three muscleblind-like genes including *MBNL1, MBNL2,* and *MBNL3.*[230–232] All three MBNL proteins share structural similarities including two pairs of highly conserved CCCH-type zinc finger domains, which bind to mRNA in a sequence-specific manner (Figure 1.3).[228,233] In both humans and mice, *Mbnl1* and *Mbnl2* are ubiquitously expressed in all body tissues, but *Mbnl1* transcript levels are highest in heart and lowest in testes.[230,233] *Mbnl2* expression is more uniform across tissues, but slightly higher in the heart and lower in spleen and testes.[230,233] *Mbnl3* gene expression is very low in all adult tissues with the highest expression in the placenta.[230,232–234] Compartmental expression is similar in fetal and adult tissues.[230,233] During mouse embryonic development, all three muscleblind-like genes are expressed starting at 6.5 days post fertilization and peak at various times during development (see Table 1.1).[230]

Table 1.1. Mammalian MBNL expression patterns.

Bodily Compartment (Human and Mouse)	***MBNL1*** **(formerly *MBNL*)**	***MBNL2*** **(formerly *MBLL*)**	***MBNL3*** **(formerly *MBXL/MBLX/CHCR*)**
Peak Embryonic Expression (Mouse Only)	13.5 – 15.5 dpf	17.5 – 18.5 dpf	11.5 – 15.5 dpf
Heart	++++	++++	+
Brain	++	+++	++
Spleen	+++	+	+
Lung	+++	+++	+
Liver	+++	+++	++
Skeletal Muscle	++++	+++	+
Kidney	+++	+++	+
Thymus	+++	++	+
Pancreas	+++	+++	+
Testes	+	+	+
Placenta	+	+	++++

dpf = days post fertilization; expression levels: ++++ = very high, +++ = high, ++ = medium, + = low. Data compiled from Kanadia, et al. 2003 & Konieczny, et al. 2014.

In skeletal muscle, MBNL1 and MBNL2 have compensatory roles, as there is a significant increase in MBNL2 protein expression when there is a functional loss of MBNL1 protein, which results in an increase in MBNL2 binding to MBNL1 RNA targets.[219] Furthermore, mice with deletion of both *Mbnl1* and *Mbnl2* are embryonic lethal.[219] Mice with a homozygous knockout of *Mbnl1* and heterozygous for *Mbnl2* have severe splicing aberrations and don't live past 20 weeks of age.[219]

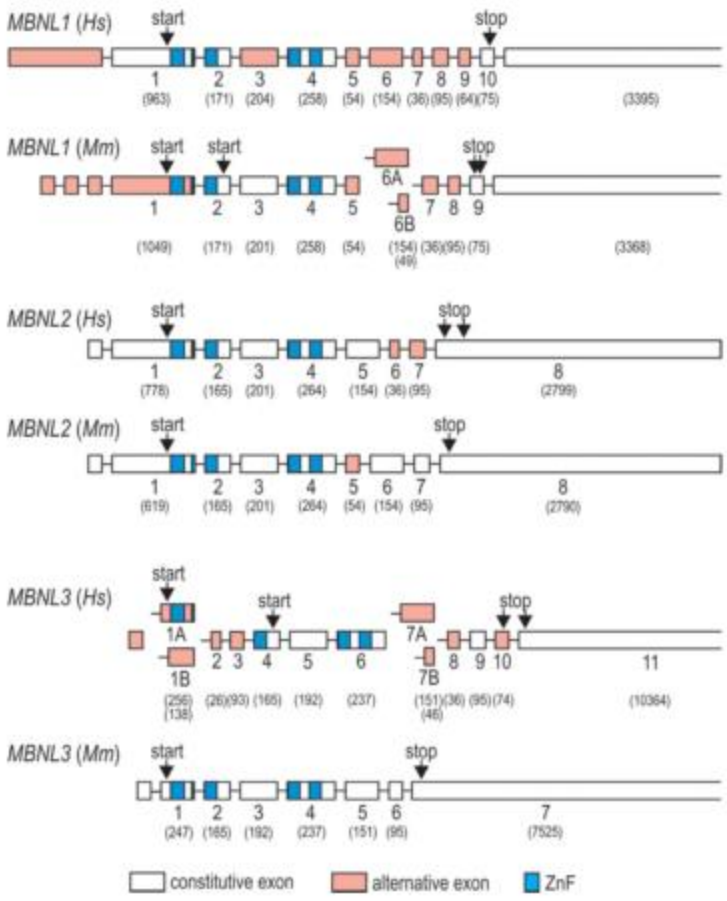

Figure 1.3. Gene structure of human (Hs) and mouse (Mm) MBNL1, 2 and 3.
Schematics are compiled from the RefSeq database sequences. Protein coding exons are numbered below each rectangle and nucleotide length of each exon is indicated in parenthesis. Red exons refer to alternatively spliced exons and blue exons refer to Zn fingers. Start and stop sights are denoted with arrows above the gene. Figure adapted from Konieczny, et al. (2014) *Nucleic Acids Research.*

MBNL proteins in the nucleus regulate alternative splicing and stabilize transcripts, and MBNL proteins in the cytoplasm localize transcripts to rough endoplasmic reticulum, membranes, and ribosomes for translation.[235,236] Some proteins such as the MBNL and HuR stabilize mRNAs by binding to AU-rich motifs within the 3' UTR, where other proteins such as CUGBP Elav-Like Family (CELF) destabilize mRNAs by binding to GU-rich motifs within the 3' UTR.[237,238] These RBPs can functionally compete for the same transcripts to either repress or stabilize transcripts, respectively.[239] Furthermore, alternative splicing of *Mbnl1* itself can impact its subcellular localization.[240] For example, inclusion of exon 5

promotes localization of *Mbnl1* to the nucleus and an increase in RNA binding affinity and alternative splicing activity.[241] Thus, subcellular localization of *Mbnl1* directly impacts its function and suggests MBNL1 acts a key mediator for transcription regulation.

1.5.2 MBNL1 as a Transcription Regulator

Depending on the binding location in the cell, MBNL proteins can regulate mRNA localization either directly in which MBNL1 has binding sites within distal 3' UTRs target mRNAs and directs them to particular subcellular compartments or indirectly by regulating APA and AS.[236] In an elegant study to assess the direct regulatory targets of MBNL1, Wang *et al*. (2012) found that MBNL proteins either suppress or activate polyadenylation. Splicing regulation was context-dependent in that MBNL proteins suppress polyadenylation in a site-specific manner by binding 5' to the polyadenylation and cleavage sites which blocks the recruitment of some components of the core polyadenylation machinery.[236] The consequence of this is observed in the cytoplasm as long 3' UTRs localize closer to membranes than short 3' UTRs with localization shifting after shRNA-mediated *Mbnl1* knockdown.[236] In an independent study from a separate lab, Batra *et al.* (2014) also showed MBNL1 is directly involved in alternative polyadenylation as MBNL knockout *in vitro* and *in vivo* causes misregulation of thousands of alternative polyadenylation events and a shift from adult to fetal APA patterns.[242] This shift to fetal splice variants has been shown in rat hearts after pressure overload.[243] Comparison of fetal rat hearts to adult hearts that underwent TAC using high-throughput sequencing of poly(A) tail mRNA showed isoforms that overlap between these groups were involved in cytoskeletal organization and RNA processing.[243] These studies emphasize the importance of this adult-to-fetal shift in cardiac remodeling, but this study was performed in a whole heart lysate in the context of pressure overload. It is still unknown if there is a shift in AS or APA patterns to fetal transcripts in the fibroblast after myocardial infarction. Prior data from our lab suggests dysregulation of MBNL1 results in destabilization of transcripts and decreased gene expression; however, how loss of MBNL1 affects AS and APA in this context is still unknown.[69]

Batra *et al*. (2014) also demonstrated that MBNL binding directs alternative polyadenylation selection, with the majority of binding occurring in the 3' UTR region of mRNAs.[242] MBNL binding in proximal 3' end processing regions suppresses polyadenylation selection, while more distal binding regions activate polyadenylation selection. This suggests that MBNL proteins show positional effects on 3' end processing and possibly recruitment of the core 3' end processing machinery. In the Wang *et al*. (2012) model in C2C12 myoblasts, they also show that cytoplasmic MBNLs bind 3' UTRs and facilitate transport along the cytoskeleton to various cellular compartments, likely through transport machineries. However, it is currently unknown what those machineries include. Furthermore, direct roles for MBNL1 in mRNA regulation and localization have not been studied in fibroblasts or myofibroblasts.

Data from our lab shows MBNL1 binds and regulates thousands of transcripts in multiple nodal signaling pathways such as the ones described above.[69] Two of these transcripts are serum response factor (SRF) and calcineurin Aβ where MBNL1 stabilizes SRF through a distal 3' UTR binding site. MBNL1 also stabilizes all the splice variants of calcineurin.[69] As described above, calcineurin and SRF are both sufficient to induce myofibroblast differentiation [69], suggesting MBNL1 endogenously stabilizes these regulatory transcripts to coordinate gene programs that promote myofibroblast differentiation.

1.5.3 MBNL1 as a Differentiation Factor

MBNL1 promotes differentiation of numerous cell types. Specifically, MBNL1 binds to mRNA targets to negatively regulate embryonic stem cell (ESC) pluripotency[244,245] as well as promote skeletal muscle differentiation,[232,246,247] cardiac muscle maturation,[218,222,248] erythrocyte differentiation,[249] and myofibroblast differentiation (Figure 1.4).[69] Alternative splicing is a widely acting mode of gene regulation in ESC pluripotency, and MBNL1 is a negative regulator of alternative splicing in ESCs.[244,245] Han *et al.* (2013) showed siRNA knockdown of MBNL1 protein in differentiated cells caused "switching" to an ESC-like alternative splicing pattern and increased formation of induced pluripotent stem cells

(iPSCs). The researchers monitored a transcription factor called FOXP1 that, with loss of MBNL1, changed its DNA binding specificity to stimulate expression of pluripotency transcription factors, such as OCT4 and NANOG, and repressed differentiation genes. In contrast, doxycycline-induced overexpression of MBNL1 promoted differentiated cell-like alternative splicing patterns, reduced pluripotency gene expression, and increased differentiated cell gene expression from all three germ lineages (endoderm, mesoderm, and ectoderm) compared to ESCs.[245] In addition to expression level of MBNL1 affecting the cell's pluripotency, where MBNL1 binds in the genome directly impacts cell fate. For example, the presence of MBNL motifs in downstream flanking intronic sequences is associated with exon skipping in ESCs, whereas their presence in upstream flanking intronic sequences is associated with exon inclusion in ESCs.[245] The opposite is true in differentiated cells where MBNL1 acts to enhance exons when it binds downstream and inhibit exons when it binds upstream.[236,244] Together, this data shows MBNL1 has a negative regulatory role in somatic cell reprogramming.

MBNL1 undergoes cytoplasmic to nuclear transition during the first three weeks of postnatal skeletal muscle development, indicative of alternative splicing function.[247] In fact, Fugier *et al*. (2011) showed that MBNL1 binds the *BIN1* pre-mRNA and regulates its alternative splicing.[246] BIN1 is required for the biogenesis of muscle T-tubules and essential for proper excitation-contraction coupling.[250] Thus, without MBNL1 present, exon skipping of *BIN1* occurs and an isoform of *BIN1* is expressed that is unable to bind tabulate membranes, which ultimately leads to disorganized T tubules and altered excitation-contraction coupling.[246] Furthermore, MBNL1 protein expression is not expressed until two days following myoblast differentiation in cultured C2C12 myoblasts, suggesting MBNL1 is important during terminal differentiation of muscle cells.[232] This can have significance impacts on phenotype as patients with defective skeletal muscle maturation due to missplicing of transcripts such as *BIN1* and the muscle chloride channel *CLCN1* experience muscle weakness and wasting, a predominant feature in myotonic dystrophy.[246,251–253]

Post-transcriptional regulation is also an important component in cardiac muscle maturation as alternative splicing plays an essential role in postnatal remodeling as cardiac transcripts must undergo fetal-to-adult changes in alternative splicing.[222,248] For example, conditional knockout of splicing factor *ASF/SF2* in cardiac muscle led to failure of a specific set of postnatal alternative splicing transitions and persistent expression of neonatal splice isoforms was closely related to the subsequent development of progressive cardiomyopathy.[254] During development, MBNL1 expression gradually in the heart,[230,241] whereas other RNA binding proteins that are regulators in alterative splicing like CELF proteins CUGBP1 and CUGBP2 are expressed at low levels in the adult compared with embryonic hearts.[218,248] CUGBP1 and MBNL1 co-regulate conserved fetal-to-adult alternative splicing transitions, and when *Mbnl1* is knocked out or *Cugbp1* is transgenically overexpressed, embryonic splicing patterns are re-expressed for over half of the these alternative splicing events without changes in overall transcript levels.[248] Phenotypically, cardiomyocyte-specific transgenic overexpression of *Cugbp1* results in T-tubule disorganization, reduced fractional shortening, and altered electrocardiograms compared to controls, mimicking electrical contraction coupling in immature cardiac tissue.[218] These studies suggest that protein isoform switches are important regulatory components during postnatal development [218,248].

MBNL1 also regulates red blood cell (erythrocyte) terminal differentiation.[249] During erythropoiesis, hematopoietic stem cells undergo multiple cell divisions followed by hemoglobinization, a reduction in cell size, chromatin condensation, and expulsion of the nucleus to reach a mature terminal erythrocyte.[255,256] Comparison of the occurrence of oligonucleotides that underwent alternative splicing with MBNL1 CLIP-seq binding clusters showed an increase of MBNL1 binding clusters in erythropoiesis-associated skipped exons in mouse fetal liver cells, suggesting MBNL1 binds mRNA transcripts to promote terminal erythrocyte differentiation.[249] MBNL1 promotes erythrocyte differentiation by alternative splicing of erythropoietic genes as there is a decrease in *Mbnl1 exon 5* exclusion during erythrocyte differentiation (indicative of nuclear localization and enhancement of

splicing activity), and shRNA knockdown of *Mbnl1* inclusion isoform impairs erythroid terminal differentiation.[241,249,257] Cheng *et al.* (2014) showed a direct mRNA target of MBNL1 that is developmentally regulated, *Ndel1,* is misspliced with shRNA knockdown of *Mbnl1.* Notably, shRNA knockdown of *Mbnl1* also inhibited erythroid terminal differentiation as indicated by fetal liver cells having more nuclei and larger cell size compared to controls as well as a reduced induction of erythropoiesis genes such as *Hbb-b1, Hbb-b2, Slc4a1, Epb4.1, Gypa, and Fech* and a 50% reduction in hemoglobin.[249] Thus, this study concludes that MBNL1 promotes regulation of RNA splicing in erythroid terminal differentiation.[249]

As noted above, MBNL1 is also an essential, albeit novel, mediator of myofibroblast differentiation and the fibrotic response after MI.[69] In mouse embryonic fibroblasts, MBNL1 protein is practically undetectable in baseline homeostatic conditions, but with profibrotic agents such as TGFβ or AngII *in vitro* or MI *in vivo,* MBNL1 protein expression significantly increases by at least 6-fold over untreated or sham conditions.[69] Deletion of *Mbnl1* prevents TGFβ-mediated myofibroblast transformation and impairs the fibrotic phase of wound healing in both mouse models of MI and dermal injury, thus leading to heart rupture and chronic open skin wounds, respectively.[69] Conversely, MBNL1 overexpression in TCF21+ cells with chronic AngII infusion resulted in fibrosis in the heart, lungs, and kidneys of MBNL1 transgenic mice. *Mbnl1* has also been discovered to be upregulated in a porcine model of MI in which pigs were subjected to coronary artery ligation and gene expression in the heart was analyzed by microarray technology. [258] Prior to thorough examination of MBNL1's role in fibrosis performed by Davis et al., MBNL1 function had minimal association with the fibrotic wound healing response and had mostly been investigated in muscular dystrophy models (see below).[219,247,251,259–263] Altogether, these studies suggest MBNL1 acts a master regulation of cell differentiation, and the MBNL1-mediated transition from fetal to adult spliced isoforms is critical for the terminal maturation of cells.

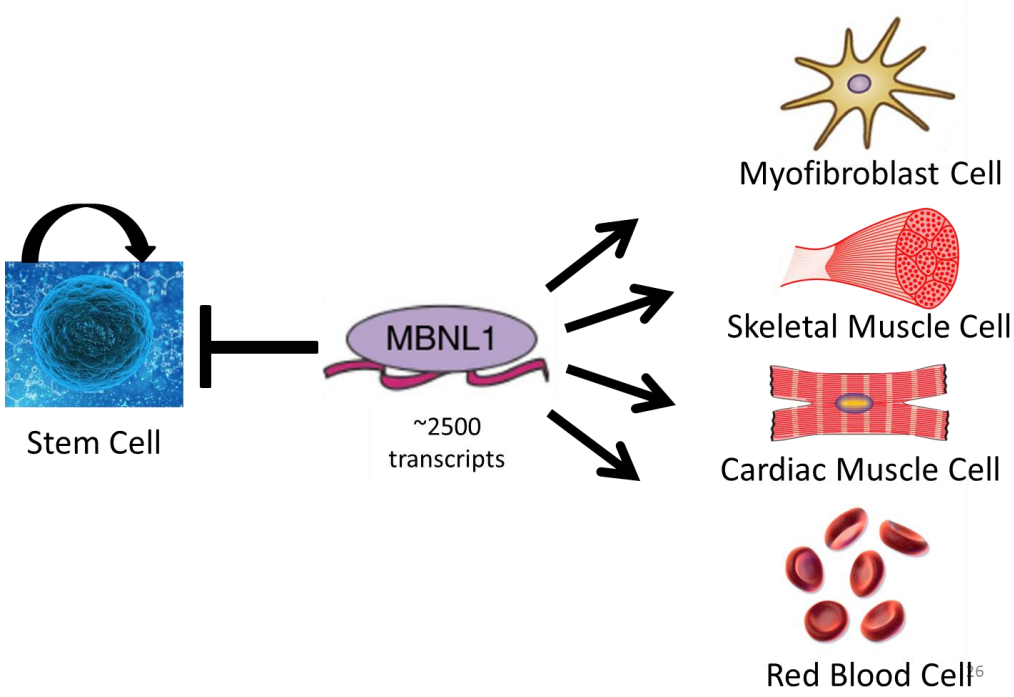

Figure 1.4. MBNL1 acts as a master regulator of cell differentiation.
MBNL1 binds to over 2500 transcripts to promote differentiation/maturation of myofibroblasts, skeletal muscle cells, cardiomyocytes, and erythrocytes. MBNL1 also inhibits stem cell self-renewal and induced pluripotent stem cell reprogramming. Stem cell image credit: CC0 Public Domain; MBNL1 image credit: Jennifer Davis; Myofibroblast cell image credit: Christensen et al. (2018) *Matrix Biology*;[264] Skeletal muscle cell image credit: Picture Lights; Cardiac muscle cell image credit: Wikipedia.org; Red blood cell image credit: https://study.com/academy/lesson/crossmatching-blood-definition-procedure-purpose.html

1.5.4 MBNL1 as a Factor in Myotonic Dystrophy

Transcription initiation, elongation, and termination are tightly coupled to mRNA processing steps such as capping, slicing, and 3' end processing (i.e. polyadenylation). These processes are also intimately connected with mRNA release, export, and translation.[265] Thus, dysregulation of 3' end processing critically interferes with other gene expression steps by altering RNA stability, localization, and translation and can lead to deleterious effects on cellular homeostasis. A prime example is when MBNL1 proteins are functionally depleted. Decreased expression of MBNL1 can cause inappropriate maturation of gene products and the expression of fetal transcript variants, resulting in pathological disease such as myotonic dystrophy.[218,234,244–246,248,262,266,267] One of the missplicing events in myotonic

dystrophy is the misregulation of *Mbnl1* itself in which there is an aberrant inclusion of exon 5.[257] Thus, not only does MBNL1 regulate proper alternative splicing of transcripts directly involved in cell maturation, it also functions in an auto-regulatory fashion, with loss of *Mbnl1* resulting in myotonic dystrophy phenotypes.

Myotonic dystrophy type 1 (DM1) is an autosomal dominant disorder that affects multiple organ systems including skeletal muscle, heart, and brain.[268] DM1 is the most common form of adult-onset muscular dystrophy and is the second most common form overall.[268] In DM1, all three muscleblind-like proteins bind to aberrant double-stranded mRNA hairpin structures containing long $(CUG)_n$ or $(CCUG)_n$ repeats and are sequestered away from their normal RNA targets into nuclear foci.[230,232,262,267] Disease severity typically correlates with the number of CUG repeat expansions[232]; however, phenotype variability has been observed in patients with the same inherited repeat length.[269] Increasing numbers of CUG repeats leads to increased binding of MBNL1 to double-stranded CUG RNA, and thus sequesters MBNL1 into CUG-protein aggregates or foci within the nucleus and decreases free MBNL1 levels.[232,247]

Postmortem DM1 hearts have notable interstitial fibrosis, fatty infiltration, cardiomyocyte hypertrophy, multi-focal myocardial fiber death and calcification, and mouse models of DM1 (where MBNL1 is globally deleted) have significant cardiac dysfunction with the persistence of embryonic splice isoforms.[219,239,249,270–272] The development of fibrosis in adult DM1 patients is likely due to altered splicing of sarcomeric contractile proteins such as titin and myomesin I, resulting in expression of large, elastic embryonic isoforms that have reduced recoil of flaccid titin and myomesin filaments.[273–277] Thus, the phenotypes observed in DM1 such as arrhythmias and dilated cardiomyopathies show how dysregulated splicing can be causal for heart disease. Furthermore, progressive depletion of MBNL1 using siRNA in myoblasts results in an increase in the number and severity of splicing defects.[278] This suggests that variable MBNL1 dose can have differential impacts on disease pathology.

1.6 Summary and Thesis Aims

Cardiac fibrosis is a significant problem in myocardial infarction, and is largely caused by the over-activation of myofibroblasts that infiltrate the wound area and secrete large amounts of ECM. Contractile properties of myofibroblasts and added mechanical load subsequently result in maladaptive cardiac remodeling and advancement toward heart failure. Tremendous progress has been made recently to understand the mechanisms of myofibroblast differentiation from resident mesenchymal cells. However, there are still significant hurdles that need to be addressed for any hope of developing an effective therapy to reverse fibrosis such as what signaling factors are needed for initiation and maturation of myofibroblasts and do all myofibroblast populations mature to the same extent and what about in different types of cardiac fibrosis models? Previous work from our lab defined a new mechanism of myofibroblast differentiation by post-transcriptional maturation of transcripts in nodal signaling pathways that are directed by MBNL1 (Figure 1.2). However, there were several limitations to this study that need to be further evaluated. First, it is currently unknown which cells contribute to the MBNL1-dependent fibrotic phenotype observed after MI since these experiments were performed in global loss of function and AngII mouse models. Secondly, extensive work from our lab as well as others proposes MBNL1 acts as a master regulator of myofibroblast differentiation and cardiac remodeling. MBNL1 accomplishes this by binding and regulating thousands of transcripts. However, to date, no one has identified the functional MBNL1-protein "interactome" and how the titration of MBNL1 complexes on RNA regions leads to myofibroblast differentiation and fibrotic remodeling. This is an important question to understand how protein complexes coordinate signaling pathways to regulate cellular phenotypes such as terminal differentiation of myofibroblasts. The research described in this dissertation aimed to address these limitations described above by better defining the role of MBNL1 in cardiac remodeling by genetically modifying its expression in cardiac fibroblasts and cardiomyocytes and evaluating remodeling

of the myocardium after MI. This research has significant impacts in advancing our knowledge of cell-specific transcriptome maturation in the development of cardiac fibrosis and adverse remodeling.

2 MBNL1 Promotes Cardiac Fibroblast and Cardiomyocyte Maturation in Mouse Cardiac Fibrotic Remodeling After Myocardial Infarction

2.1 Introduction

Cardiac fibrosis is common in most myocardial diseases and is characterized by extracellular matrix (ECM) deposition in the myocardium. [35,43,45] Generation of fibrotic scar by ECM remodeling is critical for wound healing after acute injury to the heart to maintain ventricular wall integrity. However, chronic fibrosis can become pathological and contribute to deteriorating cardiac performance and progression to heart failure.[4]

Cardiac fibrosis is often the result of a natural wound healing response to cardiomyocyte death. For example, up to one billion cardiomyocyte can die after an acute myocardial infarction (MI) and cannot be replaced due to the heart's limited regenerative capacity.[17,19,21,22] A lack of regenerative capability is due to limited cardiomyocyte cell division and the lack of resident stem cell population, and an increase in cell cycle activity results in cardiomyocyte hypertrophy.[279,280] After acute MI, necrotic myocardium is replaced by a collagen-based scar and uninjured cardiomyocytes undergo hypertrophy during the progression of the reparative response.[4]

Myofibroblasts are primarily responsible for fibrosis and scarring because of its ability to secrete ECM in the interstitial space during cardiac remodeling.[42,43,45] However, understanding of the role of programmed conversion of fibroblasts to myofibroblasts in the cardiac fibrotic response is still largely unknown. Clinically, there are limited therapeutics to treat fibrosis after myocardial infarction.[39,53,281,282] Thus, understanding the mechanism of myofibroblast transformation could lead to more promising therapies for patients who have had a MI.

Our lab previously identified a RNA-binding protein called MBNL1 as a regulator of myofibroblast differentiation.[69] MBNL1 directly binds to mRNA transcripts and regulates their expression by alternative splicing, alternative polyadenylation, mRNA stability, and mRNA localization for translation.[236] Global deletion of *Mbnl1* in mice results in heart rupture after permanent ligation of the left anterior descending coronary artery (a mimetic to MI) due to a significant decrease in cardiac fibrosis, suggesting MBNL1 is necessary for a protective scar formation after acute MI.[69] However, the specific cellular contribution to MBNL1-mediated fibrotic remodeling seen in the global *Mbnl1* knockout animals still remains unknown. Experiments performed *in vitro* on mouse embryonic fibroblasts (MEFs) show MBNL1 is necessary and sufficient for myofibroblast differentiation, suggesting MBNL1 may regulate the fibrotic response.[69] Thus, we hypothesized that cardiac fibroblasts are the main contributor to MBNL1-mediated fibrosis in the heart post MI.

It is also unclear if cardiac remodeling is due to direct adverse effects of the fibrotic response or results from a reparative response to prominent cardiomyocyte injury. Since cardiomyocytes are the main contractile unit of the heart[18], we also tested if cardiomyocytes contribute to MBNL1-mediated fibrotic remodeling post MI. Here, we used newly engineered fibroblast- and cardiomyocyte-specific MBNL1 loss and gain of function adult mouse models and performed coronary artery ligations to assess the role of these cells in fibrotic remodeling post-MI. We demonstrated that loss of MBNL1 function in fibroblasts and cardiomyocytes reduced fibrosis and protected the heart against adverse cardiac remodeling, whereas activation of MBNL1 caused increased fibrosis and cardiac dysfunction. Our results show that the fibrotic remodeling response after MI in the global *Mbnl1* knockout mouse model is due to MBNL1 activity both in the cardiac fibroblast and the cardiomyocyte.

In addition to promoting myofibroblast differentiation, MBNL1 also promotes maturation of skeletal muscle cells, cardiomyocytes, and erythrocytes and negatively regulates ESC pluripotency.[234,244–246,248,249] Studies from our lab suggest that MBNL1 binds over 2500 transcripts regardless of cell type.[69]

Additionally, studies from the laboratories of Eric Wang and Chris Burge show MBNL1 binds the same transcripts regardless of cell type.[239,283] However, it is unclear how MBNL1 regulates its target transcripts to promote cell differentiation. In particular, no studies have examined the MBNL1 protein "interactome" during myofibroblast differentiation to elucidate how MBNL1 binds to and regulates thousands of transcripts and impact cardiac remodeling. Using an unbiased mass spectrometry proteomics approach, we identified novel protein-protein interactions with MBNL1 and revealed a potential new role in MBNL1-dependent RNA elongation that could have implications as a novel therapeutic target for cardiac fibrosis.

2.2 Methods

2.2.1 Animal Models

All mouse experiments were performed with approval by the University of Washington Institute for Animal Care and Use Committee (IACUC). Power analysis was executed prior to all experiments with mouse numbers given in results or figure legends. LoxP-targeted *Mbnl1* mice were mated with mice containing MerCreMer (MCM) cDNA knocked into the *Tcf21* genomic locus in a C57BL/6 background, thus allowing for MBNL1 removal in *Tcf21*+ cells upon tamoxifen treatment. Tamoxifen-inducible MBNL1 transgenic (Tg) mice were made by mating *Tcf21* MCM mice with B6 agouti mice engineered with a cytomegalovirus-β-actin promoter construct in which MBNL1 cDNA was cloned downstream of a LoxP-flanked chloramphenicol SV40-polyA stop sequence. These mice allow for *Mbnl1* to remain out of frame until tamoxifen treatment. Pharmaceutical-grade tamoxifen dissolved in 5% ethanol in peanut oil was intraperitoneal injected for 5 consecutive days (25 mg/kg/day) in control and experimental mice, followed by maintenance on tamoxifen-citrate chow (400 mg/kg, Envigo Teklad Diets) until the experimental end point (Figure 2.1). For cardiomyocyte experiments, homozygous loxP-targeted *Mbnl1* mice ($MBNL1^{F/F}$) were crossed with mice containing constitutively active cre recombinase cDNA expressed in the alpha myosin heavy chain (*αMhc*) genetic locus allowing for deletion of the *Mbnl1* gene

only in cardiomyocytes expressing *αMhc*. These mice we termed MBNL1$^{F/F}$ αMHC^{Cre}. For *Mbnl1* overexpression in cardiomyocytes, αMHC^{Cre} mice were mated with our MBNL1 Tg mice described above.

MI injury was performed by thoracotomy followed by permanent ligation of the left anterior descending (LAD) coronary artery. Mice were anesthetized with 2% isoflurane gas, intubated through the mouth, and ventilated throughout the procedure. Mice were also given a single subcutaneous injection of a mixture of lidocaine (4 mg/kg body weight) and bupivacaine (2 mg/kg body weight) at the local surgical incision site. A single dose of sustained-release buprenorphine (1 mg/kg body weight) was administered post-operatively after mice had regained consciousness. Mice were taken off tamoxifen chow 3 days prior to surgery until 3 days post-surgery to increase survival rate. All animal experiments included both sexes and were performed at approximately 8 weeks of age. Genotypes were confirmed at weaning and again post-mortem.

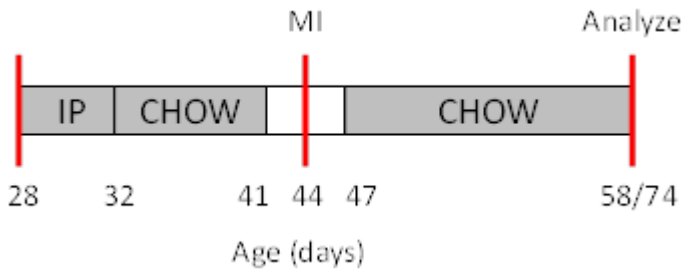

Figure 2.1. Tamoxifen dosing scheme.

M-mode and B-mode echocardiography was used to assess ventricular geometry and function 3 days prior to surgery and 14 or 30 days after surgery in mice anesthetized with inhaled 2% isoflurane for the duration of measurements (Visual Sonics 2100 instrument). Tissue Doppler imaging and pulse wave echocardiography was used to assess diastolic dysfunction in MBNL1 Tg TCF21^{Cre} mice, MBNL1 Tg αMHC^{Cre} mice, and littermate controls at 8 weeks of age. All echocardiography analyses were performed with five repeated measures. For mice used in histological studies, hearts were removed at the

completion of the study and perfused in phosphate-buffered saline followed by saturated potassium chloride to remove blood and preserve diastolic dimensions. Hearts were then fixed in 10% formalin, dehydrated in a serial series of increasing ethanol concentration, embedded in paraffin, and sectioned at 5um using a Leica RM 2125 RT sliding microtome. Fibrosis was assessed at two weeks and four weeks after MI injury by Sirius red/fast green staining in two transverse sections 200um apart from below the suture point to the apex. The percent fibrotic area was determined by total red pixel area divided by total colored pixel area using National Institute for Health (NIH) FIJI software. For myofibroblast identification, cardiac tissue sections were first progressively rehydrated in a series of xylenes followed by solutions with decreasing ethanol percentages. Sections were then subjected to antigen retrieval in 1x Biogenex antigen-retrieval solution (citrate buffer) by steam penetration. Tissues were rinsed in phosphate buffer saline (PBS) and blocked in a solution containing 1% bovine serum albumin (BSA), 0.1% cold fish skin gelatin, 0.5% Triton X-100, and 0.05% sodium azide (pH 7.4) for 1 hour at room temperature following by incubation overnight at 4°C with αSMA antibody (1:500, mouse monoclonal antibody, Clone 1A4, Sigma). Slides were washed with PBS followed by incubation for 1.5 hours at room temperature with goat anti-mouse 568 secondary antibody (1:2000, Alexa Fluor) and isolectin-B4 (10 µg/mL (1:100), Vector Biolabs) for identification of endothelial cells. After a second round of washes with PBS, heart tissues were dyed with dapi (1:1000, Invitrogen) and mounted with VectaShield mounting medium. Cardiomyocyte-specific paraffin-embedded cardiac tissue sections were stained with wheat germ albumin to visualize cardiomyocyte cross-sectional area. Stained slides were imaged and z-stacks were created using a Nikon A1R confocal mounted on a Nikon TiE inverted microscope with an oil-immersed 40x objective. Cardiomyocyte cross-sectional area was measured using National Institute of Health (NIH) FIJI software.

2.2.2 Cell Cultures and Treatments

Cardiac fibroblasts were isolated from ventricles and perfused using a langendorff apparatus with type II collagenase (2 mg/mL) and liberase blendzyme (0.4 mg/mL) in Krebs-Henseleit buffer and cultured in Dulbecco's Modified Eagle's Medium (DMEM; Gibco) without sodium pyruvate supplemented with 20% fetal bovine serum (FBS; Gibco) and 1% penicillin streptomycin (pen strep; 10,000 U/mL penicillin G sodium and 10,000 µg/mL streptomycin sulfate in 0.85% saline, Gibco). Passage two or three were used for experimentation. Cardiac fibroblasts were maintained in DMEM with either 10% or 20% FBS and passaged at 70% confluence.

For the myofibroblast differentiation assay, 30,000 cells were seeded on 18mm glass coverslips in a 12-well culture plate, serum-starved in 2% FBS DMEM media, and treated with recombinant porcine TGFβ (10 ng/mL, R&D Systems) or adenovirus delivery of serum response factor (AdSRF) and analyzed 72 hours later. Media was exchanged with fresh treatments 48 hours after seeding. Cells were fixed in 4% paraformaldehyde for 15 min, washed with PBS and blocked in PBS containing 0.5% Triton X-100 and 10% normal goat serum. Primary and secondary antibodies were diluted in PBS containing 0.5% Triton X-100 and 2% normal goat serum, and cardiac fibroblasts were incubated with αSMA primary antibody (1:500, mouse monoclonal antibody, Clone 1A4, Sigma) for 1.5 hours at room temperature. Cells were blocked again for 30 min incubation before incubation with mouse IgG Alexa 568 conjugated secondary antibody (1:1000) for 1 hour at room temperature. DAPI (1:1000, Invitrogen) was used to visualize nuclei. For myofibroblast assessment in MBNL1 Tg TCF21^{Cre} mice and littermate controls, cardiac fibroblasts incubated with or without an adenovirus delivering a short hairpin RNA against SRF (AdshSRF) for a minimum of four days after cell isolation. Cells were then seeded onto 2% gelatin-coated 300MPa coverslips and treated with or without 10 ng/mL TGFβ (R&D Systems) for 72 hours before staining with αSMA antibody and DAPI as described above. SRF antibody (1:100, rabbit polyclonal

antibody, Santa Cruz) was used to confirm knockdown of SRF protein. Alexa 488 conjugated secondary antibody directed against rabbit IgG was used to detect SRF (1:1000).

For the collagen contraction assay, 40,000 cardiac fibroblasts were seeded into collagen (freshly made from rat tail collagen type I, Sigma) gel matrices and treated with recombinant porcine TGFβ (10 ng/mL, R&D Systems) or adenovirus gene delivery of activated calcineurin truncation (AdΔCnA) or muscleblind-like 1 (AdMBNL1). Gel area was measured at 17, 41, and 65 hours after seeding. Animals were treated with tamoxifen as stated above prior to cell isolations.

For proliferation assessment, isolated cardiac fibroblasts were cultured with 10 μM 5-ethynyl-2'deoxyuridine (EDU) and DMEM supplemented with 1% pen strep, and either 10% FBS, 2% FBS, or 2% FBS + TGFβ (10 ng/mL, R&D Systems) for 72 hours. A Click-iT EDU imaging kit (Invitrogen) was used to detect EDU incorporation. Hoeschst staining was used to label all nuclei as per the kit instructions. The coverslips were imaged and analyzed for number of EDU-positive nuclei normalized to total nuclei.

Myocytes from control and MBNL1 Tg αMHC^{Cre} mice were isolated by langendorff perfusion of collagenase digestion buffer. Myocytes were then plated on laminin and allowed to settle for two hours before being fixed with 4% PFA. Cells were then stained with alexa fluor 488 wheat germ agglutinin and imaged. 200 cells per animal were analyzed from two control mice and three MBNL1 Tg αMHC^{Cre} mice.

2.2.3 Imaging

Sirius red/fast green stained heart sections and contracted collagen samples were imaged on a Nikon SMZ1500 microscope zoomed to 2x magnification. White balance was used to normalize the colors for Sirius red/fast green stained slides, and samples from the collagen contraction assay were imaged in black and white. Images were analyzed using NIH FIJI software. Immunofluorescent images were captured on a Nikon TiE inverted widefield fluorescence high-resolution microscope using an oil-immersed 40x objective. Immunofluorescent images were analyzed using Nikon NIS-Elements software.

2.2.4 Flow Cytometry and Western Blot Analysis

Cardiac fibroblasts were isolated from genetically modified mouse hearts as previously described and were immediately collected and prepared for flow cytometry by rinsing in Hanks' Balanced Salt Solution (HBSS; Gibco) supplemented with calcium, magnesium, and 2% FBS. Fibroblasts were incubated for one hour with fibroblast allophycocyanin-conjugated antibody MEF-SK4 and fluorescein isothiocyanate-conjugated CD11B antibody (1:10, Miltenyi Biotec), washed three times with buffer, and incubated with dapi (1 μg/mL, Invitrogen) to identify dead cells. Cells were flow sorting in 1% FBS HBSS buffer with 2U/μL DNase (Qiagen) using a 100 μM nozzle on an Aria III instrument. The purified fibroblast fraction was lysed in radioimmunoprecipitation assay (RIPA) buffer and denatured in 2x sample buffer (125 mM Tris-HCl pH 6.8, 4% SDS, 20% glycerol, 10mM DTT, 1M urea, 0.005% bromophenol blue). Protein lysate (20-30μg) was loaded onto a 10% SDS-PAGE gel. The protein gel was transferred onto a polyvinylidene fluoride (PVDF) membrane for two hours at 70V. Blots were blocked in 5% BSA and incubated overnight at 4°C with MBNL1 antibody (1:1000, rabbit polyclonal, Abcam) in blocking buffer, washed five times with 1x tris-buffered saline with Tween 20 (TBST), incubated for one hour with HRP-conjugated anti-rabbit secondary antibody (1:10,000, Santa Cruz), washed five times with 1x TBST, incubated briefly with ECL western blotting substrate (Thermo), and then developed with film.

2.2.5 Reverse Transcriptase-Polymerase Chain Reaction

Cardiac fibroblasts were lysed directly in the culture dish and then homogenized with Qiashredders. RNA was isolated with the Qiagen RNAeasy kit. Total RNA was reverse transcribed with random hexamer primers and Superscript III. Quantitative polymerase chain reaction was performed with SYBR green (Biorad), and 18S expression was used for normalization.

2.2.6 Sample Preparation for Mass Spectrometry

Approximately 1,000,000 mouse embryonic fibroblasts were seeded into 15cm plates and treated with AdMBNL1 for 48 hrs. Untreated cells incubated for 48 hrs. The cells were then washed in 1x PBS and flash frozen. Cells were lysed for 15 min at 4°C in lysis buffer (40 mM HEPES, 150 mM NaCl, 1 mM EDTA, 0.1% Igepal, pH 7.4). Immunoprecipitation of MBNL1 was performed by adding 2.5 µg MBNL1 antibody (Abcam rabbit polyclonal) conjugated to sepharose G beads to 1 mg protein in soluble cell lysate and incubated at 4°C for 18 hrs. Beads were washed with lysis buffer and further lysed with 1 M urea and 50 mM ammonium bicarbonate (pH 7.8). On-bead proteins were then reduced with 2 mM DTT, alkylated with 15 mM iodoacetamide, and digested overnight with a 1:50 ratio of trypsin to total protein. The resulting peptides were desalted on Waters Sep-Pak C18 cartridges.

2.2.7 Nano-LC-MS/MS Measurements and Data Analysis

Two biological replicates were run in technical quadruplicate. Peptides were measured by nano-LC-MS/MS on a Q Exactive (Thermo Scientific). Peptides were separated by online reverse-phase chromatography using a heated 50°C 40 cm C18 column (75-mm ID packed with Magic C18 AQ 5 µm/100 Å beads) in a 120 min gradient (10%-30% acetonitrile with 0.1% formic acid) separated at 300 nL/min. The Q Exactive was operated in the data-dependent mode with the following settings: 70,000 resolution, 375-1,600 m/z full scan, Top 30, and an 1.6 m/z isolation window. Identification and label-free quantification of peptides was done with MaxQuant 1.5.7.4 using a 1% false discovery rate (FDR) against the UniProt mouse proteome dataset. Perseus 1.5.6.0 was used to perform permutation-based t-tests (5% FDR), hierarchical clustering analysis, pearson's correlation, and principal component analysis.

Significant MBNL1-associated proteins were validated using western blotting as described above. Immunoprecipitation of MBNL1 was performed in parallel with the samples used for mass spectrometry. Beads were washed five times with lysis buffer and then lysed with 2x sample buffer.

Beads were centrifuged and 5 µL of sample was loaded onto a 10% SDS-PAGE gel and processed with western blotting. The following antibodies were used: MBNL1 (1:1000, rabbit polyclonal, Abcam), CDK9 (1:1000, rabbit monoclonal, Cell Signaling), Cyclin T1 (1:1000, rabbit monoclonal, Cell Signaling), HEXIM1 (1:1000, rabbit polyclonal, Bethyl Labs), MEPCE (1:1000, rabbit polyclonal, Abcam), ELAVL1/HuR (1:1000, rabbit monoclonal, Cell Signaling).

2.2.8 Statistics

Two-sided unpaired *t*-tests were used to determine statistical significance when comparing experiments with two groups. One-way ANOVA was used for experiments with > 2 groups, and statistical significance was determined by the Newman-Keuls methods for pairwise differences (GraphPad Prism software). Values of $P < 0.05$ were considered statistically significant. Power analysis with 80% criterion for significance (α) at 0.05 was used to determine a sample size of n = 6-8 for MI injury. The mean ± the standard error of the mean (SEM) is reported in all figures. *In vitro* experiments were repeated a minimum of three times, and animals from multiple litters were used for *in vivo* studies to ensure repeatability. Data was collected and analyzed blinded for all studies.

2.3 Results

2.3.1 MBNL1 Deletion in Adult Cardiac Fibroblasts Protects Against Post-Infarction Scarring and Ventricular Remodeling

To determine the fibroblast-specific role of MBNL1 in cardiac fibrosis, we used a new mouse model in which *Mbnl1* was conditionally knocked out of resident cardiac fibroblasts. For this, tamoxifen-inducible MerCreMer (MCM) cDNA was expressed from the *Tcf21* genetic locus and these mice were crossed with homozygous LoxP-targeted *Mbnl1* mice ($MBNL1^{F/F}$). We termed these new mice $MBNL1^{F/F}$ $TCF21^{Cre}$ (Figure 2.2A). Flow-sorted cardiac fibroblasts from $MBNL1^{F/F}$ $TCF21^{Cre}$ mice had about a 40%

reduction in *Mbnl1* gene expression compared to littermate MBNL1$^{F/F}$ mice after two weeks of tamoxifen treatment *in vivo* (Figure 2.2B), and echocardiographic assessment determined that MBNL1$^{F/F}$ TCF21^{Cre} mice had no change in fractional shortening (FS), intraventricular septum thickness (IVSD), left ventricular posterior wall thickness (LVPW), or left ventricular internal diameter (LVID) compared to littermate controls (Figure 2.2C-F).

We next analyzed the degree of fibrosis and cardiac function after MI to determine if fibroblast-specific deletion of MBNL1 has reduced fibrosis and a protective effect on cardiac remodeling and systolic function. Indeed, after permanent ligation of the coronary artery, mice with fibroblast-specific loss of function have a significantly reduced fibrotic area at two weeks and four weeks post-infarct compared to littermate controls when assessed from Sirius red/fast green staining of paraffin-embedded transverse heart sections (Figure 2.3A-B and Figure 2.4A-B). Cardiac sections were also quantified for αSMA-positive and isolectin B4 (IB4)-negative (endothelial marker) cells to determine the number of myofibroblasts in the scar region two weeks after MI. Isolectin B4 was used to exclude any αSMA+ vascular cells. The number of myofibroblasts was reduced in MBNL1$^{F/F}$ TCF21^{Cre} mice after injury compared to MBNL1$^{F/F}$ littermates (Figure 2.3A (right panel), C). Unlike global genetic removal of MBNL1 which caused heart rupture in a previous study[69], fibroblast-specific deletion of MBNL1 in our study had no difference in survival rate compared to littermate controls with an overall survival rate of ~90% for both genotypes (data not shown). MBNL1$^{F/F}$ TCF21^{Cre} mice had significantly reduced cardiac mass at two and four weeks post-infarct compared to littermates (Figure 2.3D and Figure 2.4C). We also used echocardiography data to perform a pairwise comparison for changes in LVID and FS before and after infarct. MBNL1$^{F/F}$ TCF21^{Cre} mice had a significantly reduced change in LVID after injury for both time points compared to MBNL1$^{F/F}$ littermates but no difference between genotypes for a change in FS, suggesting that decreasing fibrosis abrogates infarct-induced ventricular dilation but not systolic function (Figure 2.3E-F and Figure 2.4D-E).

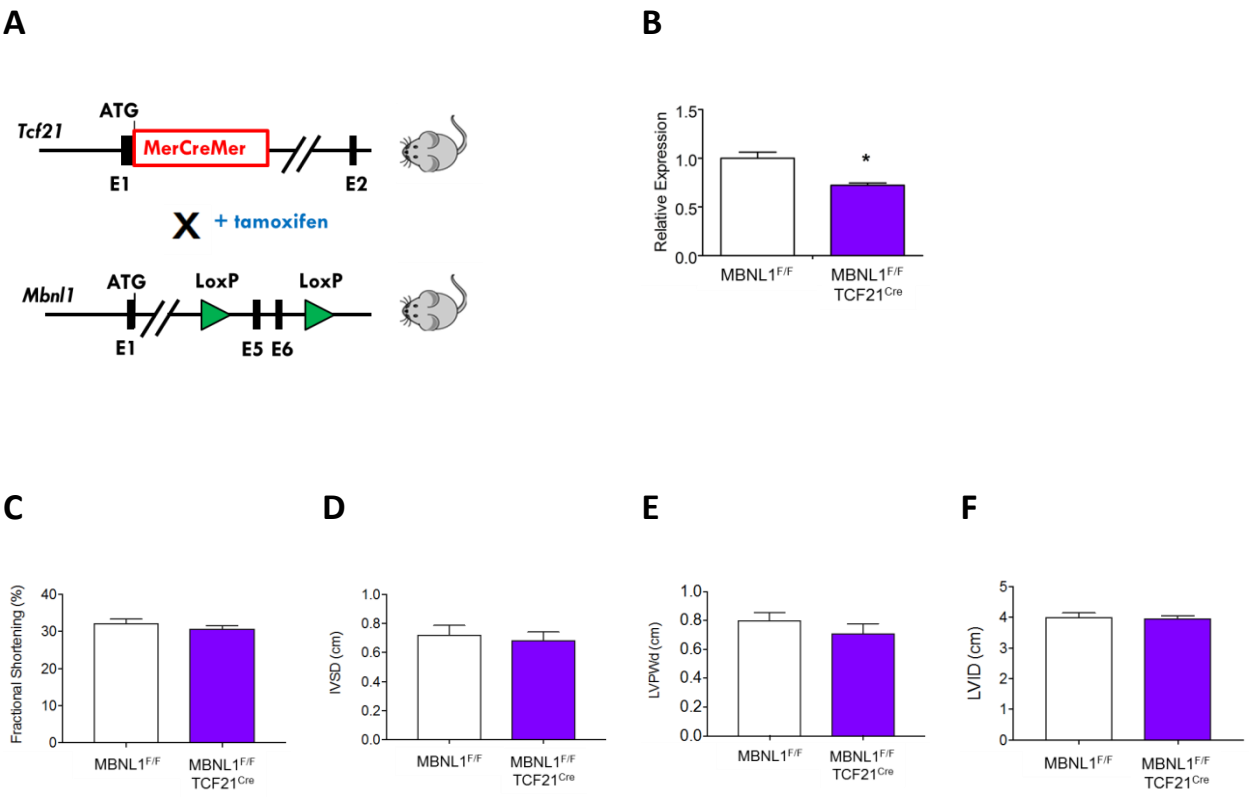

Figure 2.2. Loss of MBNL1 in adult cardiac fibroblasts does not alter cardiac structure or function.
(A) Schematic of mice with the *Tcf21* locus containing a tamoxifen-inducible MCM cDNA and a *Mbnl1*-loxP-targeted allele. Tamoxifen treatment causes Cre-dependent recombination to inactivate the *Mbnl1* gene. (B) RT-qPCR showing reduced MBNL1 gene expression in flow-sorted cardiac fibroblasts from MBNL1$^{F/F}$ TCF21^{Cre} mice compared to MBNL1$^{F/F}$ littermate controls after two weeks of tamoxifen treatment. 18S was used as a house keeping gene. Echocardiography of (C) fractional shortening, (D) intraventricular septum diameter (IVSD), (E) left ventricular posterior wall (LVPW) thickness, and (F) left ventricular interior diameter (LVID) measured in the diastolic dimension of eight week old MBNL1$^{F/F}$ and MBNL1$^{F/F}$ TCF21^{Cre} mice. Data are mean ± SEM for n ≥ 6.

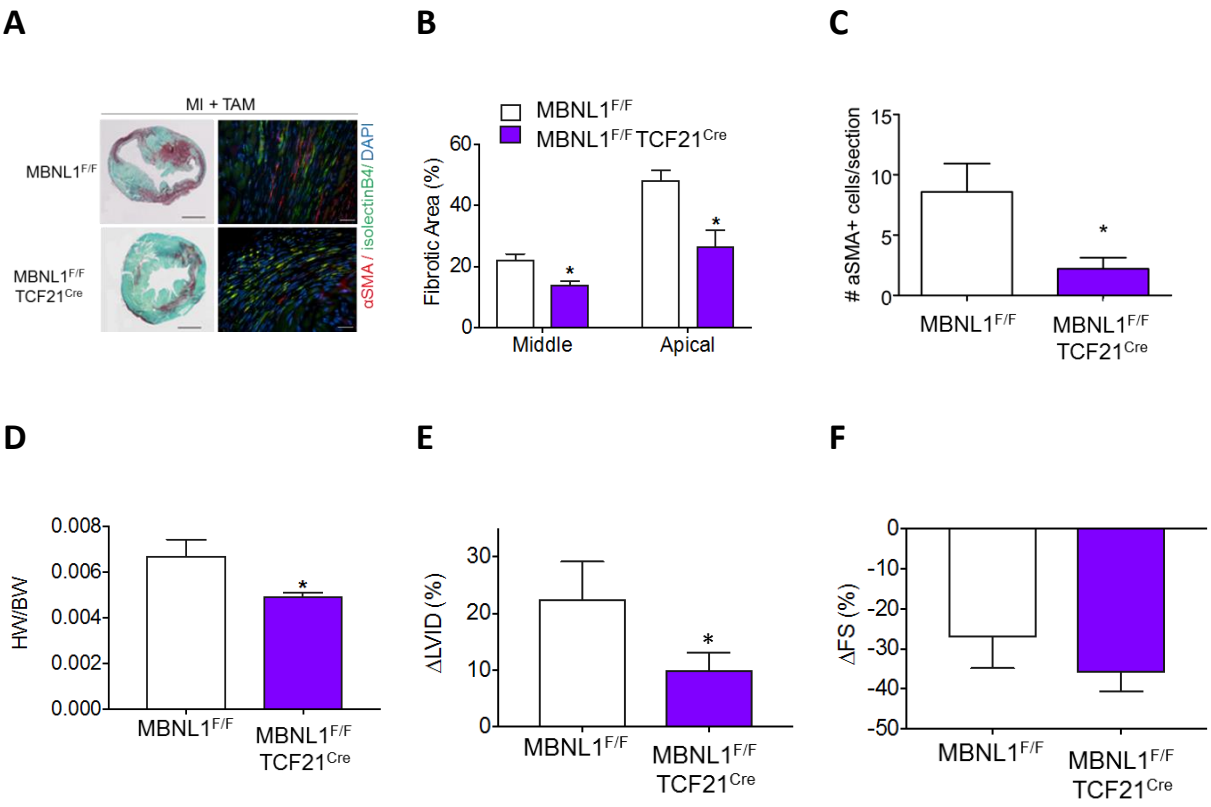

Figure 2.3. Loss of MBNL1 in resident cardiac fibroblasts reduces infarct scarring and ventricular remodeling two weeks after infarct.
(A) Transverse sections of MBNL1$^{F/F}$ and MBNL1$^{F/F}$ TCF21^{Cre} infarcted mouse hearts stained with Sirius red/fast green (left panels) or with αSMA (red) and isolectin B4 (green) antibodies (right panels) in the infarct zone two weeks after infarction. Scale bar in Sirius red images is 1 mm; scale bar in cell images is 25 µm. (B) Quantification of fibrosis in infarcted MBNL1$^{F/F}$ and MBNL1$^{F/F}$ TCF21^{Cre} mouse hearts as a percent of red area to overall stained area in (A) from middle and apical transverse sections 200µm apart. Data are averages ± SEM, n ≥ 6 mice, *t*-test, *$P < 0.05$ vs. MBNL$^{F/F}$. (C) Quantification of myofibroblasts positive for αSMA (red in (A)) and negative for the endothelial marker isolectin B4 (green in (A)) per heart section. Data are averages ± SEM, n ≥ 6 mice with 2 sections per mouse and 10 images analyzed per section, *t*-test, *$P < 0.05$ vs. MBNL$^{F/F}$. (D) Quantification of heart weight (HW) normalized to body weight (BW) for MBNL1$^{F/F}$ and MBNL1$^{F/F}$ TCF21^{Cre} mice two weeks after MI. Average ± SEM HW/BW, *t*-test, *$P < 0.05$ vs. MBNL$^{F/F}$. Echocardiography of (E) left ventricular inner diameter (LVID) and (F) fractional shortening (FS) from MBNL1$^{F/F}$ and MBNL1$^{F/F}$ TCF21^{Cre} mice. Pairwise comparison from pre-MI to 2 weeks post-MI are graphed as percent change in LVID (ΔLVID) and percent change in FS (ΔFS). Average ± SEM, n ≥ 6 mice, *t*-test, *$P < 0.05$ vs. MBNL$^{F/F}$.

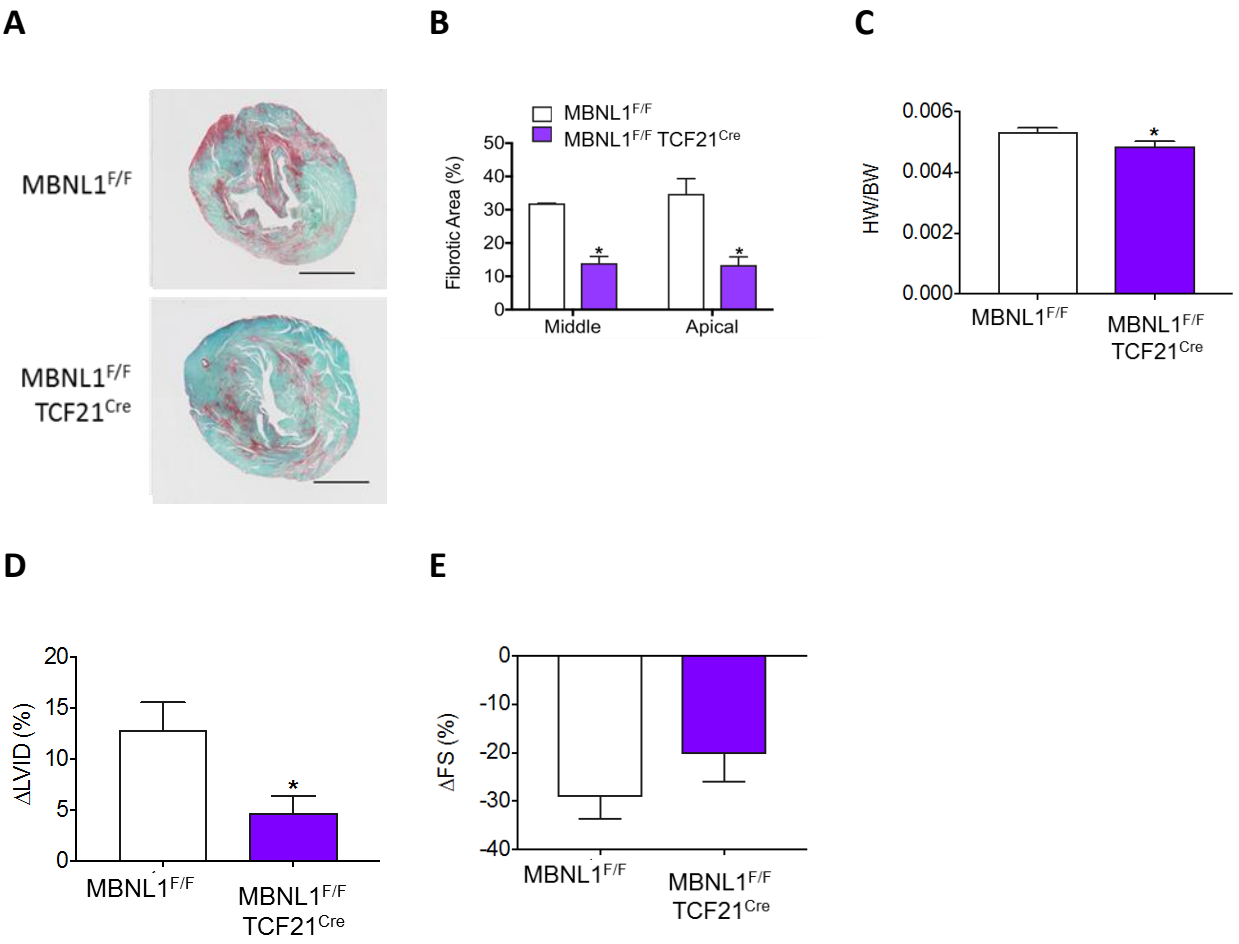

Figure 2.4. Loss of MBNL1 in resident cardiac fibroblasts reduces infarct scarring and ventricular remodeling four weeks after infarct.
(A) Images and (B) quantification of fibrotic area (red) in transverse histological sections of infarcted MBNL1$^{F/F}$ and MBNL1$^{F/F}$ TCF21^{Cre} mice stained for Sirius red/fast green four weeks after infarction. Middle and apical sections 200μm in separation were used for analysis. (C) Heart weight (HW) to body weight (BW) quantification for MBNL1$^{F/F}$ and MBNL1$^{F/F}$ TCF21^{Cre} mice four weeks after MI. (D) Percent change in left ventricular internal diameter (ΔLVID) and (E) percent change in fractional shortening (ΔFS) for MBNL1$^{F/F}$ and MBNL1$^{F/F}$ TCF21^{Cre} mice before and four weeks after coronary artery ligation. Data are average ± SEM, n ≥ 6 mice, *t*-test, *$P < 0.05$ vs. MBNL$^{F/F}$. Scale bar is 1 mm.

2.3.2 Adult Cardiac Fibroblasts Require MBNL1 for Myofibroblast Transformation

To determine if loss of MBNL1 in adult cardiac fibroblasts prevents the cells to differentiate into myofibroblasts, we isolated primary adult cardiac fibroblasts from MBNL1$^{F/F}$ and MBNL1$^{F/F}$ TCF21^{Cre} mice after two weeks of tamoxifen treatment and plated the cells in serum-reduced media with or without known agonists for myofibroblast differentiation. After three days of treatment with TGFβ, αSMA expression in matured stress fibers was increased approximately 4-fold in MBNL1$^{F/F}$ cardiac fibroblasts

compared to an untreated control. MBNL1$^{F/F}$ TCF21^{Cre} cardiac fibroblasts failed to increase αSMA expression significantly over untreated controls, confirming that MBNL1 is necessary for TGFβ-mediated myofibroblast transformation (Figure 2.5A-B).

Our past studies in MEFs showed that MBNL1 directly binds to and stabilizes SRF and calcineurin which are necessary for myofibroblast transformation in MEFs and act through MAPK and Ca^{2+} signaling pathways, respectively.[69] To confirm that SRF signaling is downstream of MBNL1 and acts as a key regulatory factor in cardiac fibroblasts, MBNL1$^{F/F}$ and MBNL1$^{F/F}$ TCF21^{Cre} cardiac fibroblasts were treated with an adenovirus expressing SRF (AdSRF) and cells were counted three days later for αSMA incorporation into stress fibers. After AdSRF treatment, both genotypes significantly increased αSMA expression to the same extent over untreated controls (Figure 2.5A-B).

We next used a collagen gel contraction assay as a functional confirmation of myofibroblast transformation. Collagen gels seeded with control cardiac fibroblasts contracted in untreated conditions likely due to spontaneous myofibroblast differentiation; however, cardiac fibroblasts devoid of MBNL1 failed to contract the collagen gel to any extent. Treatment with TGFβ amplified the contraction in control cardiac fibroblasts, but loss of MBNL1 inhibited TGFβ-mediated contraction (Figure 2.5C-D). These results functionally confirm that MBNL1 is necessary for myofibroblast transformation. To determine if MBNL1 overexpression is sufficient for collagen contraction, we treated MBNL1$^{F/F}$ and MBNL1$^{F/F}$ TCF21^{Cre} cardiac fibroblasts with an adenovirus expressing MBNL1 (AdMBNL1). We also aimed to confirm that calcineurin is downstream of MBNL1 in cardiac fibroblasts by treating cells with an adenovirus with constitutively active calcineurin (AdΔCnA). Both viruses were able to rescue the contractile phenotype seen in MBNL1$^{F/F}$ TCF21^{Cre} cardiac fibroblasts and significantly reduce the area of the collagen gel compared to untreated controls, confirming our previous data in MEFs (Figure 2.5C-D)[69].

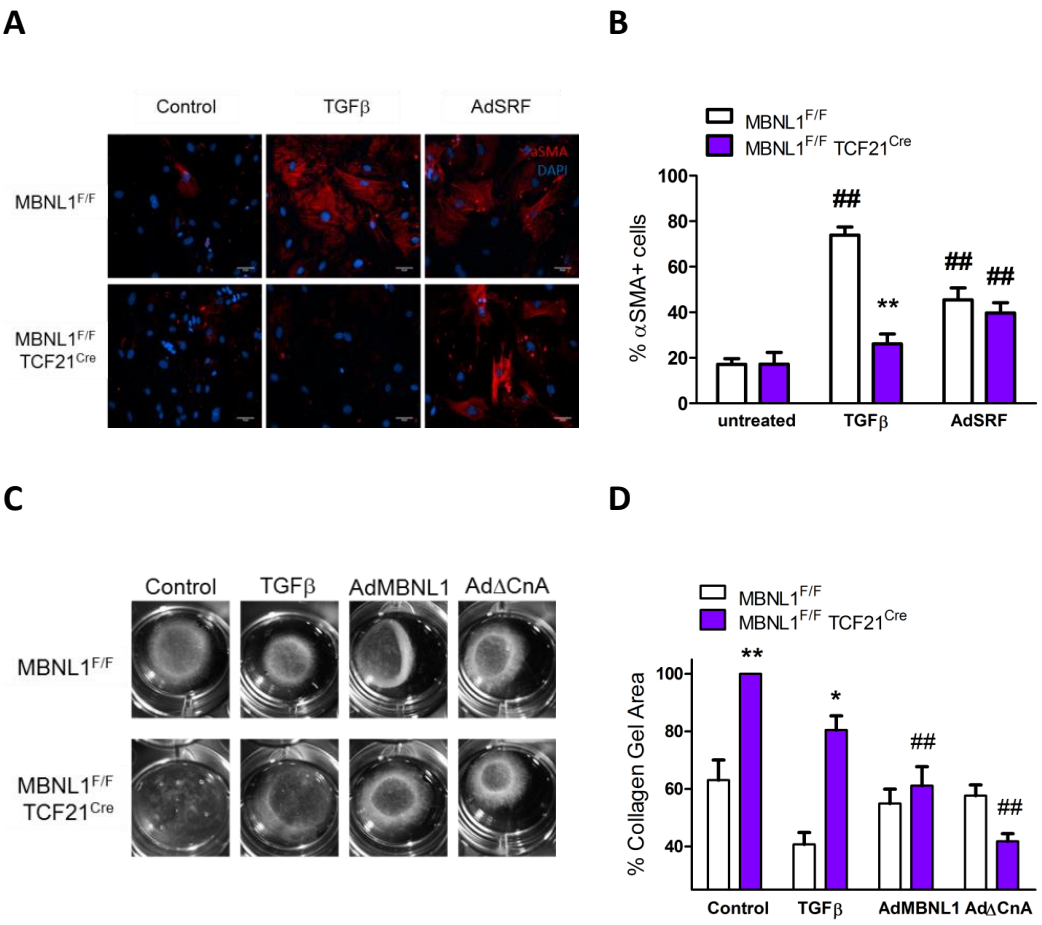

Figure 2.5. MBNL1-dependent transcriptome maturation is necessary for the programmed differentiation of resident cardiac fibroblasts into myofibroblasts.
(A) Representative immunofluorescent images and (B) quantification of the number of αSMA+ stress fibers (red) in MBNL1$^{F/F}$ vs. MBNL1$^{F/F}$ TCF21^{Cre} cardiac fibroblasts after 72 hours of TGFβ or adenovirally transduced SRF (AdSRF). Dapi (blue) was used as a nuclear stain. Scale bar = 50 μm. Data show the average number of αSMA+ cells normalized to the total number of nuclei ± SEM; n ≥ 130. **P < 0.01 vs. MBNL1$^{F/F}$, ##P < 0.01 vs. untreated. (C) Representative images and (D) quantification of contracted collagen gel matrices seeded with MBNL1$^{F/F}$ or MBNL1$^{F/F}$ TCF21^{Cre} cardiac fibroblasts. Cells were treated with TGFβ or an adenovirus containing MBNL1 (AdMBNL1) or constitutively active calcineurin (AdΔCnA) for 65 hours. The full uncontracted collagen gel is measured from the area of the bottom of one well in a 12-well culture plate. Average ± SEM; n = 3. *P < 0.05 vs. MBNL1$^{F/F}$, **P < 0.01 vs. MBNL1$^{F/F}$, ##P < 0.01 vs. control.

2.3.3 MBNL1 Depletion in Resident Cardiac Fibroblasts Reduces Proliferation

Proliferation rates in both control and MBNL1-depleted cardiac fibroblasts measured as the number of EdU+ cells were not different in low serum or differentiation conditions, suggesting that the above myofibroblast differentiation results were not due to diminished fibroblast numbers during the assay time frame. Preliminary data show there was a significant decrease in proliferation in MBNL1-

deficient cardiac fibroblasts compared to controls in high serum conditions, suggesting MBNL1 is necessary for proliferation and myofibroblast differentiation (Figure 2.7A).

2.3.4 Cardiac Fibroblast-Specific Activation of MBNL1 Induces Diastolic Dysfunction, Promotes Myofibroblast Transformation, and Decreases Proliferation

To determine if overexpression of MBNL1 *in vivo* promotes quiescent cardiac fibroblasts to differentiate into myofibroblasts and lead to cardiac dysfunction, we used an engineered transgenic (Tg) mouse model in which MBNL1 expression is elevated with tamoxifen-inducible Cre-dependent recombination in TCF21+ cardiac fibroblasts (MBNL1 Tg TCF21^{Cre}; Figure 2.6A). Here, we show after two weeks on tamoxifen, eight week old MBNL1 Tg TCF21^{Cre} mice have a significant increase in isovolumetric relaxation time (IVRT) compared to littermate controls when assessed with Tissue Doppler echocardiography (Figure 2.6B) but no change in heart weight to body weight ratio (Figure 2.6C). Upon examination of hearts for collagen deposition and myofibroblasts, we found there was no difference between genotypes (Figure 2.6D). However, when cardiac fibroblasts were enzymatically isolated from cardiac tissue and plated on soft substrates, MBNL1 Tg TCF21^{Cre} cells had an increased propensity for myofibroblast differentiation over littermate controls as indicated by the presence of αSMA+ stress fibers but not to the same extent as treatment with TGFβ (Figure 2.6E-F).

Proliferation significantly decreased in MBNL1 Tg TCF21^{Cre} cardiac fibroblasts compared to littermate controls in high serum, low serum, and differentiation conditions (Figure 2.7B). This is consistent with results from αSMA stained cells (Figure 2.3E-F) suggesting MBNL1 Tg TCF21^{Cre} cardiac fibroblasts have an intrinsic capacity for myofibroblast differentiation and thus a decreased capacity for proliferation.

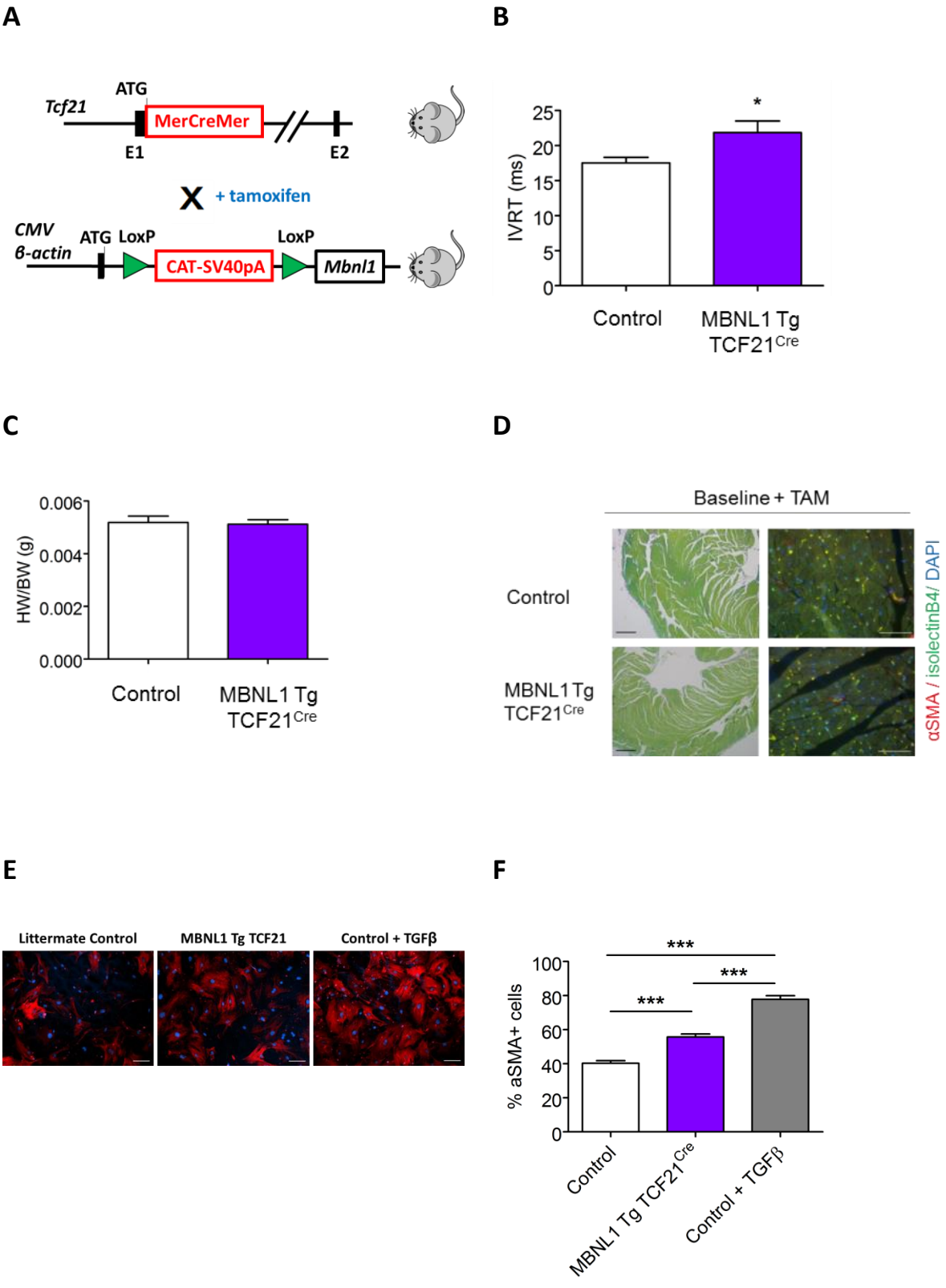

Figure 2.6. MBNL1 gain of function in cardiac fibroblasts increases the propensity for myofibroblast differentiation.

(A) **Schematic of mice with the *Tcf21* locus containing a tamoxifen-inducible MCM cDNA and loxP-targeted allele flanking a stop cassette upstream of the *Mbnl1* gene to allow for *Mbnl1* overexpression after tamoxifen treatment. (B) Graph of isovolumetric relaxation time (IVRT) assessed by Tissue Doppler echocardiography in control and MBNL1 Tg TCF21^{Cre} mice after two weeks of tamoxifen treatment. (C) Quantification of heart weight (HW) normalized to body weight (BW) at eight weeks of age. (D) Sirius red/fast green stained histological images (left) from the hearts of the indicated genotypes with representative images of immunofluorescent staining for myofibroblasts. For images in the right panel in D, myofibroblasts are defined as alpha smooth muscle actin (αSMA) positive (shown in red) and isolectin B4 (IB4) negative (shown in green). Dapi (blue) was used to mark nuclei. Scale bar = 50 μm. 10 sections were measured per heart; n ≥ 5 mice per group. (E) Representative images and (F) quantification of αSMA (red) stress fibers and dapi (blue) nuclei from control and MBNL1 Tg TCF21^{Cre} cardiac fibroblasts plated on 300 MPa substrates. Data are average ± SEM of n ≥ 500 total cells per condition, *t*-test, ***P < 0.001. Scale bar = 100 μm.**

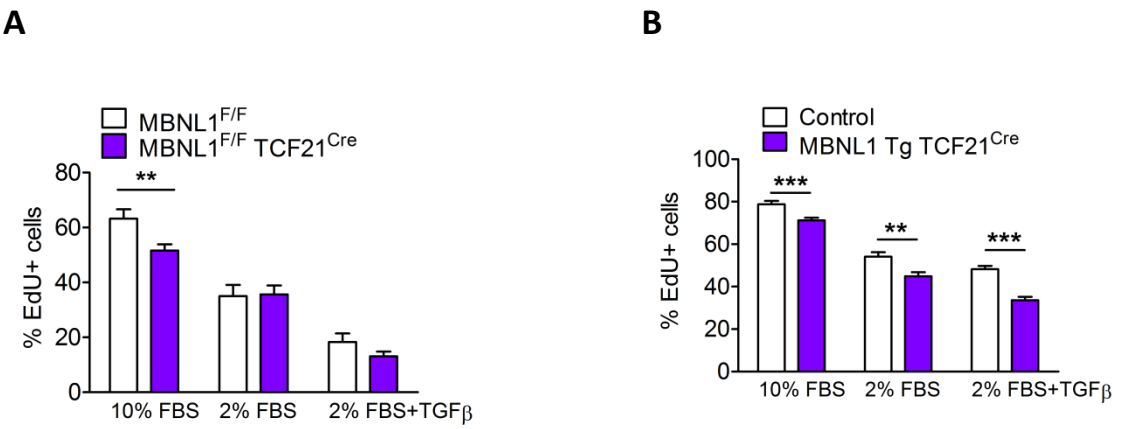

Figure 2.7. MBNL1 loss of function and overexpression in resident cardiac fibroblast decreases proliferation. Proliferation rates in (A) MBNL1$^{F/F}$ and MBNL1$^{F/F}$ TCF21^{Cre} isolated cardiac fibroblasts and (B) littermate controls and MBNL1 Tg TCF21^{Cre} isolated cardiac fibroblasts measured by incorporation of EdU after 72 hours in either 10% fetal bovine serum (FBS) media, 2% FBS media, or 2% FBS media with TGFβ treatment. Data show average cell number normalized to total nuclei ± SEM; n ≥ 175. **P < 0.01 and ***P < 0.001 vs control mice.

2.3.5 Identification of the MBNL1 Interactome Suggests MBNL1 Acts as a Scaffold Protein to Recruit RNA Processing Machinery

Since MBNL1 is a RNA-binding protein with no catalytic domain, we wanted to know what other proteins interact with MBNL1 to promote myofibroblast transformation and subsequent fibrotic remodeling. To answer this, we performed an immunoprecipitation of MBNL1 and identified novel protein complexes using an unbiased mass spectrometry approach. We quantified the MBNL1 interactome of mouse embryonic fibroblasts (MEFs) as they differentiated toward myofibroblasts using LFQ proteomics. MEFs were induced to differentiate with AdMBNL1. We immunoprecipitated (IP)

MBNL1 in both untreated and AdMBNL1-treated cells and compared them against IgG IP. Protein quantification was reproducible with an average Pearson's correlation of 0.90 across all samples (data not shown). Principal component analysis and unbiased hierarchical clustering confirmed distinction between the different samples with replicates clustering close together (data not shown). A total of 778 proteins were identified and quantified, of which 5 were significantly enriched in MBNL1 IP samples compared to IgG IP samples, with MBNL1 having the highest significance. The next most significant proteins are known to form a protein complex and regulate RNA elongation and include Cyclin-T1, Cyclin-dependent kinase 9 (Cdk9), HEXIM1, and MEPCE (Figure 2.8A). These four proteins were also significantly enriched in AdMBNL1-treated MBNL1 IP samples compared to IgG IP samples along with 16 other proteins with GO-TERM biological processes including RNA processing, splicing, localization, capping, among others (Figure 2.8B and Table 2.1). The RNA elongation complex identified was validated to interact with MBNL1 via co-IPs and western blots in both MEFs and mouse heart tissue (Figure 2.8C-D). As Elavl1/HuR is one of the proteins identified in the MBNL1 overexpression samples and plays a role in the fibrotic injury response,[226,227,284–286] we probed the interaction of MBNL1 with Elavl1/HuR using western blotting of co-IPs and reciprocal co-IPs and discovered that Elavl1/HuR is also a binding partner with MBNL1 (Figure 2.8E).

A

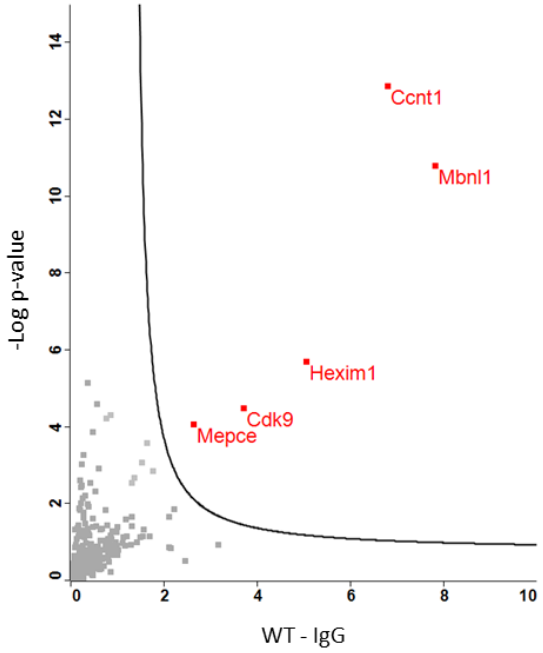
Ccnt1
Mbnl1
Hexim1
Cdk9
Mepce
-Log p-value
WT - IgG

B

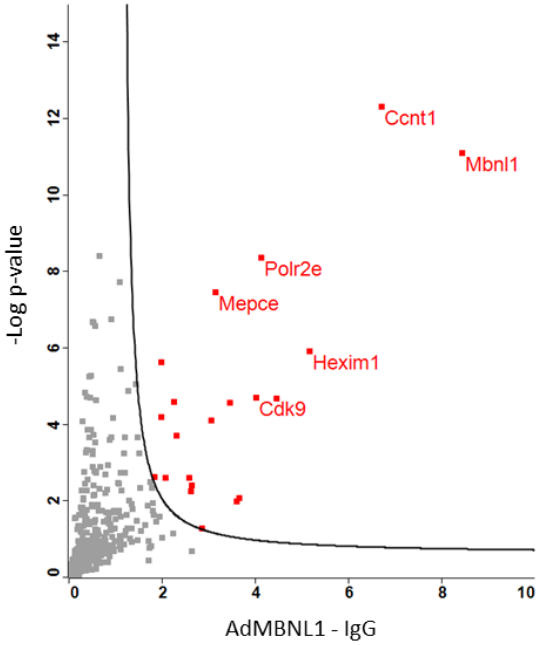
Ccnt1
Mbnl1
Polr2e
Mepce
Hexim1
Cdk9
-Log p-value
AdMBNL1 - IgG

C

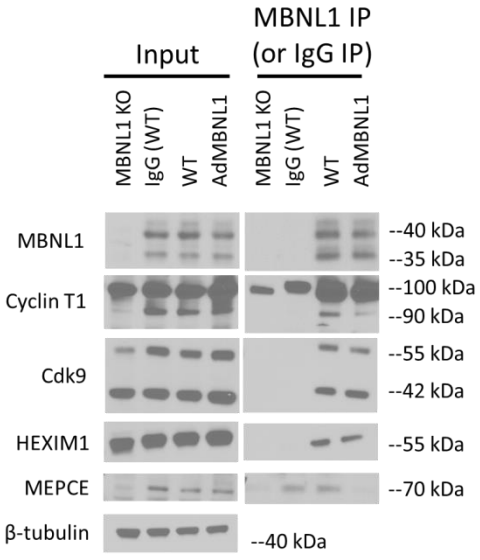
Input
MBNL1 IP
(or IgG IP)
MBNL1 KO
IgG (WT)
WT
AdMBNL1
MBNL1
Cyclin T1
Cdk9
HEXIM1
MEPCE
β-tubulin
--40 kDa
--35 kDa
--100 kDa
--90 kDa
--55 kDa
--42 kDa
--55 kDa
--70 kDa
--40 kDa

D

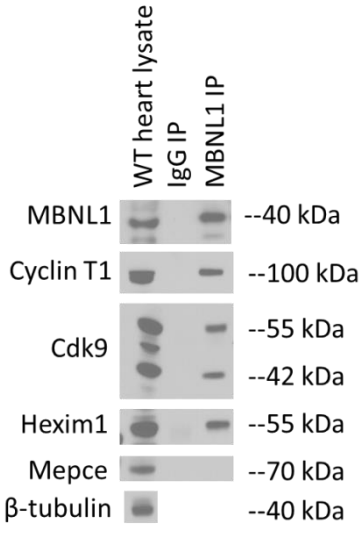
WT heart lysate
IgG IP
MBNL1 IP
MBNL1
Cyclin T1
Cdk9
Hexim1
Mepce
β-tubulin
--40 kDa
--100 kDa
--55 kDa
--42 kDa
--55 kDa
--70 kDa
--40 kDa

E

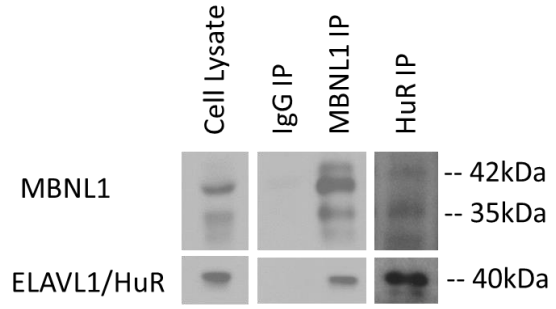

Figure 2.8. MBNL1 protein-protein interactions.
Volcano plots showing differences of (A) MBNL1 IP to IgG IP samples and (B) MBNL1 IP to IgG IP samples infected with AdMBNL1 in wild-type mouse embryonic fibroblasts (MEFs) on the x-axis vs. the –log of the p-value on the y-axis. The line denotes a 0.05% false discovery rate. Proteins in red are significantly different between conditions with some gene names denoted. Verification of MBNL1-protein interactions by western blot using MBNL1 IP in (C) MEFs and (D) heart lysates. IgG IP in wild-type MEFs and MBNL1 knockout MEFs were used as negative controls and beta-tubulin was used as a loading control. (E) Western blot of MBNL1 IP and HuR IP and reciprocal co-IPs showing MBNL1 and Elavl1/HuR are binding partners in MEFs. IgG IP was used as a non-specific binding control.

Table 2.1. GO-term/Kegg pathway analysis for proteins significantly interacting with MBNL1 in AdMBNL1 treated MEF samples.

Go-term / Kegg Pathway	Enrichment Score	Cluster frequency	P Value
RNA processing & splicing	10.41	20	6.40E-16
Spliceosome	10.41	8	8.70E-07
Nuclear lumen	6	20	2.20E-07
Posttranscriptional regulation of gene expression	3.97	10	7.10E-08
RNA localization	3.97	6	2.50E-05
mRNA capping	3.7	3	1.60E-04
Translation	1.89	7	6.40E-03
Cytoskeleton	1.79	18	3.40E-03
DNA-directed RNA polymerase II, core complex	1.62	5	1.10E-03
Muscle tissue development	0.97	4	6.40E-02
Helicase activity	0.36	13	2.90E-01

2.3.6 Loss of MBNL1 in Cardiac Myocytes Reduces Fibrotic Scarring.

Davis et al.[69] previously showed complete loss of MBNL1 in a mouse causes heart rupture in 40% of mice after MI due to a lack of fibrotic scar formation to provide structural support to the heart during the wound healing process. Because those studies (1) were performed in global MBNL1 knockout mice

and (2) MBNL1 functions in multiple cardiac cell types, the cell-specific contribution of MBNL1 function to the heart's response to MI is still unclear. Our data above shows fibroblast-specific loss of MBNL1 reduces fibrosis after MI but does not affect systolic function. Furthermore, the hearts from $MBNL1^{F/F}$ $TCF21^{Cre}$ did not rupture after MI, suggesting other cells might contribute to fibrosis and the effects seen in the MBNL1 global knockout mouse model. Since cardiomyocytes are the main contractile cell unit of the heart,[18] make up the bulk of the myocardium,[18] and directly interact with cardiac fibroblasts,[287] we aimed to understand the role of MBNL1 in cardiomyocytes during cardiac fibrotic remodeling.

To accomplish this, $MBNL1^{F/F}$ mice were crossed with mice expressing a constitutively active cre recombinase regulated by the alpha myosin heavy chain (*αMHC*) promoter, which is specific to cardiomyocytes. These mice we termed $MBNL1^{F/F}$ αMHC^{Cre} (Figure 2.9A). Echocardiographic assessment at eight weeks of age and measurement of heart weights post-mortem determined that $MBNL1^{F/F}$ αMHC^{Cre} mice had no change in heart weight to body weight ratio, fractional shortening (FS), intraventricular septum thickness (IVS), left ventricular posterior wall thickness (LVPW), or left ventricular internal diameter (LVID) compared to $MBNL1^{F/F}$ littermate controls (Figure 2.9B-F).

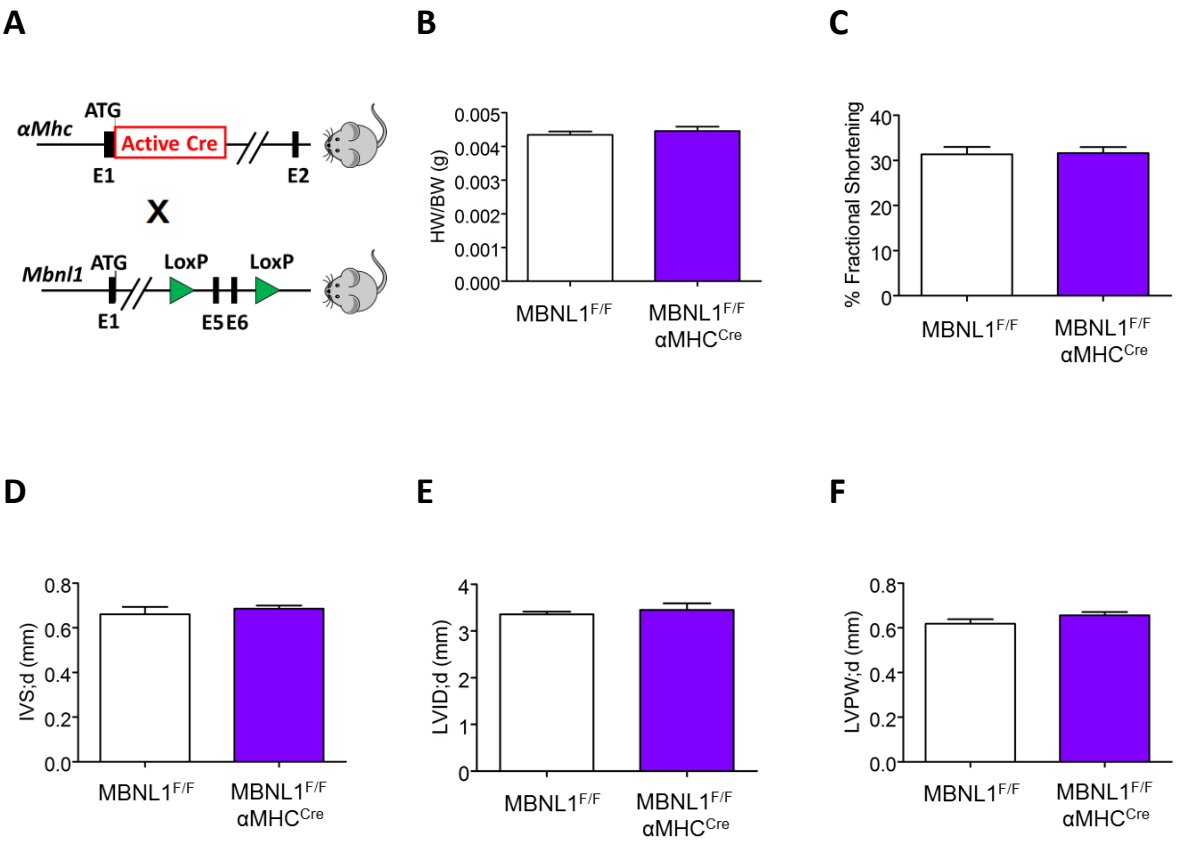

Figure 2.9. MBNL1 deletion in cardiomyocytes does not alter cardiac structure or function.
(A) Schematic of mouse breeding scheme. (B) Heart weight (HW) normalized to body weight (WT) for eight week old MBNL1$^{F/F}$ αMHC^{Cre} mice. Echocardiography of (C) fractional shortening, (D) intraventricular septum diameter (IVSD), (E) left ventricular interior diameter (LVID), and (F) left ventricular posterior wall (LVPW) thickness measured in the diastolic dimension of eight week old MBNL1$^{F/F}$ and MBNL1$^{F/F}$ αMHC^{Cre} mice. Data are mean ± SEM for n ≥ 3.

To determine if MBNL1 function in cardiomyocytes contributes to post-infarct fibrotic remodeling, MBNL1$^{F/F}$ and MBNL1$^{F/F}$ αMHC^{Cre} mice were subjected to permanent LAD ligation. Compared to MBNL1$^{F/F}$ littermate controls, MBNL1$^{F/F}$ αMHC^{Cre} mice had significantly reduced cardiac fibrosis with no change in cardiac mass four weeks post-infarct (Figure 2.10A-C). When we performed a pairwise comparison for changes in LVID and FS before and after infarct, we observed no difference between genotypes, suggesting loss of MBNL1 in cardiomyocytes does not affect ventricular dilation or systolic function after MI(Figure 2.10D-E).

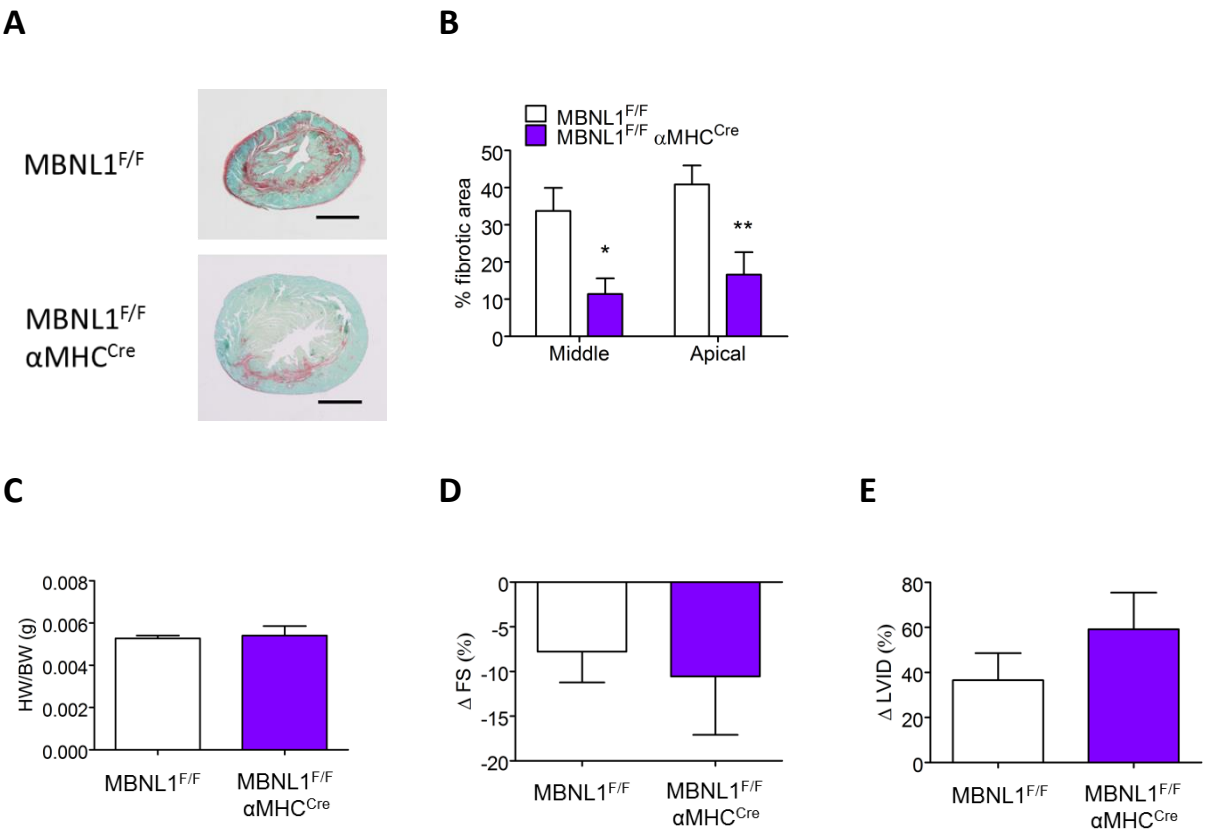

Figure 2.10. Depletion of MBNL1 in cardiomyocytes reduces ventricular scarring four weeks after infarct.
(A) Paraffin-embedded 5 µm thick transverse sections of MBNL1$^{F/F}$ and MBNL1$^{F/F}$ αMHC^{Cre} infarcted mouse hearts stained with Sirius red/fast green. Scale bar = 1 mm. (B) Quantification of fibrotic area in infarcted MBNL1$^{F/F}$ and MBNL1$^{F/F}$ αMHC^{Cre} mouse hearts as a percent of red area to overall stained area in A from middle and apical transverse sections 200 µm apart. (C) Quantification of heart weight (HW) normalized to body weight (BW) for MBNL1$^{F/F}$ and MBNL1$^{F/F}$ αMHC^{Cre} mice four weeks after MI. (D) Pairwise comparison of echocardiography from pre-MI to four weeks post-MI for percent change in fractional shortening (ΔFS) and (E) percent change in left ventricular interior diameter (ΔLVID). Data are averages ± SEM, n ≥ 3 mice, *t*-test, *$P < 0.05$ and **$P < 0.01$ vs. MBNL$^{F/F}$.

2.3.7 Cardiomyocyte-Specific Overexpression of MBNL1 Causes Dilated Cardiomyopathy and Heart Failure after MI

Given that MBNL1 promotes cardiomyocyte maturation,[218,288,289] we reasoned that cardiac myocyte specific overexpression should initiate a pathologic phenotype and worsen maladaptive remodeling. To test this hypothesis, conditional MBNL1 Tg mice were mated with the αMHC^{Cre} mice. These mice are termed MBNL1 Tg αMHC^{Cre} (Figure 2.11A). At baseline just weeks after tamoxifen

inductions, MBNL1 Tg αMHC^{Cre} mice had enlarged atria and cardiomyocyte hypertrophy compared to littermate controls (Figure 2.11B-D). When cardiomyocytes were isolated and measured for cellular dimensions, MBNL1 Tg αMHC^{Cre} cardiomyocytes had a significant increase in length, width, and area of the cell compared to littermate controls (Figure 2.11E-G). MBNL1 Tg αMHC^{Cre} mice as early has two weeks of age have enlarged atria and smaller, dilated ventricles compared to littermate controls (Figure 2.11H-I). This phenotype is even more pronounced when mice were aged to two and six months (Figure 2.11B, H-J). Echocardiography assessment shows two month old MBNL1 Tg αMHC^{Cre} mice have a significant decrease in fractional shortening and a significant increase in left ventricular interior diameter compared to littermates (Figure 2.11K-L), suggesting MBNL1 Tg αMHC^{Cre} mice experience eccentric cardiomyocyte hypertrophy. Using Tissue Doppler and pulse wave analysis, we show six month aged MBNL1 Tg αMHC^{Cre} mice have substantial ventricular remodeling, systolic dysfunction, and a restrictive filling pattern, displaying progression towards heart failure (Figure 2.11H and Table 2.2). To our surprise, we did not observe a significant difference between genotypes in spontaneous death for aged mice (data not shown).

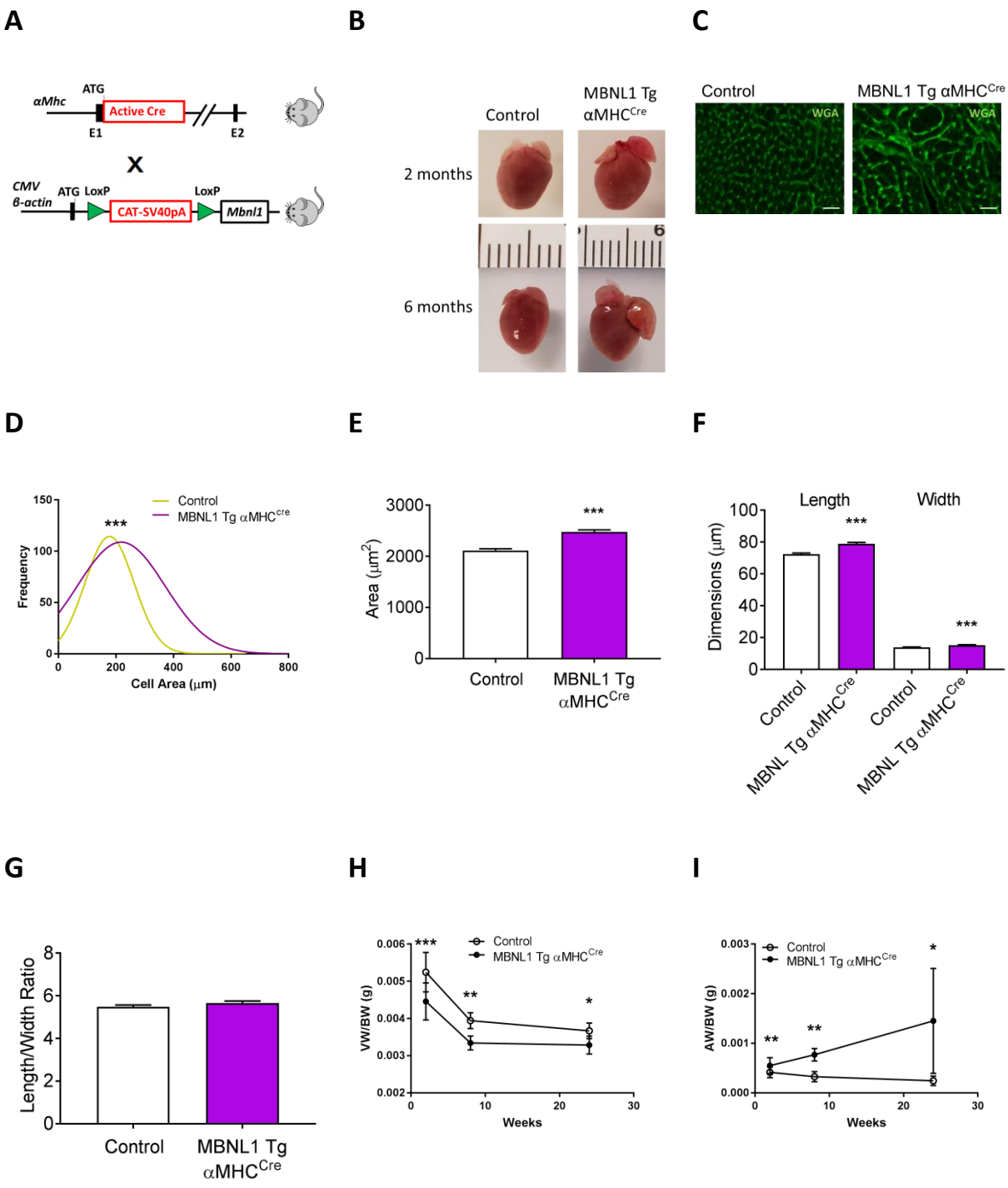
A
αMhc
ATG
Active Cre
E1
E2
X
CMV
β-actin
ATG LoxP
LoxP
CAT-SV40pA
Mbnl1
B
Control
MBNL1 Tg
αMHCCre
2 months
6 months
C
Control
MBNL1 Tg αMHCCre
WGA
WGA
D
Control
MBNL1 Tg αMHCcre
***
Frequency
Cell Area (μm)
E
***
Area (μm2)
Control
MBNL1 Tg
αMHCCre
F
Length
Width
***
***
Dimensions (μm)
Control
MBNL Tg αMHCCre
Control
MBNL Tg αMHCCre
G
Length/Width Ratio
Control
MBNL1 Tg
αMHCCre
H
***
**
*
Control
MBNL1 Tg αMHCCre
VW/BW (g)
Weeks
I
*
**
**
Control
MBNL1 Tg αMHCCre
AW/BW (g)
Weeks

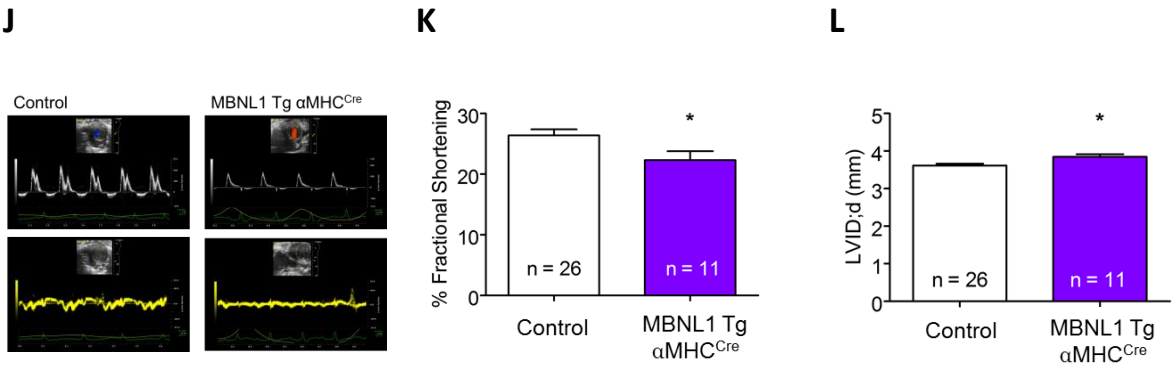

Figure 2.11. Cardiomyocyte-specific overexpression of MBNL1 causes atrial enlargement, ventricular dilation, and cardiomyocyte hypertrophy.
(A) Schematic of mouse breeding scheme. (B) Representative images for gross anatomy of control and MBNL1 Tg αMHC^{Cre} adult mouse hearts at two months and six months of age. Image of ruler in the middle measures in mm. (C) Wheat germ albumin (WGA) staining of paraffin-embedded 5 µm-thick transverse heart sections from two month old control and MBNL1 Tg αMHC^{Cre} mice. Scale bar = 25 µm. (D) Distribution of cell areas (µm) is plotted for WGA stained hearts in B. Cell areas were quantified by tracing cross-sectional cardiomyocyte cell membranes. Mann-Whitney comparison of ranks was used for testing statistical significance; n ≥ 450 cells; ***P < 0.001 between genotypes. (E) Area, (F) length and width measurements, and (G) length to width ratio of cardiomyocytes isolated from control and MBNL1 Tg αMHC^{Cre} mice. Average ± SEM, n = 200 cells per mouse, n ≥ 2 mice, t-test, ***P < 0.001 vs. control mice. Quantification of (H) ventricle weight (VW) and (I) atria weight (AW) normalized to BW over time in 2 week, 2 month, and 6 month old control and MBNL1 Tg αMHC^{Cre} mice. Average ± SEM, n ≥ 4 mice, t-test, *P < 0.05, **P < 0.01, ***P < 0.001 for each time point vs. control mice. (J) Representative traces of Tissue Doppler Imaging (top panels) and Pulse Wave (bottom panels) echocardiographs for six month old control and MBNL1 Tg αMHC^{Cre} mice. Echocardiography of (K) percent fractional shortening and (L) left ventricular interior diameter measured in the diastolic dimension (LVID;d) for two month old mice of respected genotypes. Average ± SEM, number of mice denoted on graph, t-test, *P < 0.05.

Table 2.2. Systolic and diastolic function in 6 month old mice measured by M-mode, Pulse-Wave, and Tissue Doppler echocardiography.

Genotype	n	MV IVS e'/a'	MV E/A	IVRT (ms)	MV E/e'	FS (%)	IVS;d (mm)	LVID;d (mm)	LVPW;d (mm)
Control	5	1.06 ± 0.22	1.55 ± 0.11	19.83 ± 1.89	-28.21 ± 2.85	42.26 ± 5.54	1.05 ± 0.06	3.67 ± 0.12	0.85 ± 0.04
MBNL1 Tg αMHC^{Cre}	7	0.49 ± 0.03	4.18 ± 0.93	19.68 ± 3.43	-61.16 ± 7.46	21.77 ± 3.70	0.90 ± 0.08	4.31 ± 0.23	0.71 ± 0.03
P-value		0.02*	0.02*	0.97	0.01**	0.01*	0.17	0.05*	0.01*

Values represent the mean ± standard error of the mean. MV, mitral valve; IVS, intraventricular septum; IVRT, isovolumetric relaxation time; FS, fractional shortening; LVID;d, left ventricular interior diameter measured in the diastolic dimension; LVPW;d, left ventricular posterior wall thickness measured in the diastolic dimension.

2.4 Conclusions

Prior to this study, it was unclear if cardiomyocytes and cardiac fibroblasts both contribute to MBNL1-dependent fibrotic remodeling after MI. Studies in myotonic dystrophy mouse models with depletion of MBNL1 globally in the mouse causes cardiac dysfunction as well as cardiac rupture after permanent coronary ligation.[69,242,262,269–271] Thus, we expected to observe cardiac abnormalities in the $MBNL1^{F/F}$ αMHC^{Cre} mice compared to $MBNL1^{F/F}$ mice; however, we did not observe any gross phenotypic differences. However, further in depth analyses will be needed to determine the full extent of $MBNL1^{F/F}$ αMHC^{Cre} heart function. A reduction of fibrosis was also observed in cardiomyocyte-specific MBNL1 loss of function mice compared to littermate controls after MI.(Figure 2.10) Our results also demonstrate that genetic deletion of MBNL1 in resident cardiac fibroblasts diminishes fibrosis and protects against the detrimental fibrotic remodeling response after MI (Figure 2.3 and Figure 2.4). The results of this study show that MBNL1 is both necessary and sufficient for myofibroblast differentiation from resident cardiac fibroblasts (Figure 2.7) as loss of MBNL1 in adult cardiac fibroblasts failed to differentiate into myofibroblasts and form contractile αSMA stress fibers with TGFβ stimulation. This is consistent with previous studies in mouse embryonic fibroblasts, suggesting fibroblasts are a major cell type contributing to MBNL1-dependent fibrosis.[69]

We've shown previously that MI-injured MBNL1 knockout mice have a high mortality rate due to a significant reduction in fibrotic scarring that causes ventricular wall rupture. Consistent with impaired myofibroblast differentiation in these mice, these data suggest MBNL1 is a critical factor in cardiac fibroblasts for acute wound healing.[69] However, when MBNL1 was conditionally deleted in cardiac fibroblasts, ventricular wall integrity remained intact (Figure 2.3 and Figure 2.4). This could be attributed to a number of reasons. First, due to incomplete genetic recombination there remains a population of TCF21+ cardiac fibroblast that express MBNL1 (Figure 2.2). Thus, it is possible there may be a sufficient level of MBNL1 expression for fibroblast phenotypic conversion to a contractile cell type

which prevented heart rupture. Second, it is possible that MBNL1-deficient resident cardiac fibroblasts could partially differentiate into proto-myofibroblasts due to insufficient genetic recombination, paracrine signaling from other cells, or MBNL1-independent signaling pathways, and thus have enough of a contractile phenotype maintain ventricular wall stability post-MI. Proto-myofibroblasts in which focal adhesions are immature actin stress fibers contain cytoplasmic β-actin rather than αSMA can secrete large amounts of fibrotic matrix, and thus can contribute to fibrotic scarring.[66] Third, it is possible there are other myofibroblast populations that were derived from TCF21-negative cells such as pericytes or fibrocytes that contribute to fibrotic remodeling. Finally, cardiomyocytes could contribute to ventricular wall integrity as cardiomyocytes often become hypertrophic and increase contractile properties post-MI.[4] However, our results show cardiomyocyte-specific MBNL1 loss of function results in a decrease in collagen deposition post MI compared to littermate controls without heart rupture. This suggests there could be another cell type that contributes to ventricular wall integrity in MBNL1-dependent cardiac fibrosis. One cell type of interest is the erythrocyte. MBNL1 promotes terminal differentiation of erythrocytes, and erythrocytes contribute to ECM homeostasis (discussed further in chapter 3). However, the requirement of MBNL1 in erythropoiesis after myocardial infarction is a subject of future experiments.

The results from the MBNL1 loss of function mice post-MI are not due to an underlying cardiac phenotype (Figure 2.2); however, activation of MBNL1 and downstream MBNL1-bound mRNA transcripts in what would otherwise be called quiescent fibroblasts produced αSMA-positive contractile myofibroblasts and minor diastolic dysfunction in mice (Figure 2.6). Incidentally, isolated cardiac fibroblasts from these mice spontaneously differentiate into myofibroblasts when separated from surrounding heart cells by enzymatic digestion. We plated the cells on soft substrates to maintain fibroblasts in a more quiescent state that more closely mimics their native environment. The soft coverslips we used were 300MPa, which is orders of magnitude lower than tissue culture plastic and

glass coverslips which are on the order of GPa. Nonetheless, cardiac fibroblasts isolated from control mice still spontaneously differentiated to a certain extent, albeit not to the same degree as MBNL1 Tg TCF21^{Cre} cells or those treated with TGFβ. We have previously shown MBNL1 Tg TCF21^{Cre} mice elicit a fibrotic response only after extended time on tamoxifen or with stress-dependent co-stimuli.[69] These data suggest cardiac fibroblasts overexpressing MBNL1 need a stimulation (such as mechanical forces from cell isolation) to differentiate into myofibroblasts. In fact, MBNL1 binds to *Mapk14* transcripts and suggests MBNL1 might regulate p38 mitogen-activated protein kinase signaling cascades that transduce cytokine and mechanical signals into myofibroblast differentiation through SRF and calcineurin.[154] Moreover, our data show overexpression of MBNL1 using transgenic approaches in cardiomyocytes caused eccentric hypertrophy and enlarged atria with hypertrophic ventricular cardiomyocytes and diastolic dysfunction consistent with restrictive cardiomyopathy that worsened with age (Figure 2.11). Although it has not yet been directly tested, one could hypothesize that MBNL1 Tg αMHC^{Cre} mice have increased fibrosis over littermate controls. This would thus result in a reduction of contractility and subsequent cardiac remodeling in the form of cardiomyocyte eccentric hypertrophy, enlarged atria, and smaller, dilated ventricles and could explain why aged MBNL1 Tg αMHC^{Cre} mice do not have increased mortality over littermate controls.

Furthermore, our observations suggest MBNL1 acts to potentiate myofibroblast transformation by regulating pre-existing transcripts. This is justified by the idea that MBNL1 acts as a master regulator of cell differentiation through its ability to regulate mRNA during development of skeletal muscle, cardiac muscle, and red blood cells as well as negatively regulating pluripotency of ESCs.[218,230,234,244,245,248,249] For example, sarcoplasmic reticulum transcripts that encode proteins involved in initiation of skeletal muscle differentiation are enhanced by MBNL1 for adult muscle maturation but can also be misspliced in the absence of MBNL1 which cause myotonic phenotypes.[251,253,290] Additionally, if MBNL1 acts as an early factor to accelerate differentiation, it may increase activity during the

proliferation phase and promote both differentiation and proliferation (Figure 2.4). Thus, modifying the dose of MBNL1 could have impacts in either direction, but further gene expression analyses of cell cycle and cell cycle inhibitor genes are needed to parse out this information.

From previous data in our lab, we found that MBNL1 binds over 2500 transcripts in multiple signaling pathways to direct myofibroblast differentiation which ultimately results in scar formation and fibrotic remodeling of the heart. However, it was unknown how MBNL1 guides the processing and maturation of target transcripts. MBNL1 is thought to recruit RNA processing machinery to specific genomic locations in a dose-dependent manner. Our data show there is a novel subset of MBNL1-interacting proteins unique to the MBNL1 overexpression group when compared to the IgG IP control group (Figure 2.8), suggesting that the MBNL1 interactome is dynamically context-dependent with changes in MBNL1 dose affecting protein-protein interactions. This is consistent with previous reports showing a gradual decrease in MBNL1 protein amount increases severity of missplicing of mRNA transcripts.[291] GO-term analysis of proteins that bind with MBNL1 suggests that MBNL1 interacts with RNA-binding protein complexes to regulate transcript maturation through such processes as mRNA capping, splicing, polyadenylation, and transport. Thus, missplicing events observed in myotonic dystrophy mouse models could be due to a decrease in recruitment of prominent splicing factors and a lack of transcriptome maturation. Specifically, our data show Elavl1/HuR is a direct binding partner with MBNL1 (Figure 2.8). Reciprocal co-IP with Elavl1/HuR confirms this interaction. Similar to MBNL1, Elavl1/HuR is a RBP that binds AREs and contributes to the fibrotic response after cardiac ischemic injury (reviewed in chapter 1), but we were the first to show that there is a direct interaction with these proteins in mouse fibroblasts. Also, we found a brand new interacting complex (the positive transcription elongation factor b (P-TEFb)) that has never before been associated with MBNL1, suggesting MBNL1 might have an novel role in RNA elongation. This is relevant for cell differentiation as

RNA elongation is required to produce more transcripts and evade the DNA damage response (discussed further in chapter 3).

In this study, we provide a targeted cell-specific approach to understanding MBNL1's role in myofibroblast transformation *in vivo.* MBNL1 is integral in regulating key transcripts and determining how resident cardiac fibroblasts respond to injury by differentiating into myofibroblasts. The data presented here propose a new regulatory mechanism in which MBNL1 binds to mRNA processing machinery and proteins involved in RNA elongation. Furthermore, our data suggest MBNL1 can have a protective effect against maladaptive cardiac remodeling and fibrosis if it is depleted in cardiac fibroblasts *in vivo.* As MBNL1 remains at the center of myofibroblast differentiation signaling networks and coordinates thousands of transcripts, it presents as a potential viable therapeutic target for current RNA-based strategies.

3 Future Directions and Concluding Remarks

Our study aimed to understand the contribution of MBNL1 in resident cardiac fibroblasts and cardiomyocytes to cardiac fibrosis and function after acute myocardial infarction. Previously, our lab showed global knockout of *Mbnl1* results in heart rupture after MI due to a reduction in protective scar formation.[69] MBNL1 binds and stabilizes transcripts in nodal signaling pathways such as SRF and calcineurin to promote myofibroblast differentiation from mouse embryonic fibroblasts.[69] However, this result was not tested in resident cardiac fibroblasts. Furthermore, the role of MBNL1 in cardiomyocytes after MI had not been elucidated. Here, we demonstrated that MBNL1 is required in both cardiac fibroblasts and cardiomyocytes for cardiac fibrotic remodeling after MI. We showed that MBNL1 promotes myofibroblast differentiation from resident cardiac fibroblasts and confirmed that SRF and calcineurin function downstream of MBNL1. Furthermore, constitutively active expression of *Mbnl1* in cardiomyocytes results in eccentric hypertrophy. These findings solidify the idea that MBNL1 acts as a

maturation factor and master regulator of cell differentiation.[218,230,234,244,245,248,249] Notably, the reduction in fibrosis improved cardiac function and did not result in ventricular wall rupture as seen in the global *Mbnl1* knockout animal. This suggests there is another cell type that contributes to MBNL1-mediated fibrotic remodeling after myocardial infarction.

One unexplored research avenue is the possibility of MBNL1 promoting erythrocyte terminal differentiation after myocardial infarction, which could explain the preserved ventricular integrity. MBNL1 is required for erythrocyte terminal differentiation.[249] However, it is currently unknown if MBNL1 is required for erythropoiesis after cardiac injury such as a myocardial infarction. Approximately 1% of erythrocytes are renewed daily, but this percentage can increase with stress such as with a myocardial infarction. Control of erythropoiesis expansion and colony forming unit erythroid cell differentiation into basophilic erythroblasts are regulated by the cytokine erythropoietin (EPO). EPO has cardioprotective effects on the heart by decreasing myocardial apoptosis, promoting angiogenesis, and limiting interstitial collagen deposition.[292–294] This cardioprotective effect is part of the natural wound healing response as *Epo* mRNA expression increases about 10-fold after permanent coronary artery occlusion compared to sham mice[295] as well as about a 2 fold increase in serum *Epo* levels in human patients after MI.[296] Erythrocytes also interact with extracellular matrix. For example, fetal liver erythroid progenitor cells cultured on fibronectin and treated with EPO expanded in culture to a greater extent than controls, but fibronectin was only required at later stages of terminal erythrocyte differentiation.[297] Engagement of $\alpha_4\beta_1$ integrin by fibronectin is necessary for terminal erythrocyte differentiation and proliferation.[297] Furthermore, *p38α* knockout mice have an approximately 20-fold reduction in *Epo* gene expression. These mice are defective in erythropoiesis as indicated by a reduction in erythrocyte cell progenitors in early stages of differentiation and a decrease in enucleation compared to wildtype controls, suggesting *p38α* is required for erythrocyte differentiation.[298] As mentioned above, p38α is a key regulator in myofibroblast differentiation and is a known target of MBNL1.[69,154] *Mbnl1*

gene expression is 5-10 fold higher in erythroid tissue compared to epithelial tissue although it is unclear how this expression level changes after cardiac injury.[249] Thus, erythropoiesis and migration of red blood cells to the infarct area could be sufficient to maintain ventricular wall integrity and cardiac function even despite the loss of *Mbnl1* function in fibroblasts or cardiomyocytes. However, the role of MBNL1 in the erythrocyte will need to be directly tested in the context of myocardial infarction (Figure 3.1).

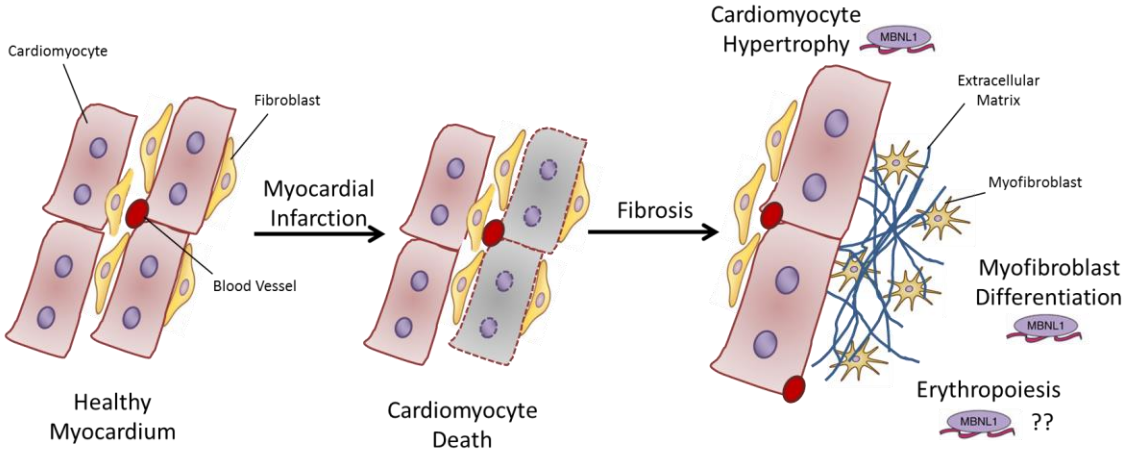

Figure 3.1. Cell-specific MBNL1 contribution to fibrosis after myocardial infarction.
Following myocardial infarction, substantial cardiomyocyte death triggers an extensive multi-cellular response that contributes to extracellular matrix deposition (fibrosis). Data from this study shows MBNL1 contributes to cardiomyocyte hypertrophy and myofibroblast differentiation, but it is known if MBNL1 plays a role in erythropoiesis after myocardial infarction.

Our data found a novel interaction of the positive transcription elongation factor b (P-TEFb) protein complex with MBNL1, suggesting MBNL1 could escape from the DNA damage response (DDR) by promoting RNA elongation and terminal cell differentiation. We hypothesize that myocardial infarction elicits a DNA damage response that stimulates transcription of nodal signaling pathways that promotes cell differentiation through a MBNL1/P-TEFb-mediated RNA elongation mechanism.

More globally, terminal cell differentiation can be a response to DNA damage (DDR) to preserve genomic integrity in numerous cell types.[299,300] For example, doxorubicin-induced double stranded breaks in ESCs repressed *Nanog* expression, which is required for ESC self-renewal. The repression of *Nanog* through a p53-dependent mechanism promotes ESC differentiation and cell-cycle arrest.[301] In terminally differentiated cells such as neurons and astrocytes, DNA repair is only maintained in genes

which are actively transcribed. For example, early studies in primary post-mitotic neurons of chick and mouse embryos showed there was a lower level of unscheduled DNA synthesis (UDS) and nucleotide excision repair.[302,303] A similar effect is seen in skeletal muscle cells in which primary rat embryonic skeletal muscle cells and chick skeletal myotubes were exposed to methyl-methanesulfate and UV light, respectively, to induce DNA damage. This resulted in a decrease in UDS as the cells matured into muscle fibers.[304,305] Although mature terminally differentiated erythrocytes do not contain nuclei and thus have no need for DNA damage repair, avian erythrocytes retain their nuclei and are unable to repair DNA strand breaks after X-ray irradiation.[306] A much more recent study investigating DNA damage in rat cardiac myofibroblasts demonstrated that although the cells were non-apoptotic as measured by flow cytometry and caspase-dependent cleavage of cytokeratin 18, they had substantial DNA damage via TUNEL staining. This suggests that myofibroblasts retain DNA damage after differentiation.[307] Human patients also have retention of DNA damage after MI. Shahzad *et al.* (2018) recently evaluated 125 patients who experienced a MI for redox status and found higher levels of DNA damage (assessed by serum 8OHdG levels) and membrane deterioration in erthryocytes in patients with MI compared to healthy individuals.[308]

DNA damage results in stalling of RNA Pol II at the lesion site, which prevents the synthesis of the gene where it is docked as well as prevents RNA Pol II from functionally transcribing other genes. This could ultimately result in RNA Pol II degradation by the ubiquitin pathway.[309] Release of pausing involves DDR signaling. Bunch *et al.* (2015) monitored phosphorylated histone variant H2AX (γH2AX) as an early marker for induction of DNA double-stranded breaks. They discovered γH2AX accumulates prior to transcription elongation, suggesting DDR signaling is required for RNA Pol II release and activation.[310]

Release of the paused RNA Pol II to allow transcription also requires the P-TEFb protein complex, which is composed of a Cyclin T1/Cdk9 heterodimer and Brd4 [311]. Brd4 is a bromodomain

protein that is thought to bind to acetylated histones and direct CyclinT1/Cdk9 to regions of the genome that are marked as transcriptionally active [312]. P-TEFb acts to phosphorylate negative elongation factor (NELF), DRB sensitivity inducing factor (DSIF), and the carboxyl terminal domain of the large subunit of RNA Pol II.[313–315] NELF inhibits elongation and only short transcripts are generated that may be prematurely terminated.[311] Phosphorylation of these proteins allows for the transition into productive elongation by the movement of the RNA polymerase II and subsequent synthesis of mRNAs. P-TEFb itself is also tightly regulated by a complex of RNA-binding proteins (RBPs) including HEXIM, MEPCE, LARP7, hnRNPs, and the 7SK snRNP. Hexamethylene bisacetamide inducible (HEXIM) is a double-stranded RBP that binds to 7SK snRNP, a non-coding RNA, and P-TEFb to functionally inhibit P-TEFb kinase activity.[316] Methylphosphate capping enzyme (MEPCE) methylates 7SK snRNP and the La-related protein 7 (LARP7) binds to the 3' end of 7SK snRNP. While the association of HEXIM and P-TEFb to 7SK snRNP is reversible, MEPCE and LARP7 are stable components and are almost always found to bind with 7SK snRNP.[317,318] The release of P-TEFb is followed by the release of HEXIM and both are replaced by heterogenous nuclear ribonucleoproteins (hnRNPs) on the 7SK snRNP molecule to allow for active P-TEFb to promote productive elongation.[319]

Components of the P-TEFb complex are directly involved in DDR signaling and maintaining genomic stability. For example, CDK9 localizes on chromatin in response to replication stress to limit the amount of single-stranded DNA, and depletion of *Cdk9* induces spontaneous DNA damage in replicating cells.[320] After ionizing radiation induces DNA damage, Brd4 suppresses γH2AX accumulation, condenses chromatin, and results in a loss of DDR signaling.[321]

P-TEFb plays a role in regulating cardiac growth and the differentiation of several cell types including skeletal muscle cells, monocytes, lymphocytes, and neurons, and an imbalance in the Cdk9/CyclinT1 ratio has been found in several cancer cell lines.[322–324] The induction of cardiomyocyte hypertrophy with calcineurin or mechanical stress in cultured cardiomyocytes results in the disruption of

the 7SK snRNP complex and activation of P-TEFb.[225,325] Consistent with this notion, the deletion of HEXIM1 from cardiomyocytes causes hypertrophy, suggesting HEXIM1 negatively regulates cardiac growth. In fact, ablation of cardiac lineage protein 1 (CLP-1), the mouse homolog of the human HEXIM1, in mice is lethal in late fetal stages. The lethality is likely caused by cardiac hypertrophy as CLP-$1^{-/-}$ fetal hearts had a reduced left ventricular chamber with thickened myocardial walls, confirming that HEXIM1 has a growth-inhibitory function during cardiac development through its inactivation of P-TEFb [326]. HEXIM1 also inhibits cell proliferation in breast epithelial cells, and its expression is down-regulated in breast tumors. Likewise, overexpression of HEXIM1 promotes stem cell differentiation and growth inhibition in multiple cell lineages, suggesting HEXIM1 is a global regulator of cellular proliferation and fate [327].

Espinoza-Derout et al. further explored the hypothesis that activated P-TEFb catalytic activity promotes cardiac hypertrophy by crossing a transgenic mouse strain in which CyclinT1 was overexpressed in the heart with a CLP-1-deleted mouse strain [328]. Thus, they wanted to create a mouse in which the level of the P-TEFb complex was considerably increased. Indeed, these mice had hearts with an increase in overall phosphorylation of the carboxyl terminus of RNA Pol II and striking ventricular hypertrophy [328]. These findings indicate there must be an appropriate equilibrium between P-TEFb and the 7SK snRNP complex in cardiomyocytes for proper functioning.

P-TEFb also plays a role in cardiac fibrosis. It was recently found that the serine kinase activity of Cdk9 not only targets RNA Pol II but also Smad3, which is downstream of TGFβ in the canonical signaling pathway [329,330]. Furthermore, the formation of a Smad3/Smad4/Cdk9 complex promotes renal fibrosis during ureteral obstruction, suggesting CLP-1 mediated changes in P-TEFb activity influences Cdk9-dependent Smad3 signaling to modulate fibrosis in multiple organs [329,330]. In fact, Mascareno et al. showed AngII overexpression in heterozygous CLP-$1^{+/-}$ mice caused cardiac hypertrophy and fibrosis with an increase in Smad3 phosphorylation [331]. These studies underlie the importance of transcriptional

regulation in remodeling the genetic response during pathological events such as hypertrophy and fibrosis. However, there is very little known about how RNA elongation via the P-TEFb complex regulates myofibroblast differentiation and fibrotic remodeling *in vivo*.

It is also unclear if deletion of each protein in these complexes functionally disrupts RNA processing during myofibroblast differentiation. This MBNL1/P-TEFb complex with RBPs could have positive or negative influences on RNA products which need to be determined in independent assays. For example, MBNL1 could bind with the P-TEFb complex and act as a scaffold to recruit transcripts and other RNA processing machinery to promote cell differentiation. Depending on where MBNL1 binds in this complex could determine if MBNL1 blocks negative regulation with HEXIM1 and the 7SK-snRNP particle or if MBNL1 recruits them. One possibility is MBNL1 could bind in between the P-TEFb and its negative regulators, such as HEXIM1 to directly interfere or promote movement of RNA Pol II. Interactions with these protein complexes are likely context-dependent, and thus capturing transient interactions with MBNL1 would be greatly advantageous. Furthermore, functional assays to determine if proteins in the identified P-TEFb are necessary and sufficient for myofibroblast differentiation and post-infarction cardiac remodeling also need to be conducted. Based on the above information, one could hypothesize that MBNL1 binds with P-TEFb to positively regulate terminal cell differentiation that subsequently results in cardiac hypertrophy and fibrosis. For example, P-TEFb [225,328] and MBNL1 (Figure 2.11) are both shown to promote cardiac hypertrophy, suggesting they could have a cooperative role in mRNA transcript maturation to induce hypertrophic phenotypes. MBNL1 could also bind and functionally inhibit HEXIM1 as loss of HEXIM1 in cardiomyocytes causes hypertrophy in mice [326], whereas loss of MBNL1 protects the heart against aversive cardiac remodeling post-MI (Figure 2.10). Furthermore, our data show MBNL1 directly binds with several components of the P-TEFb complex and knockout of MBNL1 alters expression of these components, further emphasizing that these protein complexes have co-regulatory roles in myofibroblast differentiation (Figure 2.8).

Furthermore, one could speculate that MBNL1 binding with P-TEFb could potentiate pre-existing signaling pathways that promote myofibroblast differentiation and cardiac hypertrophy. For example, our data show loss of MBNL1 in fibroblasts and cardiomyocytes reduce fibrosis to a similar extent (Figure 2.4 and Figure 2.10), suggesting similar RNA regulatory events occurs in fibroblasts and cardiomyocytes during fibrotic remodeling. This could be attributed to a loss in transcript stability as seen previously with MBNL1 knockout disrupting stabilization of SRF and TGFβR2.[69] Studies of other RNA-binding proteins further justify this hypothesis as the RBPs AUF1, HuR, and hnRNP-A1 all mediate mRNA stability of the β1-adrenergic receptor, which contributes to pathogenesis of cardiovascular disease as down-regulation of β1-adrenergic receptor in the heart results in reduced contraction.[216] Terminal differentiation of fibroblasts and cardiomyocytes could also be due to a shift in alternative polyadenylation. In heart failure patients and hypertrophied mouse hearts, there is a shift in APA towards proximal cleavage sites, which generate shortened 3' UTRs and thus increased gene expression. [221–223] APA is tightly regulated with RNA elongation .[332] For example, ELAVL1/HuR is recruited by RNA Pol II to bind to U-rich sequences near proximal polyadenylation sites to sterically block activation, resulting in pausing of RNA Pol II and long 3' UTRs. [284,286] Thus, one could propose that fibroblast- and cardiomyocyte-specific MBNL1 loss of function have elongated 3' UTRs and depressed RNA elongation, leading to decreased protein production. In contrast, MBNL1 Tg TCF21^{Cre} and MBNL1 Tg αMHC^{Cre} mice could have shorter mRNA 3' UTR isoforms that escape miRNA repression to produce more protein and cause increased fibrosis and enlargement of cardiomyocytes, respectively. Evidence in TAC models provides further support for this hypothesis as fetal gene programs are reactivated after pressure overload with transcriptome shifts towards mRNA with shorter 3' UTRs.[222] However, the temporal expression of MBNL1 has not been directly measured in the progression of cardiac remodeling, and as such, it is still unknown whether MBNL1 is needed to initiate a signaling cascade or maintain it (or both). This is an important avenue to explore to understand terminal differentiation of cellular phenotypes and

potentially filling in knowledge gaps about how maturation of cell states contributes to the transition from acute wound healing to chronic maladaptive cardiac remodeling.

APA and RNA elongation are also intimately involved in transcript localization, which is important not only for placing transcripts in the correct position of translation but also can determine where genes are expressed in discrete cellular compartments. Lessons from brain studies show us varying 3' UTR length through APA can vastly change their localization within the cell. For example, APA regulates brain-derived neurotrophic factor (BDNF) mRNA localization as short 3' UTR isoforms are found in the neuronal soma, whereas long isoforms are present in dendrites. The localization and length of these isoforms dictates their translational efficiencies, which has implications for synaptic function of the hippocampus.[333] Therefore, mRNA isoforms with different 3' UTR lengths can have distinct impacts on cellular function with different transcript decay rates and localization leading to different amounts of protein products. Importantly, MBNL proteins in C2C12 mouse myoblasts can be differentially localized, and knockdown of MBNL causes the distribution of mRNAs to change between cytosolic and insoluble fractions. mRNAs with MBNL binding sites in alternative 3' UTRs are more affected by the knockdown, suggesting that different localization patterns are mediated by MBNL.[236] These findings demonstrate that the 3' UTR region is highly dynamic during normal development as well as in disease states and plays a crucial role in orchestrating RBP function. Taken together, RBPs can regulate transcription at various levels to completely alter a cell's phenotype just through modulating their activity or expression.

One unanswered question from our data is if the MBNL1-protein interactome regulates RNA at specific genomic locations. We hypothesize that relative positioning of MBNL1 on a region of RNA with recruitment of RNA processing machinery determines how the transcriptome matures. Knowledge of the functional MBNL1-protein interactome and how it regulates transcriptome programming and cell fate is still largely underdeveloped. MBNL1 has proposed mechanisms in mRNA capping, alternative splicing and polyadenylation, transport and localization, and now elongation to functionally mature the

transcriptome during the fibrotic phase of wound healing.[236] Thus, understanding how MBNL1 simultaneously coordinates multiple arms of the myofibroblast differentiation signaling network would provide value insights into the progression from the acute wound healing response after MI to the chronic phase that results in fibrosis and scarring (Figure 3.2). Findings from those studies could produce novel druggable targets for mediating cardiac fibrotic remodeling.

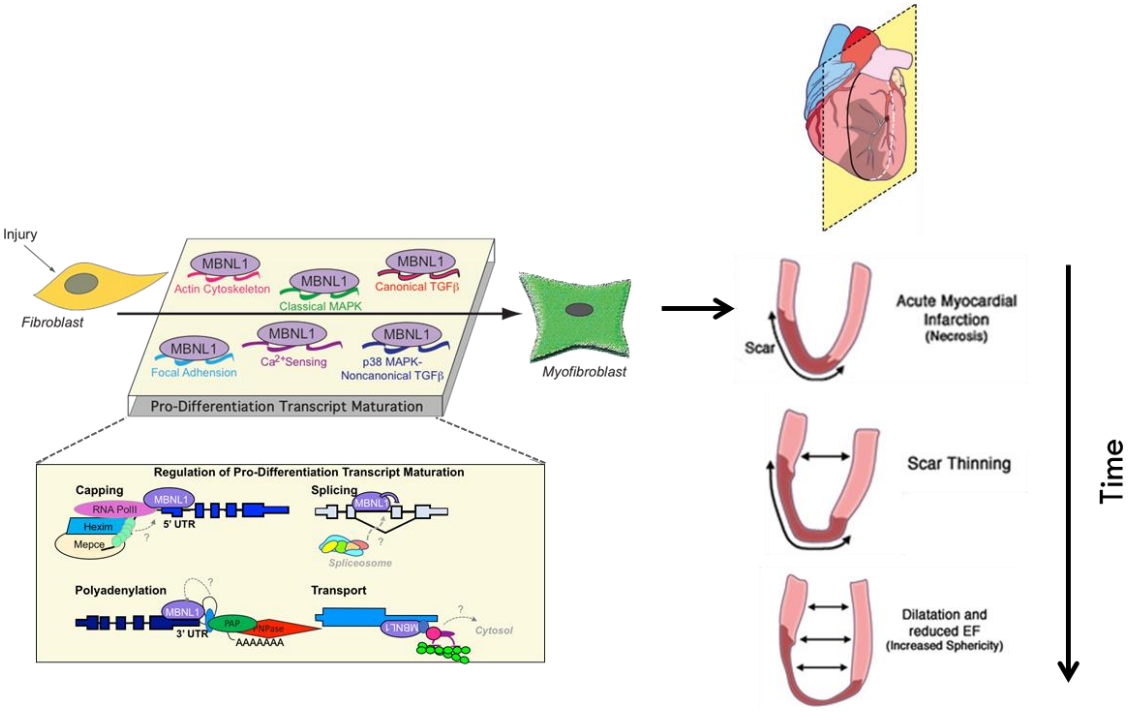

Figure 3.2. Model of MBNL1-mediated transcript maturation to promote myofibroblast differentiation.
We propose MBNL1 recruits RNA processing machinery to a specified genomic location for activation of multiple nodal signaling pathways involved in myofibroblast differentiation. Possible mechanisms include mRNA capping, splicing, polyadenylation, and transport. These mechanisms mature transcripts and could function to regulate myofibroblast differentiation and subsequent fibrotic remodeling in the heart. Image credit: Jennifer Davis and adaption from Seropian et al. (2014) *JACC.* [69,334]

But is MBNL1 a good therapeutic target? Several research groups have purposed promoting a gain of function of *Mbnl1* with the use of a nonsteroidal anti-inflammatory drug, phenylbutazone, which was shown to upregulate *Mbnl1* expression in C2C12 myoblasts as well as in the DM1 mouse model.[335] Others have proposed targeting the interaction of MBNL1 with CUG RNA repeats.[336–338] However, all of these therapeutics are aimed at increased *Mbnl1* expression in DM1 models where there is a functional

depletion of the protein. However, in the context of cardiac fibrosis, functionally depleting *Mbnl1* while still maintaining ventricular integrity would be the ideal avenue to pursue, but we can still learn from the DM1 literature. One could imagine designing a CUG repeat oligomer that is delivered with an aptamer to sequester MBNL1 away from its target transcripts.[232] However, consideration of timing of delivery, localization (i.e. which cell type to target), and dosage will be crucial for designing an effective therapy.

According to the World Health Organization, 30% of the global population dies from cardiovascular disease each year. Although there has been a significant shift in the field of cardiovascular research from basic studies towards more clinical and translational goals, it is imperative to understand the biological mechanisms of cardiac repair for the field to be successful in developing effective therapies. Every type of heart disease has a fibrotic component caused by chronic activation of myofibroblasts during the wound healing response. Despite the tissue of origin, myofibroblasts are a key cellular component to cardiac injury as they directly contribute to ECM metabolism by providing a protective scar to prevent heart rupture as well as promoting fulminant fibrosis that can lead to heart failure. Thus, understanding the molecular mechanisms of fibroblast transformation into myofibroblasts during the wound healing response can provide insights into therapeutic approaches for maintaining heart integrity and minimizing maladaptive remodeling. The information discussed in this dissertation were limited to coronary artery occlusion; however, the advancements in the field of RNA-binding protein regulation could have broad implications for other heart failure patients, such as those suffering from dilated cardiomyopathy, hypertrophic cardiomyopathy, congenital heart disease, or even myotonic dystrophy, to name a few.

Vita

Christina Jones grew up in Benbrook, TX, in a small town surrounded by cow pastures and good Tex-Mex. She completed her Bachelors of Arts at Austin College in Biochemistry with a Minor in Psychology. As an undergraduate researcher, she worked with Dr. Andrew Carr to understand gelling of ionic liquids with the Carr family organogelator and completed a senior thesis with Dr. John Richardson investigating misfolding of beta 2-microglobulin during amyloidosis. She also worked with Dr. Helmut Krämer at the University of Texas Southwestern to study mechanisms of ARC syndrome. She moved to Seattle, Washington in 2012 to pursue her PhD in Pharmacology at the University of Washington. When not working on her research, Christina enjoys playing underwater hockey, exploring the mountains of the Pacific Northwest, skiing, and sea kayaking. She also enjoys tasting the vast variety of delicious food Seattle has to offer.

4 References

1. Benjamin, E. J. *et al.* Heart Disease and Stroke Statistics-2017 Update: A Report From the American Heart Association. *Circulation* **135,** e146–e603 (2017).
2. Thygesen, K., Alpert, J. S. & White, H. D. Universal Definition of Myocardial Infarction. *J. Am. Coll. Cardiol.* **50,** 2173–2195 (2007).
3. Benjamin, E. J. *et al. Heart Disease and Stroke Statistics—2018 Update: A Report From the American Heart Association*. *Circulation* (2018). doi:10.1161/CIR.0000000000000558
4. Christia, P. *et al.* Systematic Characterization of Myocardial Inflammation, Repair, and Remodeling in a Mouse Model of Reperfused Myocardial Infarction. *J. Histochem. Cytochem.* **61,** 555–570 (2013).
5. Ongstad, E. & Kohl, P. Fibroblast-myocyte coupling in the heart: Potential relevance for therapeutic interventions. *J. Mol. Cell. Cardiol.* **91,** 238–246 (2016).
6. Chen, J. *et al.* A new model of congestive heart failure in rats. *AJP Hear. Circ. Physiol.* **301,** H994–H1003 (2011).
7. Murray, C. J. L. *et al.* Disability-adjusted life years (DALYs) for 291 diseases and injuries in 21 regions, 1990–2010: a systematic analysis for the Global Burden of Disease Study 2010. *Lancet* **380,** 2197–2223 (2012).
8. Burchfield, J. S., Xie, M. & Hill, J. A. Pathological ventricular remodeling: Mechanisms: Part 1 of 2. *Circulation* **128,** 388–400 (2013).
9. Chapman, B. L. Correlation of mortality rate and serum enzymes in myocardial infarction Test of efficiency of coronary care. *Br. Heart J.* **33,** 643–646 (1971).
10. Grande, P. & Pedersen, A. Myocardial infarct size: correlation with cardiac arrhythmias and sudden death. *Eur. Heart J.* **5,** 622–627 (1984).
11. Weber, K. T. Cardiac interstitium in health and disease: The fibrillar collagen network. *J. Am. Coll. Cardiol.* **13,** 1637–1652 (1989).
12. Anderson, K. R., Sutton, M. G. & Lie, J. T. Histopathological types of cardiac fibrosis in myocardial disease. *J. Pathol.* **128,** 79–85 (1979).
13. Hasenfuss, G. Animal models of human cardiovascular disease, heart failure and hypertrophy. *Cardiovasc. Res.* **39,** 60–76 (1998).
14. deAlmeida, A. C., van Oort, R. J. & Wehrens, X. H. T. Transverse Aortic Constriction in Mice. *J. Vis. Exp.* 7–9 (2010). doi:10.3791/1729
15. Reddy, S. *et al.* Physiologic and molecular characterization of a murine model of right ventricular volume overload. *American Journal of Physiology - Heart and Circulatory Physiology* **304,** H1314-27 (2013).
16. Shimada, Y. J. *et al.* Effects of Losartan on Left Ventricular Hypertrophy and Fibrosis in Patients with Nonobstructive Hypertrophic Cardiomyopathy. *J. Am. Coll. Cardiol.* **1,** 480–487 (2013).
17. Caulfield, J. B., Leinbach, R. & Gold, H. The relationship of myocardial infarct size and prognosis. *Circulation* **53,** I141-4 (1976).
18. Zhou, Pingzhu; Pu, W. Recounting cardiac cellular composition. **118,** 368–370 (2016).
19. Ali, S. R. *et al.* Existing cardiomyocytes generate cardiomyocytes at a low rate after birth in mice. *Proc. Natl. Acad. Sci.* **111,** 8850–8855 (2014).
20. Sun, Z. *et al.* Inhibition of Wnt/β-catenin signaling promotes engraftment of mesenchymal stem cells to repair lung injury. *J. Cell. Physiol.* **229,** 213–24 (2014).
21. Van Berlo, J. H. *et al.* C-kit+cells minimally contribute cardiomyocytes to the heart. *Nature* **509,** 337–341 (2014).
22. Senyo, S. E. *et al.* Mammalian heart renewal by pre-existing cardiomyocytes. *Nature* **493,** 433–

436 (2013).
23. Bergmann, O. *et al.* Evidence for Cardiomyocyte Renewal in Humans. *Science (80-.).* **324,** 98–102 (2009).
24. Becker, R. C. *et al.* A composite view of cardiac rupture in the United States National Registry of Myocardial Infarction. *J. Am. Coll. Cardiol.* **27,** 1321–1326 (1996).
25. Gao, X. M. *et al.* Lower risk of postinfarct rupture in mouse heart overexpressing β2-adrenergic receptors: Importance of collagen content. *J. Cardiovasc. Pharmacol.* **40,** 632–640 (2002).
26. Gao, X. M., White, D. A., Dart, A. M. & Du, X. J. Post-infarct cardiac rupture: Recent insights on pathogenesis and therapeutic interventions. *Pharmacol. Ther.* **134,** 156–179 (2012).
27. Naeim, F., De la Maza, L. M. & Robbins, S. L. Cardiac rupture during myocardial infarction. A review of 44 cases. *Circulation* **45,** 1231–1239 (1972).
28. Schuster, E. H. & Bulkley, B. H. Expansion of transmural myocardial infarction: a pathophysiologic factor in cardiac rupture. *Circulation* **60,** 1532–1538 (1979).
29. Dewald, O. *et al.* Of mice and dogs: species-specific differences in the inflammatory response following myocardial infarction. *Am. J. Pathol.* **164,** 665–677 (2004).
30. Chen, W. & Frangogiannis, N. G. Fibroblasts in post-infarction inflammation and cardiac repair. *Biochim. Biophys. Acta - Mol. Cell Res.* **1833,** 945–953 (2013).
31. van Nieuwenhoven, F. A. & Turner, N. A. The role of cardiac fibroblasts in the transition from inflammation to fibrosis following myocardial infarction. *Vascul. Pharmacol.* **58,** 182–188 (2013).
32. Sun, Y., Zhang, J. Q., Zhang, J. & Lamparter, S. Cardiac remodeling by fibrous tissue after infarction in rats. *J. Lab. Clin. Med.* **135,** 316–323 (2000).
33. Virag, J. I. & Murry, C. E. Myofibroblast and Endothelial Cell Proliferation during Murine Myocardial Infarct Repair. *Am. J. Pathol.* **163,** 2433–2440 (2003).
34. Li, L., Zhao, Q. & Kong, W. Extracellular matrix remodeling and cardiac fibrosis. *Matrix Biol.* **68–69,** 490–506 (2018).
35. Kong, P., Christia, P. & Frangogiannis, N. G. The Pathogenesis of Cardiac Fibrosis. *Cell Mol Life Sci* **71,** 549–574 (2014).
36. Frangogiannis, N. G. The extracellular matrix in myocardial injury, repair, and remodeling. *J. Clin. Invest.* **127,** 1600–1612 (2017).
37. Olivetti, G., Capasso, J. M., Sonnenblick, E. H. & Anversa, P. Side-to-side slippage of myocytes participates in ventricular wall remodeling acutely after myocardial infarction in rats. *Circ. Res.* **67,** 23–34 (1990).
38. Jugdutt, B. I., Joljart, M. J. & Khan, M. I. Rate of collagen deposition during healing and ventricular remodeling after myocardial infarction in rat and dog models. *Circulation* **94,** 94–101 (1996).
39. Brown, R. D., Ambler, S. K., Mitchell, M. D. & Long, C. S. THE CARDIAC FIBROBLAST: Therapeutic Target in Myocardial Remodeling and Failure. *Annu. Rev. Pharmacol. Toxicol.* **45,** 657–687 (2005).
40. Hinz, B. The myofibroblast: Paradigm for a mechanically active cell. *J. Biomech.* **43,** 146–155 (2010).
41. Wells, R. G. & Discher, D. E. Matrix Elasticity, Cytoskeletal Tension, and TGF-β: The Insoluble and Soluble Meet. *Sci. Signal.* **1,** 1–6 (2009).
42. Davis, J. & Molkentin, J. D. Myofibroblasts: Trust your heart and let fate decide. *J. Mol. Cell. Cardiol.* **70,** 9–18 (2014).
43. Hinz, B. *et al.* The Myofibroblast: One Function, Multiple Origins. *Am. J. Pathol.* **170,** 1807–1816 (2007).
44. Tomasek, J. J., Gabbiani, G., Hinz, B., Chaponnier, C. & Brown, R. A. Myofibroblasts and mechano: Regulation of connective tissue remodelling. *Nat. Rev. Mol. Cell Biol.* **3,** 349–363 (2002).
45. Gabbiani, G. The myofibroblast in wound healing and fibrocontractive diseases. *J. Pathol.* **200,** 500–503 (2003).

46. Chang, H. Y. *et al.* Diversity, topographic differentiation, and positional memory in human fibroblasts. *Proc. Natl. Acad. Sci.* **99,** 12877–12882 (2002).
47. Wang, H., Haeger, S. M., Kloxin, A. M., Leinwand, L. A. & Anseth, K. S. Redirecting valvular myofibroblasts into dormant fibroblasts through light-mediated reduction in substrate modulus. *PLoS One* **7,** (2012).
48. DeForest, C. A. & Anseth, K. S. Advances in bioactive hydrogels to probe and direct cell fate. *Annu. Rev. Chem. Biomol. Eng.* **3,** 421–44 (2012).
49. Camelliti, P., Borg, T. K. & Kohl, P. Structural and functional characterisation of cardiac fibroblasts. **65,** 40–51 (2005).
50. Kohl, P., Camelliti, P., Burton, F. L. & Smith, G. L. Electrical coupling of fibroblasts and myocytes: Relevance for cardiac propagation. *J. Electrocardiol.* **38,** 45–50 (2005).
51. Kohl, P., Kamkin, A., Kiseleva, I. & Noble, D. Mechanosensitive fibroblasts in the sino-atrial node region of rat heart: interaction with cardiomyocytes and possible role. *Exp. Physiol.* **79,** 943–956 (1994).
52. Souders, C. A., Bowers, S. L. K. & Baudino, T. A. Cardiac fibroblast: The renaissance cell. *Circ. Res.* **105,** 1164–1176 (2009).
53. Talman, V. & Ruskoaho, H. Cardiac fibrosis in myocardial infarction—from repair and remodeling to regeneration. *Cell Tissue Res.* **365,** 563–581 (2016).
54. Krenning, G., Zeisberg, E. M. & Kalluri, R. The origin of fibroblasts and mechanism of cardiac fibrosis. *J. Cell. Physiol.* **225,** 631–637 (2010).
55. Baxter, S. C., Morales, M. O. & Goldsmith, E. C. Adaptive Changes in Cardiac Fibroblast Morphology and Collagen Organization as a Result of Mechanical Environment. *Cell Biochem. Biophys.* **51,** 33–44 (2008).
56. Jugdutt, B. Remodeling of the Myocardium and Potential Targets in the Collagen Degradation and Synthesis Pathways. *Curr. Drug Target -Cardiovascular Hematol. Disord.* **3,** 1–30 (2003).
57. Hinz, B. It has to be the αv: myofibroblast integrins activate latent TGF-β1. *Nat. Med.* **19,** 1567–1568 (2013).
58. Munger, J. S. *et al.* Latent transforming growth factor-β: Structural features and mechanisms of activation. *Kidney Int.* **51,** 1376–1382 (1997).
59. Wipff, P. J., Rifkin, D. B., Meister, J. J. & Hinz, B. Myofibroblast contraction activates latent TGF-β1 from the extracellular matrix. *J. Cell Biol.* **179,** 1311–1323 (2007).
60. Klingberg, F. *et al.* Prestress in the extracellular matrix sensitizes latent TGF-β1 for activation. *J. Cell Biol.* **207,** 283–97 (2014).
61. Viereck, J., Bang, C., Foinquinos, A. & Thum, T. Regulatory RNAs and paracrine networks in the heart. *Cardiovasc. Res.* **102,** 290–301 (2014).
62. Porter, K. E. & Turner, N. A. Cardiac fibroblasts: At the heart of myocardial remodeling. *Pharmacol. Ther.* **123,** 255–278 (2009).
63. Slater, M. Dynamic interactions of the extracellular matrix. *Histol. Histopathol.* **11,** 175–180 (1996).
64. Snider, P. *et al.* Origin of cardiac fibroblasts and the role of periostin. *Circ. Res.* **105,** 934–947 (2009).
65. Serini, G. *et al.* The Fibronectin Domain ED-A Is Crucial for Myofibroblastic Phenotype Induction by Transforming Growth Factor-β1. *J. Cell Biol.* **142,** 873–881 (1998).
66. Hinz, B. Masters and servants of the force: The role of matrix adhesions in myofibroblast force perception and transmission. *Eur. J. Cell Biol.* **85,** 175–181 (2006).
67. Gabbiani, G., Hirschel, B. J., Ryan, G. B., Statkov, P. R. & Majno, G. Granulation tissue as a contractile organ: A study of structure and function. *J. Exp. Med.* **135,** 719–734 (1972).
68. Skalli, O. A monoclonal antibody against alpha-smooth muscle actin: a new probe for smooth

muscle differentiation. *J. Cell Biol.* **103,** 2787–2796 (1986).
69. Davis, J. *et al.* MBNL1-mediated regulation of differentiation RNAs promotes myofibroblast transformation and the fibrotic response. *Nat. Commun.* **6,** 10084 (2015).
70. Darby, I., Skalli, O. & Gabbiani, G. Alpha-smooth muscle actin is transiently expressed by myofibroblasts during experimental wound healing. *Lab. Invest.* **63,** 21–29 (1990).
71. Desmoulière, A., Redard, M., Darby, I. & Gabbiani, G. Apoptosis mediates the decrease in cellularity during the transition between granulation tissue and scar. *Am. J. Pathol.* **146,** 56–66 (1995).
72. Hinz, B., Mastrangelo, D., Iselin, C. E., Chaponnier, C. & Gabbiani, G. Mechanical tension controls granulation tissue contractile activity and myofibroblast differentiation. *Am. J. Pathol.* **159,** 1009–1020 (2001).
73. Santiago, J. J. *et al.* Cardiac fibroblast to myofibroblast differentiation in vivo and in vitro: Expression of focal adhesion components in neonatal and adult rat ventricular myofibroblasts. *Dev. Dyn.* **239,** 1573–1584 (2010).
74. Fu, X. *et al.* Specialized fibroblast differentiated states underlie scar formation in the infarcted mouse heart. *J. Clin. Invest.* **128,** 2127–2143 (2018).
75. Vracko, R. & Thorning, D. Contractile cells in rat myocardial scar tissue. *Lab. Invest.* **65,** 214–227 (1991).
76. Sun, Y. & Weber, K. T. Infarct scar: a dynamic tissue. *Cardiovasc. Res.* **46,** 250–256 (2000).
77. Willems, I. E., Havenith, M. G., De Mey, J. G. & Daemen, M. J. The alpha-smooth muscle actin-positive cells in healing human myocardial scars. *Am. J. Pathol.* **145,** 868–875 (1994).
78. Lemos, D. R. *et al.* Nilotinib reduces muscle fibrosis in chronic muscle injury by promoting TNF-mediated apoptosis of fibro/adipogenic progenitors. *Nat. Med.* **21,** 786–794 (2015).
79. Petrov, V. V, Fagard, R. H. & Lijnen, P. J. Stimulation of collagen production by transforming growth factor-beta1 during differentiation of cardiac fibroblasts to myofibroblasts. *Hypertension* **39,** 258–63 (2002).
80. Wang, H., Tibbitt, M. W., Langer, S. J., Leinwand, L. a & Anseth, K. S. Hydrogels preserve native phenotypes of valvular fi broblasts through an elasticity-regulated PI3K / AKT pathway. *Pnas* **110,** (2013).
81. Herum, K. M., Choppe, J., Kumar, A., Engler, A. J. & McCulloch, A. D. Mechanical regulation of cardiac fibroblast profibrotic phenotypes. *Mol. Biol. Cell* **28,** 1871–1882 (2017).
82. Hecker, L., Jagirdar, R., Jin, T. & Thannickal, V. J. Reversible differentiation of myofibroblasts by MyoD. *Exp. Cell Res.* **317,** 1914–1921 (2011).
83. Garrison, G. *et al.* Reversal of myofibroblast differentiation by prostaglandin E2. *Am. J. Respir. Cell Mol. Biol.* **48,** 550–558 (2013).
84. Artaud-Macari, E. *et al.* Nuclear Factor Erythroid 2-Related Factor 2 Nuclear Translocation Induces Myofibroblastic Dedifferentiation in Idiopathic Pulmonary Fibrosis. *Antioxid. Redox Signal.* **18,** 66–79 (2013).
85. Kisseleva, T. & Brenner, D. A. Inactivation of myofibroblasts during regression of liver fibrosis. *Cell Cycle* **12,** 381–2 (2013).
86. Troeger, J. S. *et al.* Deactivation of hepatic stellate cells during liver fibrosis resolution in mice. *Gastroenterology* **143,** 1073–1083 (2012).
87. Kanisicak, O. *et al.* Genetic lineage tracing defines myofibroblast origin and function in the injured heart. *Nat. Commun.* **7,** 12260 (2016).
88. Kisseleva, T. *et al.* Myofibroblasts revert to an inactive phenotype during regression of liver fibrosis. *Proc. Natl. Acad. Sci. U. S. A.* **109,** 9448–53 (2012).
89. Smith, C. L., Baek, S. T., Sung, C. Y. & Tallquist, M. D. Epicardial-derived cell epithelial-to-mesenchymal transition and fate specification require PDGF receptor signaling. *Circ. Res.* **108,**

(2011).
90. Moore-Morris, T., Cattaneo, P., Puceat, M. & Evans, S. M. Origins of cardiac fibroblasts. *J. Mol. Cell. Cardiol.* **91,** 1–5 (2016).
91. Moore-Morris, T. *et al.* Resident fibroblast lineages mediate pressure overload-induced cardiac fibrosis. *J. Clin. Invest.* **124,** 2921–34 (2014).
92. Moore-Morris, T., Tallquist, M. D. & Evans, S. M. Sorting out where fibroblasts come from. *Circ. Res.* **115,** 602–604 (2014).
93. Acharya, A. *et al.* The bHLH transcription factor Tcf21 is required for lineage-specific EMT of cardiac fibroblast progenitors. *Development* **139,** 2139–2149 (2012).
94. Ali, S. R. *et al.* Developmental heterogeneity of cardiac fibroblasts does not predict pathological proliferation and activation. *Circ. Res.* **115,** 625–635 (2014).
95. Braitsch, C. M., Kanisicak, O., van Berlo, J. H., Molkentin, J. D. & Yutzey, K. E. Differential expression of embryonic epicardial progenitor markers and localization of cardiac fibrosis in adult ischemic injury and hypertensive heart disease. *J. Mol. Cell. Cardiol.* (2013). doi:10.1080/10810730902873927.Testing
96. Aisagbonhi, O. *et al.* Experimental myocardial infarction triggers canonical Wnt signaling and endothelial-to-mesenchymal transition. *Dis. Model. Mech.* **4,** 469–483 (2011).
97. van Amerongen, M. J. *et al.* Bone marrow-derivedmyofibroblasts contribute functionally to scar formation after myocardial infarction. *J. Pathol.* **214,** 377–386 (2008).
98. Möllmann, H. *et al.* Bone marrow-derived cells contribute to infarct remodelling. *Cardiovasc. Res.* **71,** 661–671 (2006).
99. Zeisberg, E. M. *et al.* Endothelial-to-mesenchymal transition contributes to cardiac fibrosis. *Nat. Med.* **13,** 952–961 (2007).
100. Zeisberg, E. M. & Kalluri, R. Origins of cardiac fibroblasts. *Circ Res* **107,** 1304–1312 (2010).
101. Kong, P., Christia, P., Saxena, A., Su, Y. & Frangogiannis, N. G. Lack of specificity of fibroblast-specific protein 1 in cardiac remodeling and fibrosis. *AJP Hear. Circ. Physiol.* **305,** H1363–H1372 (2013).
102. Furtado, M. B. *et al.* Integrative Physiology Cardiogenic Genes Expressed in Cardiac Fibroblasts Contribute to Heart Development and Repair. *Circ. Res.* **114,** 1422–1434 (2014).
103. Kramann, R. *et al.* Perivascular Gli1+ Progenitors Are Key Contributors to Injury-Induced Organ Fibrosis. *Cell Stem Cell* **16,** 51–66 (2015).
104. Stempien-Otero, A., Kim, D.-H. & Davis, J. Molecular Networks Underlying Myofibroblast Fate and Fibrosis. *J. Mol. Cell. Cardiol.* **97,** 153–161 (2016).
105. Goldsmith, E. C. *et al.* Organization of fibroblasts in the heart. *Dev. Dyn.* **230,** 787–794 (2004).
106. Hudon-David, F., Bouzeghrane, F., Couture, P. & Thibault, G. Thy-1 expression by cardiac fibroblasts: Lack of association with myofibroblast contractile markers. *J. Mol. Cell. Cardiol.* **42,** 991–1000 (2007).
107. Doppler, S. A. *et al.* Cardiac fibroblasts : more than mechanical support. **9,** 36–51 (2017).
108. Majno, G., Gabbiani, G., Hirschel, B. J., Ryan, G. B. & Statkov, P. R. Contraction of granulation tissue in vitro: similarity to smooth muscle. *Science* **173,** 548–550 (1971).
109. Ivey, M. J. & Tallquist, M. D. Defining the Cardiac Fibroblast. *Circ. J.* **80,** 2269–2276 (2016).
110. Baum, J. & Duffy, H. S. Fibroblasts and myofibroblasts: What are we talking about? *J. Cardiovasc. Pharmacol.* **57,** 376–379 (2011).
111. Kaur, H. *et al.* Targeted Ablation of Periostin-Expressing Activated Fibroblasts Prevents Adverse Cardiac Remodeling in Mice. *Circ. Res.* CIRCRESAHA.116.308643 (2016). doi:10.1161/CIRCRESAHA.116.308643
112. Shimazaki, M. *et al.* Periostin is essential for cardiac healing after acute myocardial infarction. *J. Exp. Med.* **205,** 295–303 (2008).

113. Snider, P. *et al.* Periostin Is Required for Maturation and Extracellular Matrix Stabilization of Noncardiomyocyte Lineages of the Heart. *Circ. Res.* **102,** 752–760 (2008).
114. Horiuchi, K. *et al.* Identification and Characterization of a Novel Protein, Periostin, with Restricted Expression to Periosteum and Periodontal Ligament and Increased Expression by Transforming Growth Factor Beta. *J. Bone Miner. Res.* **14,** 1239–1249 (1999).
115. Oka, T. *et al.* Genetic manipulation of periostin expression reveals a role in cardiac hypertrophy and ventricular remodeling. *Circ. Res.* **101,** 313–321 (2007).
116. Travers, J. G., Kamal, F. A., Robbins, J., Yutzey, K. E. & Blaxall, B. C. Cardiac fibrosis: The fibroblast awakens. *Circ. Res.* **118,** 1021–1040 (2016).
117. Leask, A. Potential therapeutic targets for cardiac fibrosis: TGFβ, angiotensin, endothelin, CCN2, and PDGF, partners in fibroblast activation. *Circ. Res.* **106,** 1675–1680 (2010).
118. Frangogiannis, N. G. Cardiac fibrosis: Cell biological mechanisms, molecular pathways and therapeutic opportunities. *Mol. Aspects Med.* 0–1 (2018). doi:10.1016/j.mam.2018.07.001
119. Davis, J., Burr, A. R., Davis, G. F., Birnbaumer, L. & Molkentin, J. D. A TRPC6-dependent pathway for myofibroblast transdifferentiation and wound healing in vivo. *Dev. Cell* **23,** 705–715 (2012).
120. Hinz, B., Celetta, G., Tomasek, J. J., Gabbiani, G. & Chaponnier, C. Alpha-Smooth Muscle Actin Expression Upregulates Fibroblast Contractile Activity. *Mol. Biol. Cell* **12,** 2730–2741 (2001).
121. Phan, S. H. Biology of Fibroblasts and Myofibroblasts. *Proc. Am. Thorac. Soc.* **5,** 334–337 (2008).
122. Zhang, H. Y., Gharaee-Kermani, M., Zhang, K., Karmiol, S. & Phan, S. H. Lung fibroblast alpha-smooth muscle actin expression and contractile phenotype in bleomycin-induced pulmonary fibrosis. *Am. J. Pathol.* **148,** 527–37 (1996).
123. Walker, G. A., Masters, K. S., Shah, D. N., Anseth, K. S. & Leinwand, L. A. Valvular myofibroblast activation by transforming growth factor-β: Implications for pathological extracellular matrix remodeling in heart valve disease. *Circ. Res.* **95,** 253–260 (2004).
124. Bujak, M. & Frangogiannis, N. G. The role of TGF-beta signaling in myocardial infarction and cardiac remodeling. *Cardiovasc. Res.* **74,** 184–95 (2007).
125. Dobaczewski, M. *et al.* Smad3 signaling critically regulates fibroblast phenotype and function in healing myocardial infarction. *Circ. Res.* **107,** 418–428 (2010).
126. Hinz, B. Tissue stiffness, latent TGF-β1 Activation, and mechanical signal transduction: Implications for the pathogenesis and treatment of fibrosis. *Curr. Rheumatol. Rep.* **11,** 120–126 (2009).
127. Hinz, B. Formation and function of the myofibroblast during tissue repair. *J. Invest. Dermatol.* **127,** 526–537 (2007).
128. Vivar, R. *et al.* TGF-β1 prevents simulated ischemia/reperfusion-induced cardiac fibroblast apoptosis by activation of both canonical and non-canonical signaling pathways. *Biochim. Biophys. Acta - Mol. Basis Dis.* **1832,** 754–762 (2013).
129. Piersma, B., Bank, R. A. & Boersema, M. Signaling in Fibrosis: TGF-β, WNT, and YAP/TAZ Converge. *Front. Med.* **2,** 1–14 (2015).
130. Shi, Y. & Massagué, J. Mechanisms of TGF-beta signaling from cell membrane to the nucleus. *Cell* **113,** 685–700 (2003).
131. Verrecchia, F., Chu, M. L. & Mauviel, A. Identification of Novel TGF-β/Smad Gene Targets in Dermal Fibroblasts using a Combined cDNA Microarray/Promoter Transactivation Approach. *J. Biol. Chem.* **276,** 17058–17062 (2001).
132. Derynck, R. & Zhang, Y. E. Smad-dependent and Smad-independent pathways in TGF-. **4,** (2003).
133. Khalil, H. *et al.* Fibroblast-specific TGF-β–Smad2/3 signaling underlies cardiac fibrosis. *J. Clin. Invest.* **127,** 3770–3783 (2017).
134. Pulichino, A.-M. *et al.* Identification of transforming growth factor beta1-driven genetic programs of acute lung fibrosis. *Am. J. Respir. Cell Mol. Biol.* **39,** 324–336 (2008).

135. Takizawa, H. *et al.* Increased expression of transforming growth factor-beta1 in small airway epithelium from tobacco smokers and patients with chronic obstructive pulmonary disease (COPD). *Am. J. Respir. Crit. Care Med.* **163,** 1476–1483 (2001).
136. Zandvoort, A. *et al.* Smad gene expression in pulmonary fibroblasts: Indications for defective ECM repair in COPD. *Respir. Res.* **9,** 1–10 (2008).
137. Uemura, M. *et al.* Dominant maternal-effect mutations causing embryonic lethality in Caenorhabditis elegans. *Mol. Biol. Cell* **16,** 4214–4224 (2005).
138. Fukasawa, H. *et al.* Down-regulation of Smad7 expression by ubiquitin-dependent degradation contributes to renal fibrosis in obstructive nephropathy in mice. *Proc. Natl. Acad. Sci.* **101,** 8687–8692 (2004).
139. Meng, X. M. *et al.* Smad2 Protects against TGF-β/Smad3-Mediated Renal Fibrosis. *Journal of the American Society of Nephrology : JASN* **21,** 1477–1487 (2010).
140. Saika, S. *et al.* Smad3 Signaling Is Required for Epithelial-Mesenchymal Transition of Lens Epithelium after Injury. *Am. J. Pathol.* **164,** 651–663 (2004).
141. Sato, M., Muragaki, Y., Saika, S. & Roberts, A. B. Targeted disruption of TGF-β1 / Smad3 signaling protects against renal tubulointerstitial fibrosis induced by unilateral ureteral obstruction. *J. Clin. Invest.* **112,** (2003).
142. Wang, W. *et al.* Essential Role of Smad3 in Angiotensin II–Induced Vascular Fibrosis. *Circ. Res.* **98,** 1032–1039 (2006).
143. Bujak, M. *et al.* Essential role of Smad3 in infarct healing and in the pathogenesis of cardiac remodeling. *Circulation* **116,** 2127–2138 (2007).
144. Nomura, M. & Li, E. Smad2 role in mesoderm formation, left-right patterning and craniofacial development. *Nature* **393,** 786–790 (1998).
145. Divakaran, V. *et al.* Adaptive and Maladaptive Effects of SMAD3 Signaling in the Adult Hearth Following Hemodynamic Pressure Overloading. *Circ. Hear. Fail.* **2,** 633–642 (2009).
146. Lal, H. *et al.* Cardiac fibroblast glycogen synthase kinase-3β regulates ventricular remodeling and dysfunction in ischemic heart. *Circulation* **130,** 419–430 (2014).
147. Koitabashi, N. *et al.* Pivotal role of cardiomyocyte TGF-β signaling in the murine pathological response to sustained pressure overload. *J. Clin. Invest.* **121,** 2301–2312 (2011).
148. Watkins, S. J., Jonker, L. & Arthur, H. M. A direct interaction between TGFβ activated kinase 1 and the TGFβ type II receptor: Implications for TGFβ signalling and cardiac hypertrophy. *Cardiovasc. Res.* **69,** 432–439 (2006).
149. Zhang, Y. E., Yu, L. & He, M. C. TGF- b receptor-activated p38 MAP kinase mediates Smad-independent TGF- b responses. **21,** 3749–3759 (2002).
150. Zhang, Y. E. Non-Smad pathways in TGF-β signaling. *Cell Res.* **19,** 128–139 (2009).
151. Horowitz, J. C. *et al.* Activation of the Pro-survival Phosphatidylinositol 3-Kinase/AKT Pathway by Transforming Growth Factor-β1 in Mesenchymal Cells Is Mediated by p38 MAPK-dependent Induction of an Autocrine Growth Factor. *J. Biol. Chem.* **279,** 1359–1367 (2004).
152. Zhang, D. *et al.* TAK1 is activated in the myocardium after pressure overload and is sufficient to provoke heart failure in transgenic mice. *Nat. Med.* **6,** 556–563 (2000).
153. Liao, P. *et al.* The in vivo role of p38 MAP kinases in cardiac remodeling and restrictive cardiomyopathy. *Proc. Natl. Acad. Sci. U. S. A.* **98,** 12283–12288 (2001).
154. Molkentin, J. D. *et al.* Fibroblast-Specific Genetic Manipulation of p38 Mitogen-Activated Protein Kinase in Vivo Reveals Its Central Regulatory Role in Fibrosis. *Circulation* **136,** 549–561 (2017).
155. Braz, J. C. *et al.* Targeted inhibition of p38 MAPK promotes hypertrophic cardiomyopathy through upregulation of calcineurin-NFAT signaling. *J. Clin. Invest.* **111,** 1475–1486 (2003).
156. Zhang, S. *et al.* The role of the Grb2 – p38 MAPK signaling pathway in cardiac hypertrophy and fibrosis. *In Vitro* **111,** 833–841 (2003).

157. Rosenbloom, J., Ren, S. & Macarak, E. New frontiers in fibrotic disease therapies: The focus of the Joan and Joel Rosenbloom Center for Fibrotic Diseases at Thomas Jefferson University. *Matrix Biol.* **51,** 14–25 (2016).
158. Wang, C. *et al.* TAK1 is a ubiquitin-dependent kinase of MKK and IKK. *Nature* **412,** 346–351 (2001).
159. Nilius, B. TRP channels in disease. *Biochim. Biophys. Acta - Mol. Basis Dis.* **1772,** 805–812 (2007).
160. Adapala, R. K. *et al.* TRPV4 channels mediate cardiac fibroblast differentiation by integrating mechanical and soluble signals. *J. Mol. Cell. Cardiol.* **54,** 45–52 (2013).
161. Du, J. *et al.* TRPM7-mediated Ca2+ signals confer fibrogenesis in human Atrial Fibrillation. *Circ. Res.* **106,** 992–1003 (2010).
162. Ishii, T. *et al.* TRPV2 channel inhibitors attenuate fibroblast differentiation and contraction mediated by keratinocyte-derived TGF-β1 in an in vitro wound healing model of rats. *J. Dermatol. Sci.* **90,** 332–342 (2018).
163. Thodeti, C. K., Paruchuri, S. & Meszaros, J. G. A TRP to cardiac fibroblast differentiation. *Channels* **7,** 211–214 (2013).
164. Harada, M. *et al.* Transient receptor potential canonical-3 channel-dependent fibroblast regulation in atrial fibrillation. *Circulation* **126,** 2051–2064 (2012).
165. Thodeti, C. K. *et al.* TRPV4 channels mediate cyclic strain-induced endothelial cell reorientation through integrin to integrin signaling. *Circ. Res.* **104,** 1123–1130 (2009).
166. Rahaman, S. O. *et al.* TRPV4 mediates myofibroblast differentiation and pulmonary fibrosis in mice Find the latest version : TRPV4 mediates myofibroblast differentiation and pulmonary fibrosis in mice. *J. Clin. Invest.* **124,** 5225–5238 (2014).
167. Bosc, L. V. G., Layne, J. J., Nelson, M. T. & Hill-eubanks, D. C. Nuclear Factor of Activated T Cells and Serum Response Factor Cooperatively Regulate the Activity of an alpha-Actin Intronic Enhancer *. **280,** 26113–26120 (2005).
168. Gooch, J. L., Gorin, Y., Zhang, B. & Abboud, H. E. Involvement of Calcineurin in Transforming Growth Factor-beta- mediated Regulation of Extracellular Matrix Accumulation *. **279,** 15561–15570 (2004).
169. Herum, K. M. *et al.* Syndecan-4 signaling via NFAT regulates extracellular matrix production and cardiac myofibroblast differentiation in response to mechanical stress. *J. Mol. Cell. Cardiol.* **54,** 73–81 (2013).
170. Huang, X. *et al.* Matrix Stiffness – Induced Myofibroblast Differentiation Is Mediated by Intrinsic Mechanotransduction. *Am. J. Respir. Cell Mol. Biol.* **47,** 340–348 (2012).
171. Bataller, R. *et al.* In vitro and in vivo activation of rat hepatic stellate cells results in de novo expression of L-type voltage-operated calcium channels. *Hepatology* **33,** 956–962 (2001).
172. Kojima, N., Hori, M., Murata, T., Morizane, Y. & Ozaki, H. Different profiles of Ca2+responses to endothelin-1 and PDGF in liver myofibroblasts during the process of cell differentiation. *Br. J. Pharmacol.* **151,** 816–827 (2007).
173. Hai, L., Kawarabayashi, Y., Imai, Y., Honda, A. & Inoue, R. Counteracting effect of TRPC1-associated Ca 2 ƨ influx on TNF-a -induced COX-2-dependent prostaglandin E 2 production in human colonic myofibroblasts. *AJP -Gastrointestinal Liver Physiol.* **301,** 356–367 (2011).
174. Kemeny, L. V. *et al.* Na+/Ca2+ exchangers regulate the migration and proliferation of human gastric myofibroblasts. *AJP Gastrointest. Liver Physiol.* **305,** G552–G563 (2013).
175. Rice, N. A. & Leinwand, L. A. Skeletal myosin heavy chain function in cultured lung myofibroblasts. *J. Cell Biol.* **163,** 119–129 (2003).
176. Miano, J. M. Serum response factor: Toggling between disparate programs of gene expression. *J. Mol. Cell. Cardiol.* **35,** 577–593 (2003).
177. Zhang, S. X. *et al.* Identification of direct serum-response factor gene targets during Me 2SO-

induced P19 cardiac cell differentiation. *J. Biol. Chem.* **280,** 19115–19126 (2005).
178. Sun, Q. *et al.* Defining the mammalian CArGome. *Genome Res.* **16,** 197–207 (2006).
179. Lutz, S. *et al.* Structure of Gaq-p63RhoGEF-RhoA Complex Reveals a Pathway for the Activation of RhoA by GPCRs. *Science (80-.).* **318,** 1923–1927 (2007).
180. Vardouli, L., Vasilaki, E., Papadimitriou, E., Kardassis, D. & Stournaras, C. A novel mechanism of TGFβ-induced actin reorganization mediated by Smad proteins and Rho GTPases. *FEBS J.* **275,** 4074–4087 (2008).
181. Wang, D. Z. *et al.* Activation of cardiac gene expression by myocardin, a transcriptional cofactor for serum response factor. *Cell* **105,** 851–862 (2001).
182. Wang, D.-Z. *et al.* Potentiation of serum response factor activity by a family of myocardin-related transcription factors. *Proc. Natl. Acad. Sci.* **99,** 14855–14860 (2002).
183. Miralles, F., Posern, G., Zaromytidou, A. I. & Treisman, R. Actin dynamics control SRF activity by regulation of its coactivator MAL. *Cell* **113,** 329–342 (2003).
184. Posern, G. & Treisman, R. Actin' together: serum response factor, its cofactors and the link to signal transduction. *Trends Cell Biol.* **16,** 588–596 (2006).
185. Yoshida, T. *et al.* Myocardin is a key regulator of CArG-dependent transcription of multiple smooth muscle marker genes. *Circ. Res.* **92,** 856–864 (2003).
186. Hoofnagle, M. H. *et al.* Myocardin is differentially required for the development of smooth muscle cells and cardiomyocytes. *Am. J. Physiol. Heart Circ. Physiol.* 1707–1721 (2011). doi:10.1152/ajpheart.01192.2010.
187. Small, E. M. *et al.* Myocardin-related transcription factor-a controls myofibroblast activation and fibrosis in response to myocardial infarction. *Circ. Res.* **107,** 294–304 (2010).
188. Olson, E. N. & Nordheim, A. Linking actin dynamics and gene transcription to drive cellular. **11,** 353–365 (2011).
189. Sandbo, N., Kregel, S., Taurin, S., Bhorade, S. & Dulin, N. O. Critical role of serum response factor in pulmonary myofibroblast differentiation induced by TGF-beta. *Am. J. Respir. Cell Mol. Biol.* **41,** 332–338 (2009).
190. Velasquez, L. S. *et al.* Activation of MRTF-A – dependent gene expression with a small molecule promotes myofibroblast differentiation and wound healing. *Proc. Natl. Acad. Sci.* **110,** 16850–16855 (2013).
191. Luchsinger, L. L., Patenaude, C. A., Smith, B. D. & Layne, M. D. Myocardin-related transcription factor-A complexes activate type I collagen expression in lung fibroblasts. *J. Biol. Chem.* **286,** 44116–44125 (2011).
192. Li, J. *et al.* Myocardin-related transcription factor B is required in cardiac neural crest for smooth muscle differentiation and cardiovascular development. *Proc. Natl. Acad. Sci.* **102,** 8916–8921 (2005).
193. Oh, J., Richardson, J. A. & Olson, E. N. Requirement of myocardin-related transcription factor-B for remodeling of branchial arch arteries and smooth muscle differentiation. *Proc. Natl. Acad. Sci.* **102,** 15122–15127 (2005).
194. Yang, Y., Zhe, X., Phan, S. H., Ullenbruch, M. & Schuger, L. Involvement of Serum Response Factor Isoforms in Myofibroblast Differentiation During Bleomycin-Induced Lung Injury. *Am. J. Respir. Cell Mol. Biol.* **29,** 583–590 (2003).
195. Chai, J., Norng, M., Tarnawski, A. S. & Chow, J. A critical role of serum response factor isoforms in myofibroblast differentiation during experimental oesophageal ulcer healing in rats. *Gut* **56,** 621–630 (2007).
196. Brock, J., Midwinter, K., Lewis, J. & Martin, P. Healing of incisional wounds in the embryonic chick wing bud: Characterization of the actin purse-string and demonstration of a requirement for Rho activation. *J. Cell Biol.* **135,** 1097–1107 (1996).

197. Haudek, S. B. *et al.* Rho kinase-1 mediates cardiac fibrosis by regulating fibroblast precursor cell differentiation. *Cardiovasc. Res.* **83,** 511–518 (2009).
198. Shiwen, X. *et al.* A Role of myocardin related transcription factor-A (MRTF-A) in scleroderma related fibrosis. *PLoS One* **10,** 1–20 (2015).
199. Wang, J. H. C., Thampatty, B. P., Lin, J. S. & Im, H. J. Mechanoregulation of gene expression in fibroblasts. *Gene* **391,** 1–15 (2007).
200. Kessler, D. *et al.* Fibroblasts in Mechanically Stressed Collagen Lattices Assume a 'Synthetic' Phenotype. *J. Biol. Chem.* **276,** 36575–36585 (2001).
201. Chan, M. W. C., Chaudary, F., Lee, W., Copeland, J. W. & McCulloch, C. A. Force-induced myofibroblast differentiation through collagen receptors is dependent on mammalian diaphanous (mDia). *J. Biol. Chem.* **285,** 9273–9281 (2010).
202. Georges, P. C. *et al.* Increased stiffness of the rat liver precedes matrix deposition: implications for fibrosis. *AJP Gastrointest. Liver Physiol.* **293,** G1147–G1154 (2007).
203. Herum, K., Lunde, I., McCulloch, A. & Christensen, G. The Soft- and Hard-Heartedness of Cardiac Fibroblasts: Mechanotransduction Signaling Pathways in Fibrosis of the Heart. *J. Clin. Med.* **6,** 53 (2017).
204. Rouillard, A. D. & Holmes, J. W. Mechanical regulation of fibroblast migration and collagen remodelling in healing myocardial infarcts. *J. Physiol.* **590,** 4585–4602 (2012).
205. Sandbo, N. *et al.* Delayed stress fiber formation mediates pulmonary myofibroblast differentiation in response to TGF-β. *Am. J. Physiol. Cell. Mol. Physiol.* **301,** L656–L666 (2011).
206. Qiu, P., Feng, X. H. & Li, L. Interaction of Smad3 and SRF-associated complex mediates TGF-β1 signals to regulate SM22 transcription during myofibroblast differentiation. *J. Mol. Cell. Cardiol.* **35,** 1407–1420 (2003).
207. Herrmann, J., Haas, U., Gressner, A. M. & Weiskirchen, R. TGF-β up-regulates serum response factor in activated hepatic stellate cells. *Biochim. Biophys. Acta - Mol. Basis Dis.* **1772,** 1250–1257 (2007).
208. Hirschi, K. K. *et al.* Transforming growth factor-beta induction of smooth muscle cell phenotype requires transcriptional and post-transcriptional control of serum response factor. *J Biol Chem* **277,** 6287–6295 (2002).
209. Arsenian, S., Weinhold, B., Oelgeschlä Ger, M., Rü Ther, U. & Nordheim, A. Serum response factor is essential for mesoderm formation during mouse embryogenesis. *EMBO J.* **17,** 6289–6299 (1998).
210. Das, S., Becker, B. N., Hoffmann, F. M. & Mertz, J. E. Complete reversal of epithelial to mesenchymal transition requires inhibition of both ZEB expression and the Rho pathway. *BMC Cell Biol.* **10,** 1–18 (2009).
211. Clarke, Samantha A.; Goodman, Norman C.; Ailawadi, Gorav; Holmes, J. W. Effect of Scar Compaction on the Therapeutic Efficacy of Anisotropic Reinforcement Following Myocardial Infarction in the Dog. **8,** 353–361 (2015).
212. Friedman, S. L., Sheppard, D., Duffield, J. S. & Violette, S. Therapy for fibrotic diseases: nearing the starting line. *Sci. Transl. Med.* **5,** 167sr1 (2013).
213. Camacho, P., Fan, H., Liu, Z. & He, J. Small mammalian animal models of heart disease. **6,** 70–80 (2016).
214. Guallar, D. & Wang, J. RNA-binding proteins in pluripotency, differentiation, and reprogramming. *Frontiers in Biology* **9,** 389–409 (2014).
215. De Bruin, R. G., Rabelink, T. J., Van Zonneveld, A. J. & Van Der Veer, E. P. Emerging roles for RNA-binding proteins as effectors and regulators of cardiovascular disease. *Eur. Heart J.* **38,** 1380–1388 (2017).
216. Suresh Babu, S., Joladarashi, D., Jeyabal, P., Thandavarayan, R. A. & Krishnamurthy, P. RNA-

stabilizing proteins as molecular targets in cardiovascular pathologies. *Trends Cardiovasc. Med.* **25,** 676–683 (2015).
217. Hu, Z. *et al.* Revealing Missing Human Protein Isoforms Based on Ab Initio Prediction, RNA-seq and Proteomics. *Sci. Rep.* **5,** 1–15 (2015).
218. Giudice, J. *et al.* Alternative splicing regulates vesicular trafficking genes in cardiomyocytes during postnatal heart development. *Nat. Commun.* **5,** 1–15 (2014).
219. Lee, K. Y. *et al.* Compound loss of muscleblind-like function in myotonic dystrophy. *EMBO Mol. Med.* **5,** 1887–1900 (2013).
220. Tang, Z. Z. *et al.* Muscle weakness in myotonic dystrophy associated with misregulated splicing and altered gating of Cav1.1 calcium channel. *Hum. Mol. Genet.* **21,** 1312–1324 (2012).
221. Creemers, E. E. *et al.* Genome-Wide Polyadenylation Maps Reveal Dynamic mRNA 3'-End Formation in the Failing Human Heart. *Circ. Res.* **118,** 433–438 (2016).
222. Park, J. Y. *et al.* Comparative Analysis of mRNA Isoform Expression in Cardiac Hypertrophy and Development Reveals Multiple Post-Transcriptional Regulatory Modules. *PLoS One* **6,** e22391 (2011).
223. Soetanto, R. *et al.* Role of miRNAs and alternative mRNA 3 ' -end cleavage and polyadenylation of their mRNA targets in cardiomyocyte hypertrophy. *BBA - Gene Regul. Mech.* **1859,** 744–756 (2016).
224. Mayr, C. & Bartel, D. P. Widespread Shortening of 3' UTRs by Alternative Cleavage and Polyadenylation Activates Oncogenes in Cancer Cells. *Cell* **138,** 673–684 (2009).
225. Sano, M. *et al.* Activation and function of cyclin T-Cdk9 (positive transcription elongation factor-b) in cardiac muscle-cell hypertrophy. *Nat. Med.* **8,** 1310–1317 (2002).
226. Krishnamurthy, P. *et al.* Myocardial knockdown of mRNA-stabilizing protein HuR attenuates post-MI inflammatory response and left ventricular dysfunction in IL-10-null mice. *FASEB J. Off. Publ. Fed. Am. Soc. Exp. Biol.* **24,** 2484–2494 (2010).
227. Woodhoo, A. *et al.* HuR contributes to Hepatic Stellate Cell activation and liver fibrosis. *Hepatology* **56,** 1870–1882 (2012).
228. Begemann, G. *et al.* muscleblind, a gene required for photoreceptor differentiation in Drosophila, encodes novel nuclear Cys3His-type zinc-finger-containing proteins. *Development* **124,** 4321–31 (1997).
229. Artero, R. *et al.* ThemuscleblindGene Participates in the Organization of Z-Bands and Epidermal Attachments ofDrosophilaMuscles and Is Regulated byDmef2. *Dev. Biol.* **195,** 131–143 (1998).
230. Kanadia, R. N. *et al.* Developmental expression of mouse muscleblind genes Mbnl1, Mbnl2 and Mbnl3. *Gene Expr. Patterns* **3,** 459–462 (2003).
231. Fardaei, M. *et al.* Three proteins, MBNL, MBLL and MBXL, co-localize in vivo with nuclear foci of expanded-repeat transcripts in DM1 and DM2 cells. *Hum. Mol. Genet.* **11,** 805–814 (2002).
232. Miller, J. W. *et al.* Recruitment of human muscleblind proteins to (CUG)(n) expansions associated with myotonic dystrophy. *EMBO J.* **19,** 4439–48 (2000).
233. Konieczny, P., Stepniak-Konieczna, E. & Sobczak, K. MBNL proteins and their target RNAs, interaction and splicing regulation. *Nucleic Acids Res.* **42,** 10873–10887 (2014).
234. Squillace, R. M., Chenault, D. M. & Wang, E. H. Inhibition of Muscle Differentiation by the Novel Muscleblind-Related Protein CHCR. *Dev. Biol.* **250,** 218–230 (2002).
235. Pascual, M., Vicente, M., Monferrer, L. & Artero, R. The Muscleblind family of proteins: an emerging class of regulators of developmentally programmed alternative splicing. *Differentiation.* **74,** 65–80 (2006).
236. Wang, E. T. *et al.* Transcriptome-wide regulation of pre-mRNA splicing and mRNA localization by muscleblind proteins. *Cell* **150,** 710–24 (2012).
237. Rattenbacher, B. *et al.* Analysis of CUGBP1 Targets Identifies GU-Repeat Sequences That Mediate

Rapid mRNA Decay. *Mol. Cell. Biol.* **30,** 3970–3980 (2010).
238. Vlasova, I. A. *et al.* Conserved GU-Rich Elements Mediate mRNA Decay by Binding to CUG-Binding Protein 1. *Mol. Cell* **29,** 263–270 (2008).
239. Wang, E. T. *et al.* Antagonistic regulation of mRNA expression and splicing by CELF and MBNL proteins. *Genome Res.* **25,** 858–871 (2015).
240. Terenzi, F. & Ladd, A. N. Conserved developmental alternative splicing of muscleblind-like (MBNL) transcripts regulates MBNL localization and activity. *RNA Biol.* **7,** 43–55 (2010).
241. Terenzi, F. & Ladd, A. N. Conserved developmental alternative splicing of muscleblind-like (MBNL) transcripts regulates MBNL localization and activity. *RNA Biol.* **7,** (2010).
242. Batra, R. *et al.* Loss of MBNL leads to disruption of developmentally regulated alternative polyadenylation in RNA-mediated disease. *Mol. Cell* **56,** 311–322 (2014).
243. Ames, E., Lawson, M., Mackey, A. & Holmes, J. Sequencing of mRNA identifies re-expression of fetal splice variants in cardiac hypertrophy. *J. Mol. Cell. Cardiol.* **62,** 99–107 (2013).
244. Venables, J. P. *et al.* MBNL1 and RBFOX2 cooperate to establish a splicing programme involved in pluripotent stem cell differentiation. *Nat. Commun.* **4,** 1–10 (2013).
245. Han, H. *et al.* MBNL proteins repress ES-cell-specific alternative splicing and reprogramming. *Nature* **498,** 241–5 (2013).
246. Fugier, C. *et al.* Misregulated alternative splicing of BIN1 is associated with T tubule alterations and muscle weakness in myotonic dystrophy. *Nat. Med.* **17,** 720–725 (2011).
247. Lin, X. *et al.* Failure of MBNL1-dependent post-natal splicing transitions in myotonic dystrophy. **15,** 2087–2097 (2006).
248. Kalsotra, A. *et al.* A postnatal switch of CELF and MBNL proteins reprograms alternative splicing in the developing heart. *Proc. Natl. Acad. Sci. U. S. A.* **105,** 20333–20338 (2008).
249. Cheng, A. W. *et al.* Muscleblind-like 1 (Mbnl1) regulates pre-mRNA alternative splicing during terminal erythropoiesis. *Blood* **124,** 598–610 (2014).
250. Razzaq, A. *et al.* Amphiphysins 1 and 2 are enriched in the mammalian brain and are proposed to recruit dynamin to sites of endocytosis. Shorter amphiphysin 2 splice variants are also found ubiquitously, with an enrichment in skeletal muscle. At the. *Genes Dev.* **15,** 2967–2979 (2001).
251. Kanadia, R. N. *et al.* Reversal of RNA missplicing and myotonia after muscleblind overexpression in a mouse poly(CUG) model for myotonic dystrophy. *Proc. Natl. Acad. Sci.* **103,** 11748–11753 (2006).
252. Ho, T. H. *et al.* Muscleblind proteins regulate alternative splicing. **23,** 3103–3112 (2004).
253. Kimura, T. *et al.* Altered mRNA splicing of the skeletal muscle ryanodine receptor and sarcoplasmic/endoplasmic reticulum Ca2+-ATPase in myotonic dystrophy type 1. *Hum. Mol. Genet.* **14,** 2189–2200 (2005).
254. Xu, X. *et al.* ASF/SF2-regulated CaMKIIδ alternative splicing temporally reprograms excitation-contraction coupling in cardiac muscle. *Cell* **120,** 59–72 (2005).
255. Chateauvieux, S., Grigorakaki, C., Morceau, F., Dicato, M. & Diederich, M. Erythropoietin, erythropoiesis and beyond. *Biochem. Pharmacol.* **82,** 1291–1303 (2011).
256. Hattangadi, S. M., Wong, P., Zhang, L., Flygare, J. & Lodish, H. F. From stem cell to red cell: regulation of erythropoiesis at multiple levels by multiple proteins , RNAs , and chromatin modifications. *Blood* **118,** 6258–6269 (2015).
257. Gates, D. P., Coonrod, L. A. & Berglund, J. A. Autoregulated splicing of muscleblind-like 1 (MBNL1) Pre-mRNA. *J. Biol. Chem.* **286,** 34224–34233 (2011).
258. Prat-Vidal, C. *et al.* Identification of Temporal and Region-Specific Myocardial Gene Expression Patterns in Response to Infarction in Swine. *PLoS One* **8,** (2013).
259. Onishi, H. *et al.* MBNL1 associates with YB-1 in cytoplasmic stress granules. *J. Neurosci. Res.* **86,** 1994–2002 (2008).

260. Du, H. *et al.* Aberrant alternative splicing and extracellular matrix gene expression in mouse models of myotonic dystrophy. *Nat. Struct. Mol. Biol.* **17,** 187–193 (2010).
261. Hino, S. -i. *et al.* Molecular mechanisms responsible for aberrant splicing of SERCA1 in myotonic dystrophy type 1. *Hum. Mol. Genet.* **16,** 2834–2843 (2007).
262. Kanadia, R. N. *et al.* A muscleblind knockout model for myotonic dystrophy. *Science* **302,** 1978–80 (2003).
263. Paul, S. *et al.* Expanded CUG repeats dysregulate RNA splicing by altering the stoichiometry of the muscleblind 1 complex. *J. Biol. Chem.* **286,** 38427–38438 (2011).
264. Christensen, G., Herum, K. M. & Lunde, I. G. Sweet, yet underappreciated: Proteoglycans and extracellular matrix remodeling in heart disease. *Matrix Biol.* 1–14 (2018). doi:10.1016/j.matbio.2018.01.001
265. Ogorodnikov, A., Kargapolova, Y. & Danckwardt, S. Processing and transcriptome expansion at the mRNA 3' end in health and disease: finding the right end. *Pflugers Arch. Eur. J. Physiol.* **468,** 993–1012 (2016).
266. Masuda, A. *et al.* CUGBP1 and MBNL1 preferentially bind to 3' UTRs and facilitate mRNA decay. *Sci. Rep.* **2,** 1–10 (2012).
267. Mankodi, A. *et al.* Myotonic dystrophy in transgenic mice expressing an expanded CUG repeat. *Science* **289,** 1769–73 (2000).
268. Meola, G. & Cardani, R. Myotonic dystrophies: An update on clinical aspects, genetic, pathology, and molecular pathomechanisms. *Biochim. Biophys. Acta - Mol. Basis Dis.* **1852,** 594–606 (2015).
269. Harley, H. G. *et al.* Size of the Unstable CTG Repeat Sequence in Relation to Phenotype and Parental Transmission in Myotonic Dystrophy. 1164–1174 (1993).
270. Dixon, D. M. *et al.* Loss of muscleblind-like 1 results in cardiac pathology and persistence of embryonic splice isoforms. *Sci. Rep.* **5,** 1–13 (2015).
271. Klein, A. F., Gasnier, E. & Furling, D. Gain of RNA function in pathological cases: Focus on myotonic dystrophy. *Biochimie* **93,** 2006–12 (2011).
272. Kuyumcu-Martinez, N. M., Wang, G. S. & Cooper, T. A. Increased Steady-State Levels of CUGBP1 in Myotonic Dystrophy 1 Are Due to PKC-Mediated Hyperphosphorylation. *Mol. Cell* **28,** 68–78 (2007).
273. Bertoncini, P. *et al.* Study of the Mechanical Properties of Myomesin Proteins Using Dynamic Force Spectroscopy. *J. Mol. Biol.* **348,** 1127–1137 (2005).
274. Lahmers, S., Wu, Y., Call, D. R., Labeit, S. & Granzier, H. Developmental Control of Titin Isoform Expression and Passive Stiffness in Fetal and Neonatal Myocardium. *Circ. Res.* **94,** 505–513 (2004).
275. Pinotsis, N. *et al.* Superhelical architecture of the myosin filament-linking protein myomesin with unusual elastic properties. *PLoS Biol.* **10,** (2012).
276. Schoenauer, R. *et al.* Myomesin is a molecular spring with adaptable elasticity. *J. Mol. Biol.* **349,** 367–379 (2005).
277. Guo, W. *et al.* RBM20 , a gene for hereditary cardiomyopathy , regulates titin splicing. *Nat. Med.* **18,** 766–773 (2013).
278. Jog, S. P. *et al.* RNA Splicing Is Responsive to MBNL1 Dose. **7,** 1–8 (2012).
279. Ahuja, P. *et al.* Re-expression of proteins involved in cytokinesis during cardiac hypertrophy. *Exp. Cell Res.* **313,** 1270–1283 (2007).
280. Oparil, S., Bishop, S. P. & Clubb, F. J. J. Myocardial cell hypertrophy or hyperplasia. *Hypertens. (Dallas, Tex. 1979)* **6,** III38-43 (1984).
281. Fan, Z. & Guan, J. Antifibrotic therapies to control cardiac fibrosis. *Biomater. Res.* **20,** 1–13 (2016).
282. Ertl, G. & Frantz, S. Healing after myocardial infarction. *Cardiovasc. Res.* **66,** 22–32 (2005).
283. Wang, E. T. *et al.* Transcriptome-wide Regulationof Pre-mRNA Splicing and mRNA Localization by

Muscleblind Proteins. *Cell* **150,** 710–724 (2012).
284. Zhu, H., Zhou, H. L., Hasman, R. A. & Lou, H. Hu proteins regulate polyadenylation by blocking sites containing U-rich sequences. *J. Biol. Chem.* **282,** 2203–2210 (2007).
285. Norris, A. D., Gracida, X. & Calarco, J. A. CRISPR-mediated genetic interaction profiling identifies RNA binding proteins controlling metazoan fitness. *Elife* **6,** 1–18 (2017).
286. Oktaba, K. *et al.* ELAV links paused pol II to alternative polyadenylation in the drosophila nervous system. *Mol. Cell* **57,** 341–348 (2015).
287. Tian, Y. & Morrisey, E. E. Importance of myocyte-nonmyocyte interactions in cardiac development and disease. *Circ. Res.* **110,** 1023–34 (2012).
288. Coram, R. J. *et al.* Muscleblind-like 1 is required for normal heart valve development in vivo. *BMC Dev. Biol.* **15,** 36 (2015).
289. Ladd, A. N., Stenberg, M. G., Swanson, M. S. & Cooper, T. A. Dynamic balance between activation and repression regulates pre-mRNA alternative splicing during heart development. *Dev. Dyn.* **233,** 783–793 (2005).
290. Hino, S. -i. *et al.* Molecular mechanisms responsible for aberrant splicing of SERCA1 in myotonic dystrophy type 1. *Hum. Mol. Genet.* **16,** 2834–2843 (2007).
291. Jog, S. P. *et al.* RNA Splicing Is Responsive to MBNL1 Dose. *PLoS One* **7,** 1–8 (2012).
292. Lu, J. *et al.* Erythropoietin attenuates cardiac dysfunction by increasing myocardial angiogenesis and inhibiting interstitial fibrosis in diabetic rats. *Cardiovasc. Diabetol.* **11,** 1–11 (2012).
293. Zhang, X., Dong, S., Qin, Y. & Bian, X. Protective effect of erythropoietin against myocardial injury in rats with sepsis and its underlying mechanisms. *Mol. Med. Rep.* **11,** 3317–3329 (2015).
294. Calvillo, L. *et al.* Recombinant human erythropoietin protects the myocardium from ischemia-reperfusion injury and promotes beneficial remodeling. *Proc. Natl. Acad. Sci. U. S. A.* **100,** 4802–6 (2003).
295. Mengozzi, M. *et al.* Increased erythropoietin production after myocardial infarction in mice. *Heart* **92,** 838–839 (2006).
296. Nakamura, R. *et al.* Erythropoietin in patients with acute coronary syndrome and its cardioprotective action after percutaneous coronary intervention. *Circ. J.* **73,** 1920–1926 (2009).
297. Eshghi, S., Vogelezang, M. G., Hynes, R. O., Griffith, L. G. & Lodish, H. F. α4β1 integrin and erythropoietin mediate temporally distinct steps in erythropoiesis: Integrins in red cell development. *J. Cell Biol.* **177,** 871–880 (2007).
298. Tamura, K. *et al.* Requirement for p38α in erythropoietin expression: A role for stress kinases in erythropoiesis. *Cell* **102,** 221–231 (2000).
299. Sherman, M. H., Bassing, C. H. & Teitell, M. a. DNA damage response regulates cell differentiation. *Trends Cell Biol.* **21,** 312–319 (2011).
300. Nouspikel, T. & Hanawalt, P. C. DNA repair in terminally differentiated cells. *Thierry Nouspikel, Philip C. Hanawalt. 2002. DNA repair Termin. Differ. cells. DNA Repair 1 59-75.* **1,** 59–75 (2002).
301. Lin, T. *et al.* p53 induces differentiation of mouse embryonic stem cells by suppressing Nanog expression. *Nat. Cell Biol.* **7,** 165–171 (2005).
302. Sanes, J. R. & Okun, L. M. Induction of DNA synthesis in cultured neurons by ultraviolet light or methyl methane sulfonate. *J Cell Biol* **53,** 587–590 (1972).
303. Karran, P., Moscona, A. & Strauss, B. DEVELOPMENTAL DECLINE IN D N A REPAIR IN N E U R A L RETINA CELLS OF CHICK EMBRYOS Persistent Deficiency of Repair Competence in a Cell Line Derived from Late Embryos Neural retinas of 6-day-old chick embryos synthesize DNA and are able to carry out DNA e. *J Cell Biol* **74,** 274–286 (1977).
304. Hahn, G. M., King, D. & Yang, S. J. Quantitative changes in unscheduled DNA synthesis in rat muscle cells after differentiation. *Nat. New Biol.* **230,** 242–244 (1971).
305. Stockdale, F. E. DNA synthesis in differentiating skeletal muscle cells: initiation by ultraviolet light.

Science **171,** 1145–1147 (1971).
306. Karran, P. & Ormerod, M. G. Is the ability to repair damage to DNA related to the proliferative capacity of a cell? The rejoining of X-ray-produced strand breaks. *Biochim. Biophys. Acta* **299,** 54–64 (1973).
307. Petrov, V. V. *et al.* TGF-β1-induced cardiac myofibroblasts are nonproliferating functional cells carrying DNA damages. *Exp. Cell Res.* **314,** 1480–1494 (2008).
308. Shahzad, S. *et al.* Elevated DNA Damage, Oxidative Stress, and Impaired Response Defense System Inflicted in Patients With Myocardial Infarction. *Clin. Appl. Thromb.* **24,** 780–789 (2018).
309. Bregman, D. B. *et al.* UV-induced ubiquitination of RNA polymerase II: a novel modification deficient in Cockayne syndrome cells. *Proc. Natl. Acad. Sci. U. S. A.* **93,** 11586–90 (1996).
310. Bunch, H. *et al.* Transcriptional elongation requires DNA break-induced signalling. *Nat. Commun.* **6,** 1–12 (2015).
311. Price, D. H. P-TEFb, a Cyclin-Dependent Kinase Controlling Elongation by RNA Polymerase II. *Mol. Cell. Biol.* **20,** 2629–2634 (2000).
312. Rice, A. P. Dysregulation of P-TEFb and Myocardial Hypertrophy. *Circ. Res.* **104,** 1327–1329 (2009).
313. Yamaguchi, Y. *et al.* NELF, a multisubunit complex containing RD, cooperates with DSIF to repress RNA polymerase II elongation. *Cell* **97,** 41–51 (1999).
314. Wada, T. *et al.* DSIF, a novel transcription elongation factor that regulates RNA polymerase II processivity, is composed of human Spt4 and Spt5 homologs. *Genes Dev.* **12,** 343–356 (1998).
315. Marshall, N. F., Peng, J., Xie, Z. & Price, D. H. Molecular Genetics : Control of RNA Polymerase II Elongation Potential by a Novel Carboxyl-terminal Domain Kinase Control of RNA Polymerase II Elongation Potential by a Novel Carboxyl-terminal Domain Kinase *. **271,** 27176–27183 (1996).
316. Michels, A. A. *et al.* Binding of the 7SK snRNA turns the HEXIM1 protein into a P-TEFb (CDK9/cyclin T) inhibitor. *EMBO J.* **23,** 2608–2619 (2004).
317. Jeronimo, C. *et al.* Systematic Analysis of the Protein Interaction Network for the Human Transcription Machinery Reveals the Identity of the 7SK Capping Enzyme. *Mol. Cell* **27,** 262–274 (2007).
318. Krueger, B. J. *et al.* LARP7 is a stable component of the 7SK snRNP while P-TEFb, HEXIM1 and hnRNP A1 are reversibly associated. *Nucleic Acids Res.* **36,** 2219–2229 (2008).
319. Peterlin, B. M., Brogie, J. E. & Price, D. H. 7SK snRNA: A noncoding RNA that plays a major role in regulating eukaryotic transcription. *Wiley Interdiscip. Rev. RNA* **3,** 92–103 (2012).
320. Yu, D. S. & Cortez, D. A role for cdk9-cyclin k in maintaining genome integrity. *Cell Cycle* **10,** 28–32 (2011).
321. Floyd, S. R. *et al.* The Bromodomain Protein Brd4 Insulates Chromatin from DNA Damage Signaling. *Nature* **498,** 246–250 (2013).
322. Bellan, C. *et al.* CDK9/CYCLIN T1 expression during normal lymphoid differentiation and malignant transformation. *J. Pathol.* **203,** 946–952 (2004).
323. De Falco, G. & Giordano, A. CDK9: from basal transcription to cancer and AIDS. *Cancer Biol. Ther.* **1,** 342–347 (2002).
324. De Falco, G. *et al.* Cdk9 regulates neural differentiation and its expression correlates with the differentiation grade of neuroblastoma and PNET tumors. *Cancer Biol. Ther.* **4,** 277–281 (2005).
325. Espinoza-Derout, J. *et al.* Pivotal role of cardiac lineage protein-1 (CLP-1) in transcriptional elongation factor P-TEFb complex formation in cardiac hypertrophy. *Cardiovasc. Res.* **75,** 129–138 (2007).
326. Huang, F., Wagner, M. & Siddiqui, M. A. . Ablation of the CLP-1 gene leads to down-regulation of the HAND1 gene and abnormality of the left ventricle of the heart and fetal death. *Mech. Dev.* **121,** 559–572 (2004).

327. Turano, M. *et al.* Increased HEXIM1 expression during erythroleukemia and neuroblastoma cell differentiation. *J. Cell. Physiol.* **206,** 603–610 (2006).
328. Espinoza-Derout, J. *et al.* Positive transcription elongation factor b activity in compensatory myocardial hypertrophy is regulated by cardiac lineage protein-1. *Circ. Res.* **104,** 1347–1354 (2009).
329. Alarcón, C. *et al.* Nuclear CDKs Drive Smad Transcriptional Activation and Turnover in BMP and TGF-β Pathways. *Cell* **139,** 757–769 (2009).
330. Qu, X. *et al.* The Smad3/Smad4/CDK9 complex promotes renal fibrosis in mice with unilateral ureteral obstruction. *Kidney Int.* **88,** 1323–1335 (2015).
331. Mascareno, E. *et al.* Cardiac lineage protein-1 (CLP-1) regulates cardiac remodeling via transcriptional modulation of diverse hypertrophic and fibrotic responses and angiotensin II-transforming growth factor β (TGF-β1) signaling axis. *J. Biol. Chem.* **287,** 13084–13093 (2012).
332. Katz, Y., Wang, E. T., Airoldi, E. M. & Burge, C. B. Analysis and design of RNA sequencing experiments for identifying isoform regulation. *Nat. Methods* **7,** 1009–1015 (2010).
333. An, J. J. *et al.* Distinct Role of Long 3' UTR BDNF mRNA in Spine Morphology and Synaptic Plasticity in Hippocampal Neurons. *Cell* **134,** 175–187 (2008).
334. Seropian, I. M., Toldo, S., Tassell, B. W. Van, Harm, P. D. & Aires, B. Anti-Inflammatory Strategies for Ventricular Remodeling Following ST-Segment Elevation Acute Myocardial Infarction. *J. Am. Coll. Cardiol.* **63,** 1593–1603 (2014).
335. Chen, G. *et al.* Phenylbutazone induces expression of MBNL1 and suppresses formation of MBNL1-CUG RNA foci in a mouse model of myotonic dystrophy. *Sci. Rep.* **6,** 1–11 (2016).
336. Hoskins, J. W. *et al.* Lomofungin and dilomofungin: Inhibitors of MBNL1-CUG RNA binding with distinct cellular effects. *Nucleic Acids Res.* **42,** 6591–6602 (2014).
337. Jahromi, A. H. *et al.* A Novel CUGexp ·MBNL1 Inhibitor with Therapeutic Potential for Myotonic Dystrophy Type 1. *ACS Chem Biol* **8,** 1037–1043 (2013).
338. López-Morató, M., Brook, J. D. & Wojciechowska, M. Small molecules which improve pathogenesis of myotonic dystrophy type 1. *Front. Neurol.* **9,** 1–12 (2018).